EVALUATION OF A SIMPLIFIED TECHNIQUE FOR NERVE REPAIR BY MEANS OF ENTUBULATION BY FLEXIBLE CONTROLLED RELEASE GLASS

By

L.A. Jeans

M.D. Thesis

University of Edinburgh

A.D. 2005

DECLARATION

The work presented in this thesis is the original work of the author. Any contribution made by others has been indicated clearly. This thesis has been composed by the author and not submitted for any other degree.

Signed

Lindsay Jeans

25th August 2005

ACKNOWLEDGEMENTS

Firstly I would like to acknowledge the dedication and guidance of Mr Michael Glasby. He has provided continuous motivation and encouragement to complete this work and his expertise from years of experience in peripheral nerve research has been essential throughout.

Miss Gail Valler provided invaluable technical help to myself and many others during her work in the Edinburgh Peripheral Nerve Research Group. She has been my closest companion throughout this project and I hope she gets on really well as she moves to another field of work.

The staff at the Marshall building were thorough in their care of the animals used in these experiments and helped in every possible way to make this project run smoothly. They were fun to work with and I have enjoyed my time with them very much.

I would like to thank Brendan Hawes for his expert technical help, his work in designing several pieces of apparatus for this work and for the generous way he gave of his time and his knowledge.

I also thank Mr David Healy, Mr Tom Gilchrist and all at Giltech Ltd who have supported this work faithfully and provided all the materials for this project. They have thus aided in the advancement of knowledge in the surgical repair of peripheral nerves.

ABSTRACT

The experiments presented in this thesis are a study in which the use of a biodegradable glass wrap was compared with microsurgical epineurial suturing as a means of repairing cleanly divided median nerves in a sheep model.

Twelve sheep were used in a control group and in each of four repair groups in which the following procedures were carried out:

1. Neurotmesis and repair using microsurgically placed epineurial sutures of 10/0 polyamide.
2. Neurotmesis and repair by entubulation with the biodegradable glass wrap secured by 6/0 polyglactin macrosutures
3. Neurotmesis and repair by entubulation with the biodegradable glass wrap secured by fibrin (Tisseel) glue
4. Neurotmesis and repair by entubulation with the biodegradable glass wrap secured with polycaprolactone glue.

No gap was left between the proximal and distal stumps. Electrophysiological tests on the median nerve, flexor carpi radialis muscle and flexor digitorum superficialis muscle were carried out seven months after the repair and a portion of the median nerve distal to the repair site was excised for morphometric examination after all electrophysiological testing had been completed.

The main conclusions of the present study were:

1. Nerves repaired with the biodegradable glass wrap and fibrin glue displayed distal neuronal regeneration that was no different from that which occurred after a tensionless microsurgical epineurial suture. This biodegradable glass

wrap, secured with fibrin (Tisseel) glue, could therefore be used in humans to repair simple nerve divisions.

2. Using the wrap in nerve repair is simple and is quicker and less expensive than microsurgical epineurial suture.
3. Nerve regeneration after nerve repair could be assessed in humans by measuring *maximum conduction velocity (CV_{max})* ($m\ s^{-1}$) and *transcutaneous stimulated jitter (TSJ)* (μs).

TABLE OF ABBREVIATIONS

Ach – acetylcholine

AP – action potential

BDNF – brain derived neurotrophic factor

CMAP – compound motor action potential

CNTF – ciliary neurotrophic factor

CNTRL – control group

CRG – controlled release glass

CV_{max} – maximum conduction velocity

DCV – distribution of conduction velocities

ECG – electrocardiogram

EDL – extensor digitorum longus

EEG – electroencephalography

EPNL – epineurial suture group

EPNRG – Edinburgh peripheral nerve research group

EPP – end plate potential

F_{min} – minimum F wave velocity

FCR – flexor carpi radialis

FCU – flexor carpi ulnaris

FDS – flexor digitorum superficialis

FTMG – freeze-thawed muscle graft

IPI – interpotential interval

LIF – leukaemia inhibitory factor

M lat – motor latency

MRC – medical research council

PCL – CRG-wrap + polycaprolactone glue group

PGA – polyglycolic acid

PHB – polyhydroxybutyrate

PN – peak isometric twitch tension

PT – time to peak twitch tension

PTFE – polytetrafluoroethylene

R ½ – time to R ½

SFEMG – single fibre electromyography

TSJ – transcutaneous stimulated jitter

TTI – time tension index

TTIG – Work done in contraction to time R ½

WRP/S – CRG-wrap + polyglactin suture group

TABLE OF CONTENTS

CHAPTER 1 — INTRODUCTION

'All muscles require to receive a nerve from the brain or from the spinal cord and this nerve is small to behold but no means slight in power'

Galen 2nd/3rd century AD (as cited by Bennett 1999)

HYPOTHESIS

That, using biodegradable glass-fibre wraps held in place with glue or non-microsurgical sutures, it is possible to repair divided peripheral nerves in a large animal and obtain an outcome comparable with that found after conventional microsurgical epineurial suture repair.

Peripheral nerves in humans can be over one metre long. Their cell bodies reside in the spinal cord or adjacent to the cord in the spinal roots. They conduct motor impulses, in a healthy human of middle age, at approximately 70 m s^{-1}.

When one considers that the surgeon's role in attempting to improve repair of a peripheral nerve trunk, is to aid the repair of individual cells, each with a highly specialized function in regards to its sensory or motor role, the task seems a formidable one. Even with the best outcome after peripheral nerve repair, with the exception of repairs in young children, the recovery of function in the muscles or sensory organs supplied by that nerve never reaches 100%.

NERVE ANATOMY, INJURY AND REPAIR

A brief history

It has taken centuries to reach our current understanding of the role of peripheral nerves in motor control and sensory function. Most developments have occurred during the past two centuries.

Aristotle in the 4th century B.C. believed that the heart was the central organ controlling locomotion of an animal and that peripheral sense organs passed 'their affections' through the blood stream. His theory was based on the principle that the action of an animal was dependant upon its perception by the following mechanism;

> 'If the region of the origin [the heart] is altered through perception and thus changes, the adjacent parts change with it and they too are extended or contracted, and in this way the movement of the animal necessarily follows'
>
> Aristotle, 4th century BC (as cited by Bennett 1999)

Bennett describes in his paper, 'The early history of the synapse' how the theories of Galen (2nd and 3rd centuries AD), Descartes (1596–1650), Borelli (1608–1679), Fontana (1733–1805), Galvani (1737–1798), Matteucci (1811–1865), du Bois-Reymond (1818–1896) and Helmholtz (1821–1894) have led to the understanding we now have of nerve anatomy, neuronal impulse generation, and impulse transmission (Bennett 1999).

Anatomy

Macroscopically, normal nerves are cable-like in structure, creamy-yellow in colour and have a soft but firm texture. Individual neurones are arranged in bundles called fascicles. A nerve may contain many fascicles, in which case it is termed polyfascicular; a few fascicles, in which case it is termed oligofascicular; or only one fascicle, termed monofascicular. The fascicles in polyfascicular nerves may be organized into groups within the structure of the nerve or remain alone. The structure of an oligofascicular peripheral nerve is shown in the sketch in figure 1 and fascicles from a section of median nerve are shown as seen using a light microscope in figure 2.

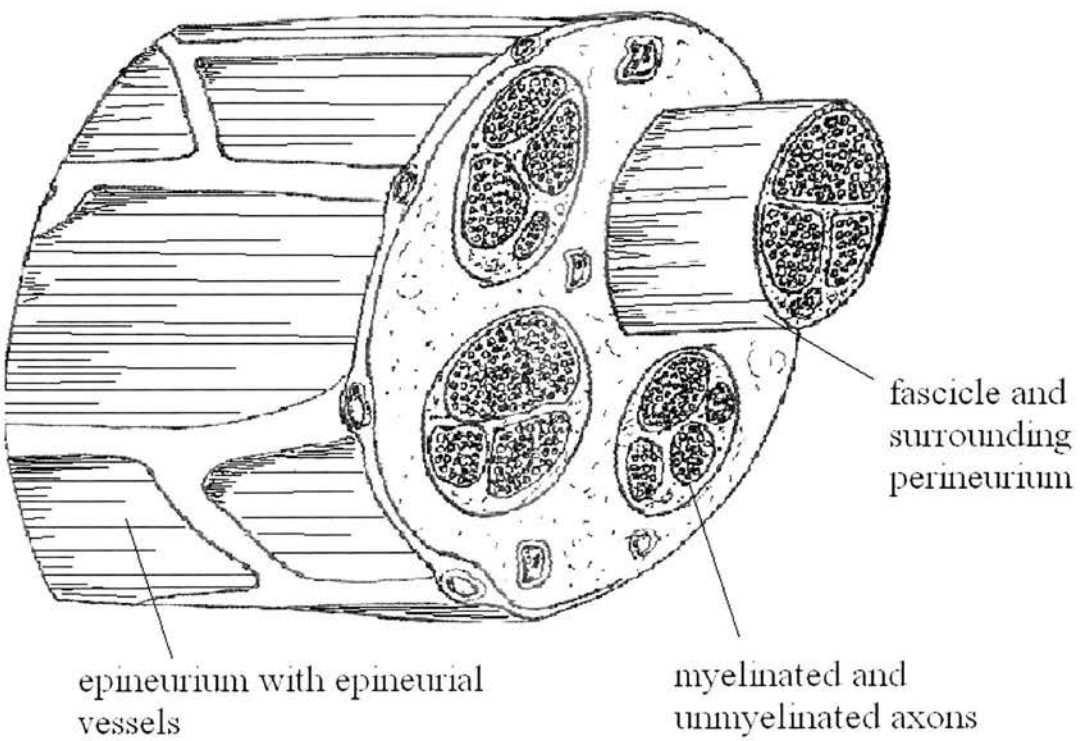

Figure 1

Diagram of an oligofascicular peripheral nerve

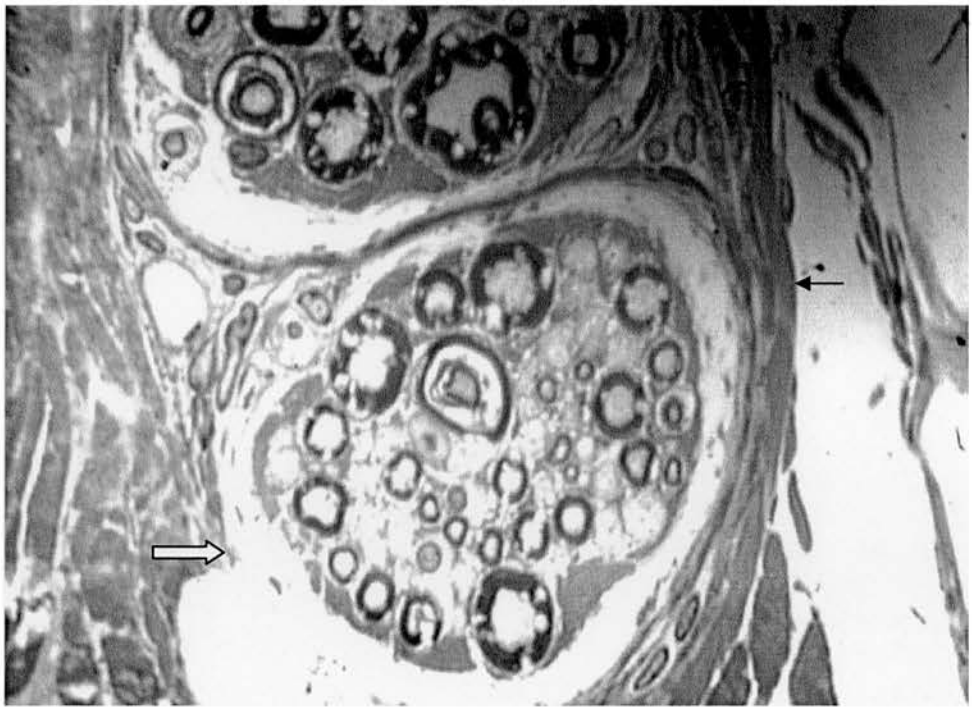

Figure 2

Light microscopy image (× 1000 magnification) of nerve fascicles in a median nerve of a sheep
(The perineurium is indicated by the light arrow and the epineurium by the dark, fine arrow)

Connective tissues

Three layers of connective tissue surround the nerve axons; the endoneurium, the perineurium and the epineurium. The endoneurium consists of longitudinally aligned collagen fibres and fibroblasts and surrounds the axon as shown in figure 3. In myelinated axons this is then surrounded by the myelin sheath and the Schwann cell.

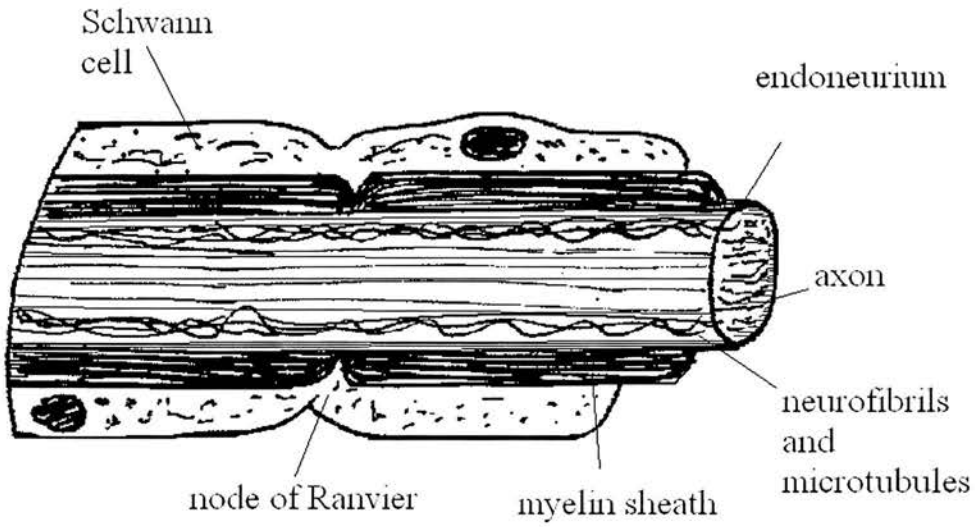

Figure 3

A myelinated neurone

The perineurium is composed of flattened cell processes linked by tight junctions, and alternating layers of collagen. It provides a barrier to diffusion thus maintaining a separate intrafascicular and extrafascicular environment (Lundborg 1988) and plays an important role in maintaining the internal environment of the endoneurial space. It is most likely the perineurium that allows nerves to maintain their activity when traversing a pyogenic focus (Kelly 2002).

The epineurium is composed of loose, strong connective tissue which surrounds the whole nerve and embeds, separates and protects the nerve fascicles. It is more abundant near joints. Its cells and collagen fibrils are aligned longitudinally (Birch, Bonney, & Wynn Parry 1998).

Blood supply

An intrinsic network of blood vessels supplies the nerve along its length. This is composed of an intrafascicular network (capillaries), a network supplying the perineurium itself, and vessels outwith the perineurium between the fascicles. A 'blood-nerve-barrier' exists between the endoneurial vessels and the surrounding intrafascicular tissues (Lundborg 1981). Extrinsic vessels supply the nerve from the surrounding vasculature at regular intervals along its length.

Lundborg found it possible to divide the extrinsic vessels over a length of 7 cm in a rabbit tibial nerve and still maintain an adequate blood supply at the distal end via the intrinsic system (Lundborg 1988). In the sheep therefore (a larger animal than the rabbit), it is likely that the intrinsic supply would be adequate when the extrinsic supply was removed over an even longer length than 7 cm.

Tensile properties

Peripheral nerves have a high tensile strength. Often it is the nerve which remains in continuity after avulsion injuries when other surrounding soft tissues are torn (Yoshimura et al 1989). This is attributed to the strength of the connective tissue surrounding the axons.

Neurones in peripheral nerves are arranged in a wave-like alignment called the 'spiral bands of Fontana' which give peripheral nerves a banded appearance in longitudinal section when examined using magnification. This banded appearance disappears as a nerve is stretched—the fibres are straightened (Birch et al 1998).

The neurones in the central nervous system (CNS) are surrounded mainly by oligodendrocytes, glial cells and astrocytes whereas in the peripheral nervous system they are surrounded by Schwann cells and fibroblasts. The Schwann cells and fibroblasts produce the endoneurium, perineurium, and epineurium. Nervous tissue of the spinal cord and the brain does not have the same tensile strength as peripheral nerves. Most of the tensile strength in peripheral nerves has been found to come from the perineurium (Yoshimura et al 1989) which requires the presence of fibroblasts for the production of the collagen found within it (Bunge 1981).

In the present study, the tensile strength of the repaired nerves seven months after surgery was tested to determine the force and the site in the nerve's length at which breakage occurred. This was important to determine that there was no weakness at the sites of repair because the effect that polycaprolactone glue, and indeed the other types of repair, would confer on the nerve and the formation of connective tissue was unknown.

Also, the force required to pull a repair apart immediately after its completion was considered to be an indication of how likely dehiscence was to occur *in vivo*. The ultimate force (force required to break the repair) was therefore measured for each type of repair used in this study.

Injury

The most common nerve injury treated in man is complete division of the nerve trunk (Seddon 1954; Sunderland 1978). This is most frequently caused accidentally by a sharp agent such as broken glass (59%) or a knife (19%), or related to a suicide attempt (19%) (Rosberg et al 2005). Nerve injury in the forearm is often associated with tendon injury and is most common in young males (Rosberg et al 2005). The median time reported for

sick-leave in a recent study from Sweden regarding patients with an injury to the median or ulnar nerve in the forearm, requiring repair was 210 days (Rosberg et al 2005). (No similar studies have been done in Britain. The Swedish welfare system probably provides more support than the equivalent system in the United Kingdom, therefore, the duration of sick-leave taken by a Briton may not be as long as the mean duration of sick-leave found in this Swedish study.) With such a long delay before patients return to work and with most injuries occurring in young males, expedient nerve repair and recovery is important for economic reasons.

Neuronal degeneration after injury

The process of degeneration and repair of neurones following injury is fundamental to this present study and will now be described in more detail.

Degeneration

In 1850, Augustus Waller described the distal degeneration of the neurone after neurotmesis, a process now known by the eponym 'Wallerian degeneration'. The degeneration process is different in the proximal and distal segments of the neurone. In both segments, there is an accumulation of organelles at the nodes of Ranvier and then a disappearance of the microtubules, swelling of the mitochondria and disappearance of the axon. In the proximal section of the nerve, the myelin sheath degenerates to the point of the most distal node of Ranvier. The rest of the proximal neurone retains its structure and a bulbous swelling develops at its distal end owing to the collection of transported proteins and axoplasm.

In the distal portion of the divided neurone, more extensive changes occur; the myelin sheath degenerates, there is an influx of fibroblasts, and a proliferation of the Schwann cells. Degradation of the myelin is carried out by the Schwann cells initially, and then by haematologically recruited macrophages. The Schwann cells elongate, proliferate, and arrange themselves into longitudinal bands within the residual basal lamina of the now degenerated axons. These Schwann cell lines are called the 'bands of Büngner'.

Regeneration

The proximal ends of the divided neurones produce multiple pioneering axon sprouts—hundreds per axon in the human (Kline et al 1981). These axons advance as the 'growth cone' toward the distal end of the divided nerve. Neurones have a mitogenic effect on Schwann cells and Schwann cells have a trophic effect on regenerating neurones (Bunge 1981). When pioneering axons reach the distal stump of a divided nerve, they grow along the bands of Büngner. Newly regenerated axons will only survive if they reinnervate their original axon type, e.g. a sensory nerve to a sensory organ (Aitken, Sharman, & Young 1947).

Classification of injury

Two classifications of nerve injury are used in clinical practice. The first is a three point classification constructed by Sir Herbert Seddon which is the most widely used in clinical practice (Seddon 1954). The second classification, based on histological anatomy, was constructed by Sir Sidney Sunderland (Sunderland 1978) and included two further grades.

Seddon's classification of nerve injuries is as follows:

Neurapraxia

Neurapraxia (equivalent to Sunderland Grade I) is derived from the Greek '*neuron*' meaning a 'nerve' or 'sinew', and '*apraxia*', meaning 'non-functional'.

Causes are most frequently; local compression, ischaemia, local blunt trauma, and toxins or disease causing local demyelination.

The changes in function are temporary and recover fully in days to weeks providing there has been removal of the insult causing the injury. The endoneurium, perineurium, epineurium and axons remain intact although, in severe cases, there may be thinning of the axon and localized mild myelin sheath degeneration. Clinically there is usually a small amount of residual function with a proportionally greater motor than sensory loss, and some residual autonomic function. Spontaneous return of function within days to months confirms the diagnosis. A classic clinical example of neurapraxia is 'Saturday night palsy'. In this, the radial nerve is compressed against the posterior surface of the shaft of the humerus due to the position in which the patient sleeps. Pain caused by compression of the nerve fails to wake the patient from his slumber and a conduction block ensues. This recovers usually over a period of six weeks, though may take several months.

Axonotmesis

Axonotmesis (equivalent to Sunderland Grade II) is derived from the Greek '*axono*' meaning 'shaft' or 'axon' and '*tmesis*' meaning 'cutting'.

Clinically there is loss of function of the nerve. Anatomically, there is division of the axons and their myelin sheaths but the endoneurium, perineurium and epineurium remain

intact. Recovery occurs spontaneously and to an excellent degree after removal of the insult as the neurones grow into their original endoneurial tubes, which have remained in continuity, and thus make appropriate distal connections. Wallerian degeneration occurs distal to the site of injury and so recovery takes longer than in neurapraxia.

Neurotmesis

Neurotmesis (equivalent to Sunderland grade V), is derived from the Greek, '*neuron*' meaning 'nerve' or 'tendon', and '*tmesis*' meaning 'cutting' .

Injury usually arises from incised wounds, lacerations, or missile wounds. Anatomically there is division of the whole nerve: the axon, myelin sheath, endoneurium, perineurium and epineurium. Loss of function of the nerve will not spontaneously resolve and the nerve must be repaired surgically. The recovery of function is never complete (except on occasion in young children). This is because the regenerating axons do not always find an endoneurial tube through which to proceed or make appropriate peripheral connections.

Sunderland described another two grades of injury; grades III and IV.

Grade III describes loss of axonal continuity and connective tissue disruption within the fascicle of injury but with intact extrafascicular tissue. In grade IV injuries, there is also damage to the extrafascicular connective tissue and perineurium but the epineurium remains intact. The intact epineurium in these two grades of injury disguises the severed axons beneath and it is possible to mistake a grade III or IV injury as an axonotmesis or neurapraxia thus leading to a falsely optimistic prognosis (Birch et al 1998; Seddon 1954; Sunderland 1978).

The macroscopic appearance of the damaged nerve depends on the exact mechanism of injury and the time at which the nerve is examined after the injury. A nerve which is visualized within approximately forty-eight hours after a compression or abrasion injury—for example, after a blunt injury causing a flap laceration—is hyperaemic, swollen and has a more 'fleshy' appearance proximal to the site of compression. If a nerve has been chronically compressed, it is pale and firm at the site, and distal to, the area of compression.

After sharp division of a peripheral nerve trunk the ends becomes swollen and the fascicles 'mushroom' from the proximal epineurium. If the two ends are not co-apted, they become swollen and develop into two fibrous bulbs of tissue; a *neuroma* at the proximal end (fibrous tissue containing immature and unaligned axons); and a *glioma* at the distal end (Schwann cell extensions encased in fibrous tissue) (Birch et al 1998). Figure 4 shows a neuroma and a glioma that formed after the dehiscence of an epineurial repair in the present study.

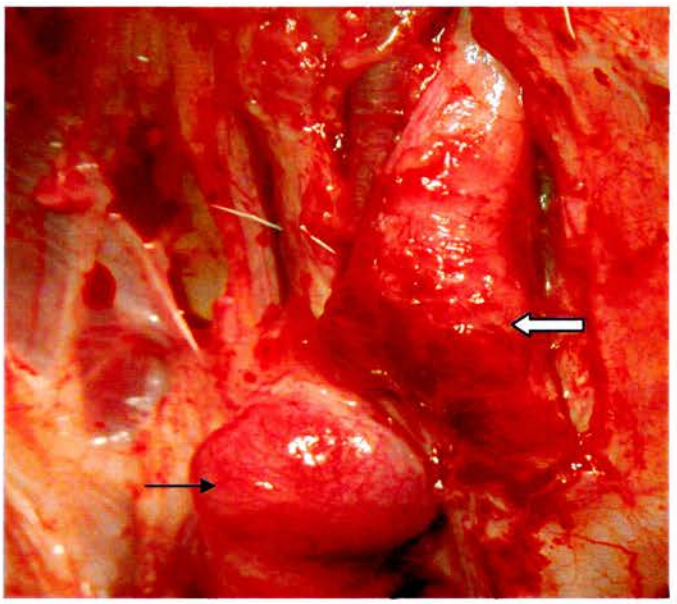

Figure 4

Neuroma (dark arrow) and glioma (light arrow) at the site of dehiscence of an epineurial nerve repair

After successful nerve repair and regeneration, the repaired nerve is usually wider in diameter and again has a softer, more 'fleshy' texture. Figure 5 shows a repaired median nerve from the present study adjacent to a normal, undamaged ulnar nerve.

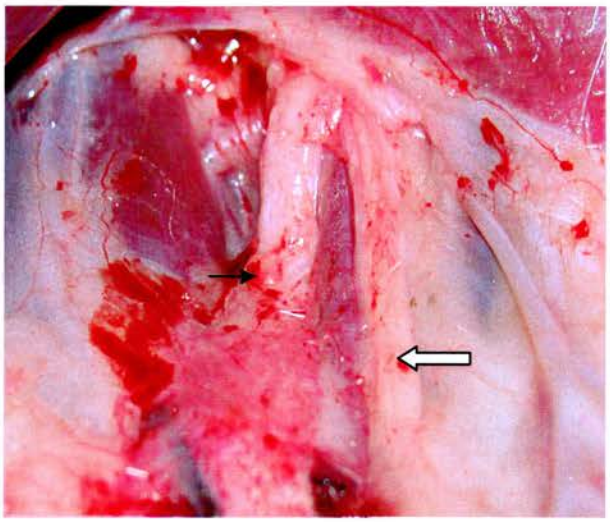

Figure 5

A repaired median nerve (black arrow) adjacent to an undamaged ulnar nerve (white arrow)

Nerve repair

Throughout the centuries

Galen (130–200 AD) was the first to distinguish nerves from tendons. William of Saliceto (1210–1277) and Rhazes (an Arabian physician from Baghdad) (865–925), carried out the earliest reported suturing of peripheral nerves (as cited by Dellon (2004)). Gabrielle Ferrara in 1608 described repairing a nerve using the split tendons of a tortoise (Dellon 2004). Sir James Paget in 1847 carried out primary suture on the divided ends of the median nerve in an 11 year old child with an apparently excellent result (Boyes 1976).

Until approximately 1600, there was a generally held view that nerve repair should not be attempted because it was thought that divided nerves were responsible for 'convulsions' and that nerves would not heal, no matter the course of treatment employed. Co-aptation of nerve stumps was attempted until 1850 by aligning the surrounding tissues (Millesi

1981). It was believed at that time that nerves would repair without bringing the divided ends together and that suture material would cause infection and be a barrier to spontaneous recovery, and that nerves which had been sutured may even cause worse pain (Dellon 2004).

Millesi (1981) cites Heuter as the first to recommend end-to-end nerve repair by using epineurial sutures in the 1870's.

The First and Second World Wars resulted in a great number of nerve injuries and comprehensive studies of war injuries were carried out in Britain and the United States of America. Soldiers sustaining nerve injuries during the Second World War in Britain were treated and followed up in five centres across the United Kingdom. The results of treatments and findings at these five centres were collated and published under the guidance of Sir Herbert Seddon to produce the Medical Research Council (MRC) special report series number 282 (Seddon 1954). Woodhall collated and published similar work in the U.S.A (Woodhall & Beebee 1956). Seddon concluded in the MRC report that secondary nerve suturing was more appropriate than primary nerve suturing but that both gave a poor outcome. These findings were not surprising given that the injuries being treated were usually surrounded by a great deal of soft tissue disruption, had a high infection risk and were often treated several days after the insult. Since then, studies carried out to determine the most appropriate timing for nerve repair have compared cleanly divided nerves in controlled laboratory situations and have shown that primary repair gives the best outcome for clean divisions of peripheral nerves in the middle or distal portions of limbs (Brunelli & Brunelli 1990; Grabb & Arbour 1968).

Current techniques

The type of injury being studied in the present study is that of a sterile, clean-cut nerve division without a gap: a tensionless repair. In clinical practice, the current standard method of repair of such an injury is by primary microsurgical epineurial suture. Millesi states that epineurial suturing gives better results when using a microscope (Millesi, Meissl, & Berger 1972). Tissue which initially bridges the gap between the divided nerve ends is peripheral to the epineurium and tends to push suture material into the epineurium and so decrease the available space for regenerating axons (Millesi et al 1972). Therefore, the finest suture material possible should be used and the minimum number of sutures placed to keep the nerve ends co-apted.

Millesi describes in detail the four steps to neurorrhaphy (Millesi 1981):

1. Preparation of the stumps, often involving resection or interfascicular dissection with separation of individual fascicles or groups of fascicles.
2. Approximation, with special reference to the gap between the stumps as well as the amount of tension present.
3. Co-aptation of the nerve stumps. Co-aptation describes the opposition of corresponding nerve ends with special attention to bringing divided fascicles into contact. A direct co-aptation (neurorrhaphy) can oppose stump to stump, fascicle to fascicle or fascicle group to fascicle group from the proximal and distal ends. An indirect co-aptation can be performed by interposing a nerve graft.
4. Maintenance of co-aptation, involving the use of, for example, stitches, glue, or a natural fibrin clot.

In current clinical practice, some surgeons insist on the use of an operating microscope, 10/0 polyamide sutures and the use of microsurgical instruments while other surgeons use only loupe magnification (× 2.5 or × 3.5 magnification) with 8/0 or 9/0 polyamide sutures despite Millesi's recommendations.

Fascicular repair

Whether epineurial or fascicular repair should be attempted depends on the proximity of the lesion and the arrangement of the fascicles within the nerve at the site of the lesion (Kline et al. 1981). The fascicles in proximal regions of a nerve are not organized within the fascicles according to their sensory or motor function and so fascicular repair at a proximal level is of no benefit. Distally, neurones are more likely to be arranged according to whether they supply a sensory or motor end-organ. If the nerve is oligofascicular; or polyfascicular with the fascicles grouped into discreet, recognizable bundles; it is more likely that fascicles can be matched and co-apted appropriately, and therefore a fascicular repair is more likely to be beneficial.

MacKinnon doubts the necessity of fascicular alignment in view of the neurobiological factors influencing nerve repair and suggests that increased manipulation of the nerve ends, required during microsurgical fascicular repair, could be detrimental (Mackinnon & Dellon 1988).

Tension at the site of repair

Tension across the site of repair between the nerve ends causes an increase in the collagen deposition between the nerve ends (Millesi, Meissl, & Berger 1972), a decrease in intraneural circulation and vascular anastomosis formation (Miyamoto & Tsuge 1981)

and stretching and kinking of the regional and nutrient vessels thus decreasing blood flow. (Stretching of the perineurium increases intrafascicular pressure and causes closure of the blood vessels piercing it obliquely, first the venules, then the arterioles and capillaries. Lundborg and Rydevik found than an 8% elongation of a rabbit sciatic-tibial nerve began to cause venular obstruction and stretching by 15% stopped all arteriolar flow (Lundborg 1988)). These factors result in a functionally poorer outcome.

Driscoll et al also demonstrated an independent effect of strain and tension on conduction velocity in rabbit tibial nerves (Driscoll, Glasby, & Lawson 2002): Despite a similar decrease in blood flow, there was a greater decrease in conduction velocity with a larger strain.

Options for repair to avoid tension at the suture site with direct co-aptation of the nerve ends or where there is a non-functioning proximal nerve trunk (e.g. in brachial plexus injury) are currently:

- Interposed cable or single nerve autograft
- Vascularized interposed nerve graft (pedicled or free)
- Entubulation (Dahlin, Anagnostaki, & Lundborg 2001; Lundborg et al. 2004)
- Denatured muscle graft (Norris et al. 1988; Pereira et al. 1991)
- Neurotization or nerve transfer; e.g. suturing the radial digital nerve of the ring finger (proximal stump) to the ulnar digital nerve of the ring finger (distal stump) (Brunelli 2004); or suturing an intercostal nerve (proximal stump) to the axillary nerve (distal stump) (Birch et al 1998).

Although the model of injury being studied in the present study is a tensionless epineurial repair, the CRG-wrap being tested may prove beneficial in some of the above techniques in the future.

Timing

Early work by Holmes and Young (1942) demonstrated an increase in the rate of the axonal regeneration after delayed suturing of the tibial and peroneal nerves. Brunelli and Brunelli (1990) demonstrated that amino acid production and the fibroblast activity required to form connections between the stumps is best at 20–40 days after the initial injury. However, comparison of primary and secondary repair of bluntly and sharply divided median and ulnar nerves in rhesus macaque monkeys demonstrated a better return of motor function after primary repair (Grabb & Arbour 1968).

Many factors conspire against carrying out delayed repair in clinical practice. These are:

- Requirement for a second operation
- Disturbance of surrounding tissues and less ability to easily identify nerves especially in hand injuries
- Longer recovery time
- Longer hospital stay and expense
- Limited amount of amino acids required in distal lesions
- Possibility of two scars e.g. on fingers, contributing to a poor result

(Brunelli & Brunelli 1990)

With most traumatic nerve injuries occurring in young men, return of function as quickly as possible is important (Rosberg et al 2005). With a simple peripheral nerve division where the wound can be adequately cleaned, primary nerve repair, where possible, is now recognized as optimal for nerve regeneration (Grabb 1968).

When a nerve is not cleanly divided, e.g. a lacerated nerve, it is difficult to decide on the length of damaged nerve that should be resected from the stumps. This is one weakness of primary nerve repair: if this length is underestimated, it will be difficult for pioneering axon sprouts to traverse the damaged tissue that remains (Millesi 1981) but if a large length of nerve is removed, there will be increased tension at the site of repair and it may even be necessary to insert a nerve graft. Where there has been a large amount of soft tissue damage or loss, as is often the case in battlefield injuries, a secondary nerve repair is preferred and is carried out once the surrounding tissues are known to be viable and have been repaired adequately.

Neurotropism, neurotrophism and contact guidance

A neurotropic substance grows towards or has an affinity for neural tissue. Neurotrophism is the ability of one tissue or cell to aid in the survival of neural tissue. Contact guidance refers to the ability of the surrounding tissue to determine the direction of axonal growth.

All these factors contribute to successful and expedient axonal sprouting and growth. The ability of a neurone to regenerate depends both on its intrinsic properties and its environment. Sensory neurones show an ability to regenerate within the peripheral nervous system where they are surrounded by Schwann cells and fibroblasts but not within the CNS where they are surrounded by ependymal cells, astrocytes and oligodendrocytes. However, Ramon y Cajal demonstrated that motor neurones from the ventral horn can form recurrent branches and regenerate for a certain length into the spinal cord (as quoted by Lasek, McQuarrie, & Wujek 1981). Lundborg demonstrated selective growth of the proximal end of a divided nerve towards its distal stump within a silicone tube. It was shown that the neurones from the proximal nerve stump would grow in a curve toward a distal nerve stump rather than in a straight direction towards a tendon or a muscle. This phenomenon was attributed to neurotropic factors directing axonal regeneration (Lundborg 1988). Brunelli demonstrated that when the proximal ends of the sural and tibial nerves of a rabbit were inserted into one end of a vein graft and the distal ends randomly sutured to the other end of the graft, after a sufficient time for nerve recovery to take place, stimulation of the proximal tibial nerve produced a normal electromyographic response in the gastrocnemius muscle. Nerve sections taken from within the vein graft after nerve regeneration showed a mixture of sensory and motor

fibres. They concluded that regenerating axons were able to find their way to appropriate distal targets. The postulated reason for this was that Schwann cells may exhibit different surface antigens according to their function or that laminin secreted by Schwann cells might have a slightly different biochemical composition depending on function (Brunelli & Brunelli 1990). It is possible however that this phenomenon could have occurred simply due to growth of pioneering neurones in a random manner.

Contact guidance by the negative charges on laminin, fibronectin and collagen molecules was demonstrated by Letorneau (as cited by Dellon 2004). Much experimental work has been carried out to incorporate these substances within conduits in the hope of increasing the length of gap across which a nerve will regenerate (Archibald et al 1995; Chen et al 2000; Haber et al 1988; Itoh et al 2003b; Matsumoto et al 2000a; Matsumoto et al 2000b; Mosahebi et al 2002; Rodriguez et al 2000; Yu & Bellamkonda 2003; Zhao et al 1997). Cajal believed that Schwann cells provided most of the trophic support for the growth of peripheral axons. Schwann cells produce neurotrophic factors such as nerve growth factor, NEFR and peptides with molecular weights of 225K, 210K, 90K, 66K and 50K which provide necessary nutritional support for nerve cells and their processes (Birch et al 1998; Bryan, Wang, & Chakalis-Haley 1996; Bunge 1981).

Bridging the gap

Many nerve injuries are unfortunately not clean divisions and often some amount of trimming of the nerve ends is required in primary or secondary repair. In brachial plexus surgery, in primary or secondary repairs, this is often the case. Usually several nerve gaps are present in these patients. Currently these gaps are repaired by cable autografting or neurotization. If sufficient donor nerves are not available, certain nerves may be left

unrepaired. Currently the greatest problem for interested parties in peripheral nerve surgery is how to most appropriately bridge nerve gaps of different lengths and to find a successful method of bridging a gap without using an autologous nerve graft.

Nerve grafts

Balance and Duel had the earliest success in interposed nerve grafting when using autografts within the facial canal (quoted by Holmes & Young 1942). Early work on nerve autografts was carried out by Seddon in 1947 and continued in 1967. Unfortunately he had poor results owing to the long length of the grafts that were used and because many of the patients initially had difficult, scarred wounds which subsequently became infected. Millesi carried out work on the value of nerve grafts to avoid tension at the repair site and now the microsurgical placing of an interposed nerve autograft is the most commonly used technique in peripheral nerve surgery to bridge a gap between nerve stumps (Dellon 2004).

Interfascicular grafts

Millesi et al carried out a series of interfascicular median nerve autograft repairs in which they used only one 10/0 suture between the graft fascicle and the fascicles at the proximal and distal ends of the divided nerve. Their results showed good recovery of function in many patients, even when the injury had occurred up to thirty-six months prior to the graft placement (Millesi et al 1972).

Donor nerves

The nerves harvested for use as autografts are most commonly the sural nerve, and the lateral and medial cutaneous nerves of the forearm. Consequences of this procedure

include; scars at the sites of harvesting, painful neuromas on the nerve stumps from where the graft has been resected, and anaesthesia in the area supplied by the resected nerve. Weber et al quote rates found by other authors of 44% and 6.1% of patients complaining of loss of sensibility over the lateral foot and painful neuromas respectively after sural nerve harvesting (Weber et al. 2000).

Denatured muscle grafts

The basement membrane of freeze-thawed muscle contains laminin and fibronectin. The negative charges on these molecules guide the regenerating axons (Glasby et al. 1986a). Extensive work has been carried out by Glasby and co-workers on the use of autologous denaturated muscle grafts as an alternative to autologous nerve grafting (Fullarton, Glasby, & Lawson 1998; Gattuso et al. 1989; Glasby et al. 1995; Glasby, Carrick, & Hems 1992a; Glasby, Evans, & Huang 1989; Glasby, Fullerton, & Lawson 1998; Glasby, Hems, & Pell 1992b; Glasby, Mountain, & Murray 1993; Hems & Glasby 1992b; Hems & Glasby 1993; Lawson & Glasby 1998; Lawson & Glasby 1995; Lenihan, Carter, & Glasby 1998; Mountain et al. 1993; Pereira et al 1991).

To prepare the denatured muscle autograft, a block of muscle is excised that is twice the size of the nerve defect (50% shrinkage occurs during the processing). The muscle is wrapped in silver foil and then submerged in liquid nitrogen (-196 °C) until thermal equilibrium is reached. It is then slowly thawed by transfer to sterile distilled water where the hypo-osmolar environment causes fracture and destruction of the cells leaving the basement membrane network intact. The graft is joined to the nerve stumps either by suture or fibrin glue (Glasby et al. 1990; Glasby et al 1992a; Glasby et al 1992b).

Denatured muscle grafts have successfully been used to aid in the repair of digital nerve defects between 15–25 mm in length (Norris et al 1988) and have been shown to successfully bridge 3 cm gaps in the ulnar nerve in marmosets (*Callithrix jacchus*) (Glasby et al. 1986b). Gaps of 4 cm were repaired giving an outcome comparable to that obtained with an epineurial suture repair in rabbit sciatic nerves. However, attempts to use similar grafts in the repair of 5 and 10 cm gaps in rabbit sciatic nerves were not successful (Hems & Glasby 1993).

Defects of between 25–60 mm in three median nerves and nine posterior tibial nerves gave promising results when bridged by denatured muscle autografts in leprosy patients (Pereira et al 1991).

Sandwich grafts

Whitworth et al demonstrated regeneration of neurones to be comparable in freeze thawed muscle and autologous nerve 'sandwich grafts' compared with autologous nerve grafts over a gap of 5 cm. (The sandwich grafts consisted of FTMG lengths of 1cm adjacent to 2–3 mm lengths of fresh autologous nerve followed by a further 1 cm length of muscle and so on to bridge a gap of 5 cm). The growth of neurones was much less through the 5 cm FTMG (Whitworth et al. 1995b). The use of autologous nerve grafts in this way however still requires the harvesting of donor nerves.

Other techniques to enhance neuronal regeneration

Other substances used as nerve autograft substitutes include; 'pseudo-nerve' (longitudinally organized Schwann cell columns) (Zhao et al 1997), fibronectin mats

(Whitworth et al. 1995a) and other methods of Schwann cell transplantations (Mosahebi et al. 2002b; Rodriguez et al 2000).

Nerve growth factor and acid and basic fibroblast growth factors have been shown to enhance nerve regeneration in conduits (quoted from Wang and Lineweaver 2003). A solution which contained ciliary neurotrophic factor (CNTF) and brain-derived neurotrophic factor (BDNF) was found to increase the number of fibres in the distal regenerating portion of rat facial nerves when infused constantly around the site of repair for fourteen days: CNTF and BDNF were not found however to affect facial nerve regeneration in sheep when infused around the site of repair within an inert conduit. Kelly concluded that in the large animal, there was no evidence to support that the presence of these neurotrophic factors at the site of nerve repairs improved the outcome (Kelly 2002). Terris et al compared nerve autografts, collagen conduits filled with collagen gel, and collagen conduits filled with brain derived neurotrophic factor suspended in a collagen gel. They did not find any increase in the regeneration potential when using the BDNF in the gel. They did however find as good an outcome of repair with both conduit types as with the nerve autograft as assessed by axon number, mean axonal diameter and facial movements (Terris et al 2001).

McKay Hart et al (2003) reported on the effect of the addition of leukaemia inhibitory factor (LIF) to nerve repairs delayed by two and four months. Using syngeneic nerve grafts or poly-3-hydroxybutyrate (PHB) conduits, 1 cm gaps in the sciatic nerves of Sprague-Dawley rats were repaired. LIF was added to the hydrogel in two PHB conduit groups (one group repaired at two months and the other at four months after nerve division). At six weeks after repair, results of histochemical staining showed an increase

in the longitudinal nerve fibre growth through the conduits with the addition of LIF but not a significant increase in the percentage area of immunofluorescent staining for Schwann cells or nerve fibres in the groups with the added LIF. The percentage area of staining of nerve fibres and longitudinal growth of nerve fibres through the conduits was always significantly lower than across the syngeneic nerve grafts.

Schwann cells

The importance of the presence of Schwann cells for axonal regeneration has been recognized for decades. After neurotmesis, Schwann cells proliferate in the peripheral nerve stump and elongate forming tubes filled with Schwann cell protoplasm (Holmes & Young 1942; Young, Holmes, & Sanders 1940). These Schwann cell tubes or 'bands of Büngner' are the pathways down which the pioneering axons from the proximal stump proceed, between the Schwann cell cytoplasm and the cell wall (Holmes & Young 1942). The Schwann cells attract axons from the proximal stump (Holmes & Young 1942; Young, Holmes, & Sanders 1940) by the production of neurotrophic factors (Rodriguez et al 2000; Shen et al 2001).

Mosahebi et al demonstrated that allogeneic and syngeneic Schwann cells could increase the rate of axonal regeneration at six weeks after they were implanted in a polyhydroxybutyrate (PHB) conduit to repair a 10 mm gap in the sciatic nerves of rats. They demonstrated that the immediate availability of allogeneic Schwann cells may compensate for the poorer outcome obtained when compared to the outcome when autogeneic Schwann cells were used (Mosahebi et al 2002).

Rodriguez et al compared the use of autologous Schwann cells suspended in Matrigel within resorbable polyglycolic acid conduits at a concentration of 150 000 Schwann cells

per tube across a 6 mm gap in the sciatic nerve of rats. They found that nocioceptive, motor, sensory, and sweat gland function four months post-operatively was comparable after repair with this type of conduit to nerve autografts. They also demonstrated in this study that autogeneic Schwann cells survived longer than syngeneic cells.

Whitworth et al (1995b) compared freeze-thawed muscle and nerve sandwich-autografts with nerve autografts and FTMGs to bridge a 5 cm gap in rabbit sciatic nerves. They demonstrated that, 120 days after repair, Schwann cells were found along the whole length of the repaired segments of nerves in the sandwich graft and nerve autograft groups, but that Schwann cells had migrated poorly into the freeze thawed muscle grafts and that this group had a worse outcome.

Matrigel

Matrigel (a commercially available product, Colaborative Research) contains 60% laminin, 30% type IV collagen, 3% heparin sulphate proteoglycan, and 1% entactin and has been shown to promote the growth of neurones in culture and *in vivo* centrally (Haber et al 1988) and peripherally. Shen (2001) successfully produced a biocompatible and biodegradable framework using polyglactone and polydioxone filaments coated with Matrigel and used cultured newborn or adult Schwann cells within collagen tubes to repair 1.5 cm defects in rat sciatic nerves.

Conduits

Gluck (1880) and Vanlair (1882) used decalcified bone as conduits in attempted nerve repair (as quoted by Gilchrist et al 1998). Other early work used cargile membrane (pig bladder), dura, feather quill, trachea, and parchment (as described by Dellon 2004).

Buengner was the first to use arteries by repairing the sciatic nerve of a dog with a human brachial artery in 1891 (quoted from Strauch et al 1996). Fascia was used by Kirk and Lewis in 1905 and amnion by Bassett et al in 1959 (quoted from Wang and Lineaweaver 2003). The use of veins as conduits has been studied by many authors (Di Benedetto et al 1998; Brunelli et al 1993; Kelleher et al 2001; Strauch et al 1996). Veins are currently used as conduits by some peripheral nerve surgeons in the United Kingdom in the repair of nerves where a small gap is present. Gelatin conduits were used by Lotheissen in 1901 (Robinson 1989) and genipin-cross-linked gelatin more recently by Chen et al (2005).

Braun (1966) demonstrated that regeneration through a collagen tube which could be placed without a microscope gave as good functional results as epineurial suture with the use of a microscope. More recently, Archibald and Krarup demonstrated an equivocal outcome between autologous nerve grafting and collagen conduits when used to repair a 5 mm gap in the median nerve of primates (Archibald et al 1995; Krarup, Archibald, & Madison 2002). Polytetrafluoroethylene (ePTFE) (Miloro et al. 2002; Stanec & Stanec 1998a; Stanec & Stanec 1998b), polyglycolic acid (Dellon & Mackinnon 1988), polyglycolic acid-collagen (Nakamura et al. 2004) and poly-L-lactide (Seckel et al 1984) and polyhydroxybutyrate (PHB) (Huang et al. 1997) represent some of the more recent advances in the production of absorbable synthetic polymers being used as conduits. Lundborg et al studied the use of silicone conduits in comparison with standard epineurial repair in a prospective randomized study in the repair of ulnar and median nerves in the forearm. After a 5 year follow-up they concluded that there was little difference in outcome except that cold intolerance was reduced in the tubular repairs.

However, eight of the seventeen (26.7%) silicon tubes inserted required removal by a second operation because of local discomfort.

The benefits of repairing nerves with conduits in comparison to an epineurial repair are:

- No tension at the repair site
- Reduction in the time required for the operative repair
- No requirement for microsurgical equipment

The drawbacks are the extra cost and organization of having a conduit of the appropriate size available.

The benefits of using a conduit to repair nerves with a gap present that would otherwise require the placement of an interposed nerve autograft are:

- No morbidity from harvesting a graft
- No limit to the number of repairs that could be done. For example in lesions of the brachial plexus there may be one, two or even more nerve defects present that require to be repaired. It would be difficult, and at times not possible, to harvest sufficient nerve autograft to repair all the gaps present.
- Less theatre time would be required to complete the operation and there would be no need for microsurgical equipment or technique. (Rosberg in his evaluation of the costs of median and ulnar nerve damage in the forearm quotes a median operating time of 141 minutes and a median operating cost of € 2919 (£2004.00)—approximately € 20.7 (£14.20) per minute (Rosberg et al 2005).

The drawbacks in the use of a conduit include the finite gap length that can be bridged, the possible discomfort or inflammation caused by a foreign body, and the cost of purchasing the conduit if a synthetic product is used.

Repair across a gap using conduits

A technique which could allow even the bridging of gaps using conduits without the requirement of a nerve autograft would be of great benefit. In the following section recent work done using various conduits across nerve gaps is presented.

Animal studies

Vein grafts

Strauch (1996) demonstrated good axonal regeneration in rabbit sciatic nerves through vein grafts across a gap of 3 cm. Failure of regeneration with increasing gap lengths was related to fibrosis, lack of viable Schwann cells and collapse of the graft.

Smahel and Jentsch demonstrated in 1986 failure of the femoral nerve in adult male rats to regenerate across a 14 mm gap using a vein conduit, but showed successful regeneration when a 2 mm segment of femoral nerve autograft was placed in the middle of the conduit (Smahel & Jentsch 1986).

Biodegradable conduits

Controlled release glass

Biodegradable glass tubes were used by Gilchrist et al to repair divided facial nerves in sheep (n = 5). Ten months after the repairs, the conduction velocity in the five repaired nerves was compared to the conduction velocity in five normal nerves. The peak conduction velocity and the range of conduction velocities was lower in the repaired nerves but minimum conduction velocity in the repaired nerves had recovered to a level that was not significantly different from normal nerves ($p = 0.96$). Fibre diameter and

axon diameter were reduced in the repair group but this was not significantly different from the normal nerves ($p = 0.34$ and 0.96 respectively) (Gilchrist et al 1998). Lenihan repaired a gap of 1 cm in rabbit peroneal nerves using empty biodegradable glass tubes, biodegradable glass tubes filled with diced autologous denatured muscle and normal autologous denatured muscle grafts. There was a lower mean fibre and axon diameter in the nerves repaired with the glass tubes alone when compared with the other two repair groups and normal nerves. There was no significant difference in the maximum conduction velocities between the three groups (Lenihan et al. 1998; Lenihan 2000).

Polyglycolic acid

Axonal regeneration using a polyglycolic acid tube across a 15 mm gap in beagle dogs demonstrated faster regeneration of large myelinated fibres in comparison to a nerve autograft (Nakamura et al 2004).

Dellon and MacKinnon (1998) demonstrated comparable regeneration of a nerve using polyglycolic acid conduits, mesh tubes or sciatic nerve autograft across a 3 cm gap in the ulnar nerve of the forearm in *Macca cynomolgus* monkeys. They stated that 'bridging a gap of 2–3 cm therefore would appear reasonable without a nerve graft'.

Collagen

Kim et al (1993) demonstrated functional recovery through non-permeable, semi-permeable and macropore collagen conduits. Archibald et al (1995) demonstrated similar outcomes across a 5 mm gap using a nerve autograft, collagen conduit and microsurgical epineurial repair in *Macaca fascicularis* monkeys.

Axonal regeneration has been demonstrated across a 10 mm gap in peripheral nerves in rats using genepin-cross-linked gelatine conduits (Chen et al. 2005), and poly-3-hydroxybutyrate (Young, Wiberg, & Terenghi 2002).

Adjuvant strategies

Strategies used to keep collapsible conduits such as vein, mesothelial chambers and intestinal sleeves open included metal spirals, collagen coating and metal sleeve insertion (Wang et al. 1993), insertion of nerve segments (Smahel & Jentsch 1986) and injection of saline (Wang, Cetrulo, & Seckel 1999).

'Stepping stone' grafts using nerve autografts and silicone tubing (Maeda et al. 1993) and vein conduits with an inset nerve segment (Smahel & Jentsch 1986) have shown comparable outcome to nerve autografts over longer lengths.

Clinical studies

Non-biodegradable

Polytetrafluoroethylene

Stanec and Stanec used a polytetrafluoroethylene (PTFE) conduit to bridge a human ulnar nerve in the distal forearm with a 2.9 cm gap. He reported that there was excellent recovery of motor and sensory function (Stanec & Stanec 1998b).

Stanec and Stanec successfully bridged a nerve gap of 5 cm using an ePTFE conduit. All the patients in their study had a forearm median or ulnar nerve injury. The patients were separated into two groups. The first group of patients (n = 28) had a nerve gap of 1.5– 4.0 cm. In this group, 78% regained useful motor activity. The second group of patients (n = 15), had a nerve gap of 4.1– 6.0 cm. Only 13% of patients in this group regained useful motor activity. One patient had to have the tube removed at a later date because they were experiencing discomfort at the site of injury (Stanec & Stanec 1998a).

Silicone

Lundborg has reported extensively on the use of silicone conduits in the repair of peripheral nerves. There was no significant difference in the motor and sensory recovery gained by the two groups except in respect to cold intolerance. The group who had undergone silicon tube repair suffered less discomfort with a cold stimulus.

Significantly however, 8 out of 17 patients had local discomfort around the site of the tube and required a second surgical procedure to have the tube removed (Lundborg et al 2004). This is an unacceptably high complication rate for a clinical technique. Lundborg et al concluded that ideally conduits should be completely biodegradable and

biocompatable and not cause any local inflammation or discomfort (Lundborg et al 2004).

Biodegradable conduits

Polyglycolic acid

Weber et al (2005) reported on a multi-centre randomized prospective evaluation of polyglycolic acid (PGA) conduits compared with epineurial suture and autologous nerve grafts in the repair of digital nerves. The outcome was assessed by measuring moving and static two-point discrimination. There was a better outcome when defects of up to 4 mm were repaired with the PGA conduit than when repaired by standard epineurial repair. Repair of gaps over 8 mm long with the PGA conduit had a better outcome than gaps over 8 mm long repaired with a nerve autograft. There was no statistically significant difference in the outcome when standard epineurial repair was compared with repair using a PGA conduit to bridge gaps of 5–7 mm. Excellent results were obtained in 91% of the PGA group overall.

MacKinnon and Dellon (1988) used a technique of making PGA mesh tubes by heat-sealing the edges for use in digital nerve repair. The tubes had a tendency to kink and so their use was replaced by ready-made corrugated PGA tubes with a smooth internal surface. They report on results from fifteen patients with a 3 cm gap in the digital nerves and compare outcomes with a previous series of nerve autograft repairs. The results were similar between the two groups. They recognize however that this was neither a randomized nor blinded study and that the study using PGA conduits and the study using nerve autografts took place at different times.

In their recent review of the use of conduits for nerve repair, Wang and Lineaweaver (2003) concluded that a gap of 3 cm seems to be the conservative limit of possible nerve repair using a conduit.

Implantation techniques

Ideally the method used to attach the nerve ends within a conduit or wrap should be secure, quick, in-expensive and simple.

Archibald et al (1995) used a microsurgical technique to attach collagen tubes to the median nerves of primates as did Chen et al (2005). Starrit (2004) used 6/0 polyglycolic acid sutures to secure the Corglaes wrap to the median nerve of sheep and Dellon and MacKinnon (1988) used 6/0 polyamide sutures to secure their polyglycolic acid tubes to the ulnar nerves in monkeys. Lundborg et al (2004) used 6/0 or 9/0 polyamide monofilament sutures to secure silicon tubes to the ulnar and median nerves of humans. None of the listed researchers reported any difficulties in the techniques used.

An ideal method of fixing the wrap to ensure no axonal damage by trauma to the axons by a needle is to use glue. In the present study, the use of fibrin glue (Tisseel, Baxter Healthcare Ltd., Bioscience, Wallingford Road, Berkshire, U.K.) and polycaprolactone glue (Giltech Ltd, Ayr, Scotland) were compared.

Fibrin glue

Glue based on plasma substances and fibrin has been used since 1940 (Holmes & Young 1942; Young, Holmes, & Sanders 1940). Tisseel glue alone is used to secure interposed nerve autografts during brachial plexus repair by some authors (Birch et al 1998) and it is used by others in conjunction with microsurgical epineurial repair (personal

communication with Mr T.E.J. Hems). Tisseel powder and thrombin powder are made from human plasma originating in plasma collected form licensed plasmaphoresis centres. There is a possibility of Parvovirus B19 transmission and this should be considered especially in immunodeficient individuals and pregnant women (Baxter, Summary of Product Characteristics). Tisseel is licensed for use in humans but is relatively expensive (approximately £70 per vial) and requires a water bath (37 °C) or specific equipment (the 'Fibrinotherm', as shown in figure 6) to prepare it for use.

Figure 6

The Fibrinotherm

Polycaprolactone glue

Polycaprolactone glue (Giltech Ltd, 12 North Harbour Estate, Ayr, Scotland) consists of polycaprolactone (a biodegradable plastic) dissolved in chloroform solvent. It is provided sterile and ready to use in a vial from which it can be easily drawn up into a syringe and applied to the desired site. It sets in a couple of seconds and forms a good bond between the nerve surface and the wrap, and the two surfaces of the wrap. It was decided to evaluate its use in this present study as it would be an inexpensive, easy-to-use alternative to Tisseel.

6/0 Polyglactin macrosutures

The third method used in the present study was 6/0 polyglactin (Vicryl, Ethicon, Edinburgh, Scotland, U.K.) macrosutures. Four were used to secure the wrap in a cylindrical fashion around the opposed nerve stumps. The benefits of using this technique were; the suture is biodegradable, there was no requirement for microsurgical equipment and it takes less time than epineurial repair.

Potential uses for a conduit or wrap

The potential uses for an entubulation technique, especially if a wrap were being used, are outlined in figure 7:

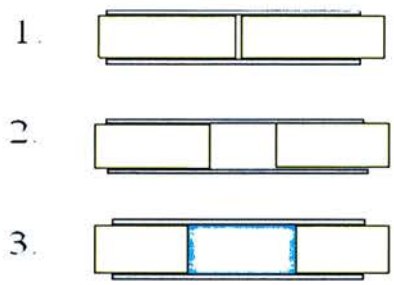

Figure 7

Potential uses of nerve conduit/wrap include:

1. Placement around the nerve stumps with virtually no gap between the nerve stumps (as in the present study)
2. Placement around the nerve stumps with a small gap (1–10 cm) between the stumps
3. Placement around the nerve stumps (when a larger gap of 10–30 mm is present) with an interposed length of autologous nerve, autologous denatured muscle graft, or other nerve graft substitute

Previous researchers have commented on the difficulty of inserting the nerve stumps into a conduit—some amount of trauma is caused to the nerve ends. One techniques used was to insert a suture through the end of the nerve stump, thread the suture through the conduit, and then use the suture to pull the stump into the conduit. With a wrap, the stump ends and any interposed graft material could simply be laid on the open wrap before it was folded to form a conduit. This technique would be much quicker and less likely to damage the nerve stumps.

CONTROLLED RELEASE GLASS (CRG)

History and development

A glass is a non-crystalline arrangement of molecules that form a solid. Metal ions are usually arranged in a crystalline form but if melted and then cooled under certain conditions; their molecular structure can be altered such that they do not form a crystalline structure.

'Corglaes' (Giltech Limited, Ayr, Scotland) is a calcium phosphate based biodegradable and biocompatible glass manufactured by Giltech Ltd., a biomedical research company in the West of Scotland. Its basic formula is Na_2O-(Ca,Mg)-O-P_2O_5 (Gilchrist et al 1998). The glass was initially developed to provide a means of introducing antimicrobial substances directly into the bladder along with catheters to prevent infection from indwelling catheters (personal correspondence with D. Healy, Giltech Ltd). The glass is produced by the fusion of a mixture of oxides of calcium, sodium and phosphorus. The glass dissolves in a simple first order fashion (from the outside inwards with no leaching) and its dissolution rate can be altered almost infinitely by altering the group I: group II ratio. Giltech has manufactured glasses with solution rates between 0.0008 and 2500 mg cm^{-2} hr^{-1}. Upon its dissolution, all compounds are released as ions in their active form. It is a versatile product and can be incorporated into most production processes. Most cationic elements, e.g. zinc, boron, copper, can be incorporated into the glass compound and can provide specific functions e.g. the addition of silver ions provide an antimicrobial effect. The company has been investigating the possible use of the glass in the field of temporary implantable stents, bone and soft tissue augmentation, tissue engineering

scaffolds e.g. for providing a framework on which to grow undifferentiated mesenchymal stem cells, investment casting, surface modifier, antimicrobial delivery, antistatic additives, trace element release, anti-corrosives, optics (personal communication with David Healy, Giltech Ltd. Ayr) and anti-adhesives in tendon repair (personal communication with Ms Elaine Davidson).

Manufacture of the wrap

The appropriate group I, group II and phosphorus compounds (and additional transition elements if required) are blended in a batch mixer. The mix is measured into suitable crucibles and placed in a furnace at about 1100 °C. After a period of time, the components fuse to form a homogenous glass melt. When the reaction is complete, the melt is poured onto a stainless steel tray to cool. As the glass cools it breaks up into small chunks. This is the glass cullet.

To produce 'CRG-wrap', the glass is next processed into fibres. The glass cullet is re-melted in a small batch furnace. Once molten, the glass is transferred to a special fibre furnace containing a small tank to hold the glass. At the bottom of the tank is a perforated plate called a 'bushing'. The furnace is designed to maintain a critical temperature gradient between the melt and the bushing. This prevents the glass from crystallising in the tank whilst maintaining sufficient viscosity for the fibres to be drawn from the bushing. The viscous glass exits the holes in the bushing and the molten glass beads drop down to a rapidly rotating drum trailing glass fibre behind them. The fibres are taken up by the drum and the fibre is then pulled at high speed through the bushing in a controlled manner. The process is outlined in figure 8.

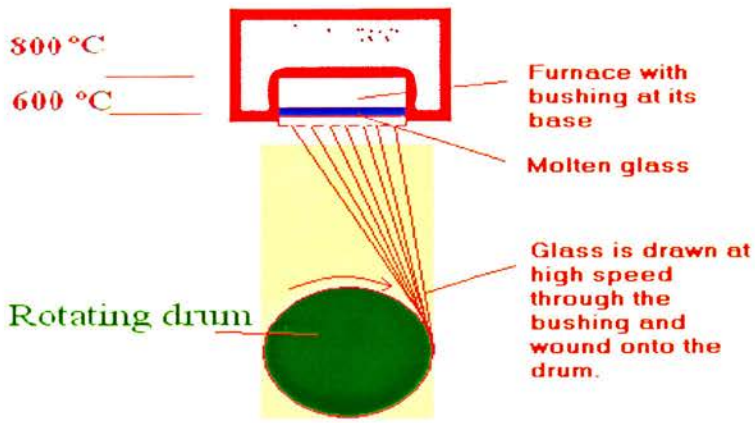

Figure 8

Diagram of furnace set up to form Corglaes fibres

Once the run is complete, the fibres are cut off the drum to produce a belt or band of linear fibres whose length is equal to the drum circumference

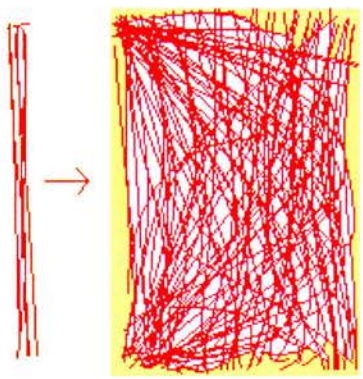

Figure 9

Diagram of fibres and mesh formed after teasing out horizontally

These belts of fibres are then teased out perpendicular to the direction of the fibres to produce a non woven mesh as shown in figure 9. This mesh is cut into sheets of approximately A4 size. The non woven sheets are then bonded using a biodegradable polymer, such as polycaprolactone, to produce 'CRG-wrap'. Once cured, the wrap can be cut to the required size of the 'CRG-wrap' (2 × 6 cm), sealed in foil and plastic bags, then irradiated to produce the sterile wrap used in the experiments in the present study.

Use of the controlled release glass in clinical practice

The Corglaes tubes have been used in humans for peripheral nerve repair in the upper arm. The tubes, being rigid, had a tendency to protrude under the skin (personal communication with Mr T. E. J. Hems). Various sizes of tubes are required for different sizes of nerves. In contrast to this, one size of CRG-wrap can be modeled around any size of nerve and the CRG-wrap, being flexible, would not protrude under the skin. If wrap were used, one size could be altered by the operator to fit around any size of nerve.

Wang and Lineaweaver 2003 suggest the nine ideal characteristics for a nerve conduit in clinical use:

1. Biocompatibility
2. Low antegenicity
3. Minimal inflammatory stimulus
4. Sustenance of axon regeneration throughout the length of the conduit
5. Biodegradability
6. No potential for entrapment or compression
7. Easy manufacturing
8. Economic availability
9. Easy technical handling characteristics

The Corglaes wrap incorporates all of these features. It is like tissue paper in texture but maintains its structure when damp. Another benefit of the CRG-wrap over a solid conduit is its porosity to macromolecules.

> 'Now we come to the next step...[If a micro-filter sheath] will aid our honest suture, which will hold it together , but at the same time will supply it with oxygen, as his pictures seem to show, then that is a step in advance. But if his system does not permit the introduction of extracellular fluids into that nerve, it is not good.'
>
> Henry C. Marble, M.D., 1960 (Dellon 2004)

Henry C. Marble, a neurosurgeon in the faculty of the Massachusetts General Hospital had a lifetime's experience in attempting to decide how to repair divided peripheral nerves and was referring to James C. Campbell's basic science and clinical experience with neural regeneration through non absorbable microfilter sheaths of cellulose acetate (Millipore) as a nerve conduit in the 1960's (Dellon 2004).

Kim et al (1993) reported that macropore collagen conduits gave better recovery of function in nerve repair with a defect of 1 cm between the cut ends than either semi-permeable or non-permeable collagen conduits. They postulated that neurotrophic macromolecules were being allowed access to the site of repair.

METHODS OF ASSESSING NEURONAL REGENERATION

Electrophysiological methods

Transcutaneous Stimulated Jitter (TSJ)

Neuromuscular coupling

Normally, each muscle fibre has one motor end plate. The arrival of acetylcholine (ACh) at the motor end plate after its release from the supplying motor axon and crossing of the neuromuscular synaptic gap generates an end plate potential (EPP) in the motor end plate. If this reaches the threshold EPP value for that muscle fibre, an action potential is generated in the muscle fibre and it contracts. If a muscle fibre is denervated, ACh receptors develop along the muscle fibre membrane outwith the motor endplate and the whole muscle fibre membrane becomes hyper-excitable (Thesleff, Vyskocil, & Ward 1974). EPPs can then be generated anywhere along its surface. After reinnervation by a motor neurone there is a gradual re-establishment of the single motor end plate and a return to normal of the remainder of the muscle fibre membrane with a loss of the ACh receptors. Before this newly created motor end plate becomes mature, the threshold EPP varies in size and rise-time and the refractory period also varies in duration causing

variability in the latency period between the stimulation of a motor axon and the contraction of the muscle fibre it supplies. This variation in latency is called 'jitter' (μs).

Measurement of jitter

Measurement of *jitter* is an electromyographic technique that has been developed over the past twenty years mainly by the work of Stålberg and Trontelj (Stålberg.E. & Trontelj 1994). In an individual muscle there is a range of values for jitter which is considered normal and has been measured for several muscles in humans (Delisa 1994; Kimura 2000).

The latency time from stimulation of the supplying nerve axon to contraction of the muscle fibre is composed of: the transmission time of the action potential (AP) along the nerve axon, chemical transmission across the synapse between the terminal axon and the motor end plate of the muscle fibre, the production of threshold end plate potentials (EPPs) in the motor end plate, and the production of the wave of depolarization in the muscle fibre (Kimura 2000). After denervation and reinnervation of a muscle fibre by the supplying axon, there is an increase in the instability of the motor end plate and a change in its refractory period. Thus the variation in latency between stimulation of the supplying axon and the development of an action potential in the muscle fibre, i.e. jitter, increases (Stålberg.E. & Trontelj 1994).

Prior to the development of electromyographs such as the Medelec Synergy EMG/EP (Oxford Instruments, Manor Way, Old Woking, Surrey, GU22 9JU, England), jitter measurement was made by photographic superimposition of recorded single fibre potentials on an oscilloscope screen. A series of 50 sweeps with 5–10 discharges in each group had to be recorded, photographed and then superimposed on one another

(Stålberg.E. & Trontelj 1994). The Medelec provided both the stimulating current and the recording and calculating facilities for jitter thus enabling measurements to be taken much more easily than when using these early techniques.

Lenihan (2000) examined jitter as a method for assessing the outcome of nerve repair. By measuring jitter values at 30, 60 and 90 days after repair of the peroneal nerve in rabbits, he demonstrated a significant decrease in jitter as the nerve repair matured with a decrease in 'blocking' (the failure of stimulation of the axon to produce an action potential in the muscle fibre), so that by 90 days, there was no longer any blocking and jitter values were not significantly different from the normal controls (Lenihan 2000). He also demonstrated that this technique reliably indicated the maturity of neuronal regeneration after repair using CRG tubes filled with either diced freeze-thawed muscle (FTM), a diced nerve, or diced nerve / FTM sandwich graft as his results for *jitter* decreased along with a histological increase in *fibre diameter* and *g-ratio* (Lenihan 2000). Jitter is recorded using single fibre electromyography (SFEMG) and can be measured during voluntarily activated muscle contractions (*voluntary jitter*) or by direct stimulation of the axons supplying the muscle fibres being measured (*stimulated jitter*). *Transcutaneous stimulated jitter* was used in this study as it is the appropriate method when the subject is unconscious or unable to co-operate for other reasons.

Single fibre electromyography (SFEMG)

SFEMG was developed by Erik Stålberg and Jan Ekstedt (Stålberg.E. & Trontelj 1994). The moving electrical field of a wave of depolarization in a muscle cell is detected outside the muscle fibre as an action potential. By using a needle with a very small recording surface area, action potentials from individual muscle fibres can be detected

and measured in a similar way to compound muscle action potentials. Measurements can be made using a single fibre electromyography needle or a concentric monopolar electrode. The SFEMG needle consists of an insulated platinum wire (25 μm in diameter) which is exposed at the side port of a steel cannula (0.5–0.6 μm in diameter). The side port is around 3 mm from the needle's tip (Stålberg.E. & Trontelj 1994) and opposite its beveled surface so that recording is not carried out from the muscle fibres that have potentially been damaged during the needle's insertion. The small recording surface of the platinum wire allows selective recording from single muscle fibres.

The concentric needle has a larger recording surface than the SFEMG needle. The cannula of the concentric needle is 0.3 mm wide and made from stainless steel. The tip is beveled with an oval end. The recording surface has dimensions of 150 by 580 μm and an impedance of 50 kΩ. Despite this, single fibre action potentials can be measured using the concentric needle and use of this needle is in fact favoured by most clinical neurophysiologists. (personal communication with Dr Moran, Department of Clinical Neurophysiology, Western General Hospital, Edinburgh)

'Blocking' describes the phenomenon of an action potential failing to cause depolarization of the muscle cell and occurs because the immature regenerating motor end plate fails to generate a threshold EPP from a stimulus that would not normally do so.

Maximum Conduction Velocity (CV_{max})

Borelli (1608–1679) believed that a muscle contraction occurred by the flow of 'nervous juice' directly from the ends of nerves into the muscle belly causing the muscle to swell and shorten. With the demonstration by Swammerdam in 1738 that the actual volume of the muscle did not change during contraction the theory that muscle contraction was

caused by a swelling of the muscle was disproved. Galvani, between the years of 1781 and 1791 showed that nerves conducted electricity and the theory of the action potential gradually developed (Bennett 1999).

Helmholtz in 1848 was the first to demonstrate that the action potential has a finite velocity. With the use of a 'frog-tracing machine' that traced the response from a frog muscle stimulated by an impulse of 'vanishingly small duration', he demonstrated that;

> 'the energy of the muscle does not develop completely at the moment of an instantaneous stimulus. Rather, in most cases after the stimulus has already ceased, it increases gradually, reaches a maximum, and again subsides.'
>
> Helmholtz, 1848 as quoted by (Bennett 1999)

We now take for granted that action potentials are conducted at a finite velocity along nerve fibres and that the speed of conduction of the action potential is dependant on the morphology of the nerve axon. Larger diameter neurones conduct impulses at a faster speed than small neurones (Cragg & Thomas 1964; Sanders & Whitteridge 1946). The speed of conduction in neurones increases as their axonal diameter and myelin sheath thickness increases (Sanders & Whitteridge 1946). Internodal distance varies linearly with the fibre diameter in normal, undamaged nerves but Sanders and Whitteridge (1946) demonstrated that internodal length did not influence conduction velocity in the peroneal nerve of rabbits which had recovered from a crush injury.

The median nerve in the sheep, and in the human, are mixed nerves containing both motor and sensory neurones. The fastest conducting neurones, the A-α motoneurones, which make up around 1% of the median nerve, have a conduction velocity in humans of 70–110 m s^{-1} and have large, myelinated axons and are the first to reach threshold

potential with an increasing stimulus. The largest and fastest myelinated fibres supply muscle fibres and conduct proprioceptive information centrally (Birch, Bonney, & Wynn Parry 1998). When a supramaximal stimulation is given to a peripheral nerve trunk, a compound muscle action potential (CMAP) can be detected in the supplied muscle which is formed from the mass effect of all the stimulated muscle fibres contracting at varying times according to the speed of conduction down the supplying motoneurones. The first negative (upward), deflection of the CMAP from the isoelectric baseline is caused by depolarization of the muscle fibres supplied by the fastest conducting fibres (assuming that threshold stimulus was reached first by the fastest conducting fibres—this could vary according to the motoneurones topographical position in the nerve trunk and their distance from the stimulating cathode). Therefore, if measured from the first upward deflection, the *maximum conduction velocity* (CV_{max}) of a mixed nerve reflects the speed of conduction in the fastest conducting fibres (Cragg & Thomas 1964; Fullarton et al. 2001; Gasser & Grundfest 1939; Lawson & Glasby 1995; Sanders & Whitteridge 1946) It has been found by many authors to be one of the best measurements to quantify the functional outcome of nerve repair and is routinely measured in clinical nerve conduction studies.

Distribution of conduction velocities (DCV)

The *CMAP* has a wave-like morphology. After nerve division and repair, there is a change from the normal bimodal distribution of nerve fibre diameter on a histogram to a unimodal distribution with a shift to the left (figure 10) therefore a much greater number of fibres conduct more slowly in a repaired nerve.

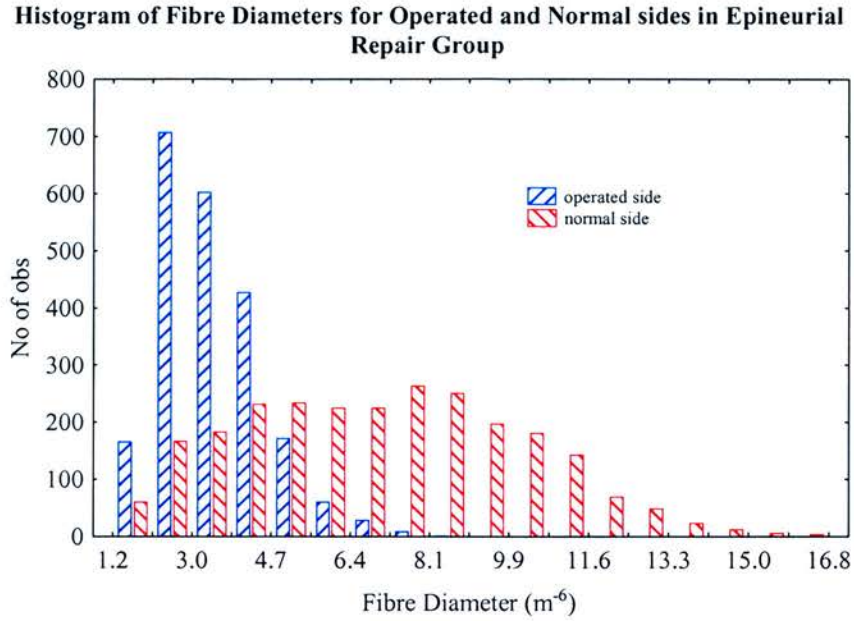

Figure 10

The diameter of neurones from a normal sheep median nerve and a section of a median nerve distal to the site of an epineurial repair (taken from a sample of 200 neurones in ten sheep—this does not reflect the total number of regenerated neurones in the repaired side compared with the un-operated side)

There is also a change in the wave morphology of the CMAP with a decrease in its amplitude (fewer fibres of the mean fibre size: there is a decrease in total fibre numbers) and a lengthening of the wave.

Starrit (2004) investigated whether the distribution of conduction velocities (*DCV*) of a CMAP would be a useful measurement in the assessment of the success of nerve repair. She concluded; 'In the case of the models of nerve injury investigated [neurapraxia, axonotmesis, neurotmesis, repair with wrap and epineurial repair], the *DCV* does not provide any more clinically useful information than conventional CV_{max}' (Starrit 2004). Thus, in the present study, only the CV_{max} was measured.

Isometric twitch tension

Stevenson et al in 1988 reported on the outcome of the repair of rat peroneal nerves by measuring the *wet muscle mass* (g), *cross-sectional area* (mm^2), *muscle fibre length* (mm), *isometric twitch tension* (N) and *maximum tetanic tension* (N) (including measurements of time to peak tension and time to half relaxation) of the extensor digitorum longus (EDL) muscle.

They stated that;

> 'One of the most valid measures of the overall effectiveness of axonal regeneration and of reinnervation of muscle fibres is the *maximum isometric tetanic force* developed by the muscle, following nerve repair, compared with that developed by contralateral control muscles.'
>
> (Stevenson, Kadhiresan, & Faulkner 1994)

Frykman et al reviewed experimental methods measuring peripheral nerve regeneration in 1988. They concluded that 'the most precise methods are muscle weight and the isometric response of muscle to tetanic contraction'. In reference to the *maximum isometric tetanic* and *maximum twitch tension* responses they state, 'these muscle strength responses give the best objective data on muscle reinnervation' (Frykman, McMillan, & Yegge 1988).

In Stevenson et al's study, a statistically significant decrease ($p = 0.05$) was found in the *maximum tetanic tension* (N) produced after repair by epineurial suturing and repair by tubular nerve guides compared with controls. The percentage of the force produced compared to the controls with each type of repair was 84% and 75% respectively. The percentage of the *maximum isometric twitch tension* (N) between the two types of repair and controls was 65% and 55% respectively. There was no significant difference

between the results in the epineurial repair group and the tubular nerve guide group. The measurement of *maximum isometric twitch tension* gives an accurate reflection of the *maximum tetanic tension* that would be obtained in the same muscle. It was therefore decided in the present study to only measure the *maximum isometric twitch tension.*

Wet muscle mass

In Stevenson et al's measurements of wet muscle mass of EDL, they found no significant difference between groups although there was a trend to a decrease in the mean wet muscle mass from the control, to the epineurial, to the tubular repair groups. Their measurements did not compare the repaired to the contralateral limb but instead used a control group of fifteen rats in which measurements were taken from normal nerves to give control values. This could have produced a skew in the results if the control group had been more active than the two repair groups but does not affect the comparison between the two methods of testing as outlined above. In this same study by Stevenson et al the *total mass of the rats* (g), *cross-sectional area of EDL* (mm^2) and *muscle fibre length* (mm) were measured but no significant difference was found between these variables. The mass of the FCR muscle compared with the mass of the whole sheep was not thought to be a useful measure as the mass of the whole sheep was so much greater that that of FCR and differences in wool thickness, which have nothing to do with the amount of muscle in the sheep, could have affected calculations. Only the *wet muscle mass* (g) of FCR was therefore compared among the groups.

Starrit found the wet muscle mass of FCR to be a good indicator of the difference in outcome between groups of sheep where the median nerve had been injured and repaired by different methods even though she had small group sizes (n = 6) (Starrit 2004).

This technique of assessing the outcome between groups, even though not applicable in the clinical situation, was therefore employed in the present study.

Morphometric analysis

Most peripheral nerves in mammals contain both myelinated and non-myelinated neurones. There is a bimodal distribution of the diameters of myelinated axons and, in humans, fibre diameters range from 0.4–1.25 μm and 2–22 μm respectively in mixed peripheral nerves (Birch et al 1998). After neurotmesis a large number of new, small diameter axons grow from the proximal stump (Aitken et al 1947; Aitken & Thomas 1962). The number of small axons reduces with time, a phenomenon that has been ascribed to a lack of space in the distal nerve as the thickness of the individual axons and their myelin sheaths increases, and also to the degeneration of fibres as they fail to make appropriate peripheral connections (Aitken et al 1947). Axon numbers in the present study was not considered to be a measure of the success of nerve regeneration. If regeneration of the nerve was incomplete at the time of excising the nerve specimen, there would have been a larger number of small axons at the time of measuring but, as some of these would fail to make appropriate peripheral connections and as the size of some fibres increased thus leaving less available space within the distal stump, the number of small axons would decrease. Counting the total number of regenerated nerve fibres could therefore overestimate the success of the regenerative process.

There is an initial large increase in fibre diameter during nerve regeneration with a proportionately greater thickness of the myelin sheath compared to the axon diameter (Sanders & Whitteridge 1946). The final diameter of the largest neurones in a repair is

less than the axons in uninjured nerves, and the axon diameter is relatively smaller than the myelin sheath thickness (Aitken & Thomas 1962).

G-ratio

As regeneration continues there is a continued increase in the diameter of the fibres but with a gradual reduction in the myelin sheath thickness in relation to the diameter of the axon itself (Aitken & Thomas 1962). The *g-ratio* is calculated by the formula:

$$g-ratio = \frac{axon\ diameter}{fibre\ diameter}$$

As the regenerated fibres mature, the g-ratio increases to an optimum value of approximately 0.50–0.60 (taken from average of normal nerves in this present study), and is a well recognized measure of nerve fibre maturity (Glasby et al. 1986c; Kettle 2003; Starrit 2004). It was concluded that in the present study the measurements of *axon diameter*, *fibre diameter*, *myelin thickness* and *g-ratio* would be used to assess the success and maturity of nerve regeneration.

Tensile testing of nerves and repairs

Peripheral nerves are strong structures and are often left in continuity during injuries when muscle, vasculature and other soft tissues have been avulsed (Yoshimura et al 1989). Any nerve repair carried out *in vivo* must be able to withstand forces of tension that it may be subjected to after closure of the skin and regeneration at the site of division. Uninjured nerves are able to withstand large tensile forces and are often the only structures that remain intact after avulsion injuries to a limb (Yoshimura et al 1989). Sunderland and Bradley (1961) reported that the ulnar nerve in the human can withstand

a maximum load of 63.7–151.9 N and the median nerve 71.5–218.5 N (12 hours after death and fixed in formalin). The maximum tensile stress supported by the nerves was 9.8–21.6 N mm^{-2} and 9.8–29.4 N mm^{-2} respectively.

It was found that the distal segment of a divided nerve has the same tensile properties as the proximal segment and so the axon itself is thought not to add strength to the nerve (Sunderland & Bradley 1961). The perineurium is a special laminated tissue heavily interlaced with finer but densely packed and mostly longitudinally aligned collagen fibrils together with specialized perineurial cells possessing individual features and a collective arrangement which imparts tensile strength and elasticity. Yoshimura et al demonstrated in their experimental studies on traction injury of peripheral nerves (with experiments carried out on the sciatic nerves of rabbits) that the nerves seemed to break most easily at the regions of low perineurial circumference lengths, thus indicating that it was the perineurium that conferred tensile strength to the nerves (Yoshimura et al 1989).

Borschel et al (2003) investigated the effect of acellularization [1] on the tensile properties of rat sciatic nerves by stretching four nerves in each of the following four different groups;

- Normal whole nerve
- Acellular whole nerves
- Normal nerves co-apted with 10/0 nylon sutures
- Acellular nerves co-apted with normal nerves using 10/0 nylon (to simulate a graft repair)

One problem they encountered was the slippage of the nerves at their attachment to the apparatus during the application of the load. They overcame this by using 4/0 silk sutures and ethyl cyanoacrylate adhesive to link the nerve specimens to stainless steel hooks which were attached to the apparatus which applied the load to the nerve specimen. The variables Borschel et al considered in their results were *burst strength* (N) (force at point of rupture), *ultimate stress* (kPa) (stress at the point of rupture), *ultimate strain* (strain at the point of rupture), *work done to failure* (N m) (obtained from the integral of the force/deformation curve), *normalized work done* (N) (work done to failure/original specimen length) and *Young's modulus* (kPa) (stress/strain). Even with their relatively small group sizes they demonstrated a significant difference in *ultimate strain, work to failure* and *normalized work to failure* which showed that whole acellular nerves had a lower tensile strength in comparison to whole normal nerves. The results for the co-apted

[1] Acellularization was carried out by immersing the excised nerves in a series of detergents (at 37°C). These were; glycerol,sodium deoxycholate, sodium dodecyl sulphate, and Triton X-100 (all reagents from Fisher Scientific, Pittsburgh, PA, USA).

nerves again showed that the acellular co-aptations had a decreased *work to failure* and *normalized work to failure* as well as decreased *burst strength* and *ultimate stress*. They concluded that the *normalized work to failure* is an excellent measure because it corrects for minor variations in initial length and so it has been used in this present study. The main question to be answered in this present study was whether the repaired nerves ruptured preferentially at the site of repair and whether one type of repair produced a regenerated nerve with a lower tensile strength compared with the other types of repair and normal nerves.

During the present study, median nerves were removed from the sheep after electrophysiological testing and frozen to -11°C. They were stored at this temperature until it was possible to access equipment to test their tensile properties.

An internet search had been carried out to investigate what effect freezing confers on the tensile properties of nerves. No information was available on the subject and therefore it was decided to investigate in the present study any changes to the tensile strength of nerves after freezing and thawing.

Uninjured median nerves that had been frozen for several weeks at -11 °C and then thawed had their tensile properties tested and compared with freshly excised, normal median nerves. The region of the nerve and the force at which rupture occurred was recorded.

To test the initial strength of the different types of repair used in the present study, one specimen of each type of repair was excised from the sheep immediately after being formed and had its tensile properties measured.

SUMMARY OF THE OBJECTIVES OF THE PRESENT STUDY

1. The controlled release glass wrap (CRG-wrap) used in the present study is completely biodegradable and biocompatible. It can be easily manufactured and fully sterilized. The technique of nerve repair when using the wrap in the repair of the sharply divided median nerves in sheep was compared with the current clinical standard technique of microsurgical epineurial suturing in tensionless repairs.

2. When using the CRG-wrap in the clinical setting it is important to know which method of securing the wrap gives the best results of regeneration of the nerve. Three methods of securing the CRG-wrap were used in the present study. The outcome of nerve regeneration with each method was compared with the outcome after microsurgical epineurial suturing and normal nerves.

3. Electromyography, morphometry, isometric twitch tension testing and wet muscle mass were used to assess the outcome of the nerve regeneration in the different repair groups. The most appropriate methods of assessing the outcome of nerve repair in humans will be considered.

CHAPTER 2 — MATERIALS AND METHODS

THE SHEEP AS A MODEL FOR HUMAN NERVE REPAIR

In order for animal experiments to predict events in the human, the properties and environment of the animal and human should be similar (Kline, Hayes, & Morse 1964). Regeneration of nerves in rabbits, rats, dogs and other animals such as the Australian opposum is much faster than in humans (Di Benedetto et al 1998; Kline, Hayes, & Morse 1964; Sunderland 1978; Seddon 1954). It is therefore difficult to correlate clinically the results of studies in rats, rabbits, cats and dogs to humans (Frykman et al 1988).

The animal model chosen for the present study was the sheep. There has been considerable experience using the sheep as a large animal model in the Edinburgh Peripheral Nerve Research Group (EPNRG). It has been found to be a very good model for the human with a similar potential as humans for nerve regeneration (Kettle 2004; Lawson & Glasby 1995; Lawson & Glasby 1998; Starrit 2004).

The site chosen for neurotmesis and repair was the median nerve in the upper forelimb. The size of the median nerve in the sheep at this level approximates to the size of the ulnar and median nerves at the wrist in the human (Lawson & Glasby 1998). The maximum conduction velocity in the proximal median nerve in the upper forelimb in sheep is 69 m s^{-1} (range 50–85 m s^{-1}) (mean conduction velocity found in normal median nerves in this study). In the median nerve of adult humans, from the elbow to wrist, the maximum conduction velocity is 63 m s^{-1} (range 51–75 m s^{-1}) (quoted from a study by Gamstrop, 1963 (Sunderland 1978)).

The median nerve supplies the flexors of the forelimb in the sheep (May 1970). After high division of the median nerve in the proximal forelimb, flexion of the forefoot and wrist is weakened but the extension which is essential for mobilization is not affected. The sheep can therefore mobilize well after division of the median nerve at the site chosen for this study. Cross-innervation from the radial and ulnar nerves supplies sensation to the hoof and therefore trauma and sepsis due to anaesthesia has not previously occurred (Lawson & Glasby 1998) and did not in the present study.

Seven months was considered adequate to allow regeneration of the nerves and re-establishment of the muscle supply. Results of a previous study by Lawson & Glasby (1995) examining the flexor carpi radialis (FCR) function and nerve morphometry in sheep six months after median nerve injury and repair using autologous freeze-thawed muscle grafts showed the g-ratio was smaller in the repaired groups than the normal groups suggesting that satisfactory maturation had occurred in the repaired neurones. It was therefore considered that seven months would allow complete regeneration of the repaired nerves in this study where no graft was being inserted and no gap was being left between the nerve ends. All sheep were examined at the same time interval after repair and therefore, even if maturation of the regenerated nerve fibres were not complete, comparison between the groups would still be valid.

Age

There is a decreasing rate of both nerve regeneration and muscle recovery after nerve re-innervation with increasing age (Grieve, Kristmundsdottir, & Glasby 1991). An attempt was therefore made to keep the sheep the same average age at the time of operation: at the time of neurotmesis and repair, all the sheep were over one year old with an average age of around two years.

Breeds

The breeds used were Texals, Booroolas, Finns, Blackfaces, Border Leicesters, Suffolks, and Greyfaces. The different breeds and sexes were used randomly throughout the groups.

Experimental groups

The different experimental groups compared in this study were:

1. Normal sheep (matched for age and weight)
2. Neurotmesis and repair with CRG-wrap secured by Tisseel glue
3. Neurotmesis and repair with CRG-wrap secured by polycaprolactone glue
4. Neurotmesis and repair with CRG-wrap secured by suturing
5. Neurotmesis and repair by conventional epineurial suturing using a microscope and 9/0 polyamide (Nylon, Ethilon, Ethicon ltd, UK)

The normal sheep were the first group to undergo electrophysiological testing and did not undergo any operation prior to this. Electrophysiological testing and morphometric analysis were carried out on both the operated side and the normal side in all groups. The

ratio of the results from the operated side divided by the results from the normal side was used to compare the outcome between the groups and so reduced within-groups variation.

Group size

Figures from experimental work carried out by Starrit (2004) were used to calculate an appropriate group size. Starrit had concluded that the maximum conduction velocity (CV_{max}) (m s^{-1}) and wet muscle mass (g) of flexor carpi radialis (FCR) had varied significantly according to the degree of median nerve damage and type of repair when comparing normal nerves to nerves injured by axonotmesis or neurotmesis and repair by nerve graft, CRG-wrap or epineurial suture repair. Using the *Power analysis* module in the statistics programme Statistica (Statsoft, Tulsa, USA) and the measurements obtained in Starrit's study, it was calculated that a group size of seven for CV_{max} (m s^{-1}) measurements and nine for *wet muscle mass* (g) would be required in order to show a difference between the groups. Starrit had not been able to show a significant difference in CV_{max} measurements between repairs carried out by epineurial suture, CRG-wrap and nerve grafts. In this present study, to be sure that a statistical difference in the results of the measured variables among the repair groups would not be missed because the number of animals in each group was too small, a group size of twelve was chosen. This allowed for possible fatalities in the groups and aimed to improve on the power obtained by Starrit.

Animal husbandry

The appropriate personal and project licenses were obtained according to the Home Office Animals (Scientific Procedures) Act 1986 (HMSO 1986).

The sheep used in the experiments were housed at the Marshall Building, Roslin. This is a joint University of Edinburgh and Medical Research Council establishment. The sheep were housed in barns during the winter in groups of twelve per pen and in the spring and summer months they were kept in the fields. Tups and ewes were penned separately. Their diet, while housed in the barns, was of hay supplemented by a once daily feed of 'Emerald Ewe nuts' (Carrs Billington, Cunard building, Liverpool, L3 1E2). This compound feed for adult sheep contains 5% oil, 15% protein, 8.5% fibre, 10% ash, vitamins A, E, D3 and selenium. Water was in constant supply in automatically refilling troughs. Their bedding of straw and shavings was changed as necessary, usually once per week. The sheep were monitored and cared for by two animal handlers.

Health of the sheep postoperatively

Generally, the sheep kept very well throughout the period of the study. Two sheep were treated for lice with one 5 ml dose of Coopers 'Spot-on' (Shering-Plough Animal Health Division of Shering-Plough Ltd, Welwyn Garden City, AL7 1TW) applied to the midline of their backs. One sheep died while being fasted in isolation pre-operatively. The sheep had seemed well prior to this and no *post mortem* was undertaken. The cause of death remained unknown. The most stress inducing situations for sheep are fasting and isolation. It was speculated that this sheep may have had an underlying cardiac condition. From this time onwards, sheep being fasted pre-operatively were penned along with one other sheep and within sight of the other sheep. They were also allowed to drink water.

NEUROTMESIS AND REPAIR

Anaesthesia

The sheep was placed on a weighing crate prior to induction of anaesthesia to measure its mass (kg). In the preparation room, the lateral side of the sheep's neck was shaved to expose the external jugular vein. Intravenous thiopentone sodium BP (Intraval Sodium, Merial Animal Health Ltd, Essex, UK) (5 mg kg^{-1}) was used as an induction agent and injected directly into the external jugular vein. The sheep were then intubated using a cuffed endotracheal tube (between size 8.5–11.0 depending on the size of the sheep) and had an oro-gastric tube inserted prior to being transferred to the operating table.

Maintenance of anaesthesia

The sheep was positioned supine on the operating table with supports on each side to maintain its position. General anaesthesia was maintained by a mix of halothane BP 1% to 2% (Halothane-Vet, Merial Animal Health Ltd, Essex, UK) in 5 l min^{-1} of oxygen (O_2) and 2 l min^{-1} of nitrous oxide (N_20) (BOC gases, Manchester, UK) administered with the pressure-controlled ventilator shown in the photograph in figure 11. Waste gases were removed via a corrugated plastic pipe to the outdoor atmosphere.

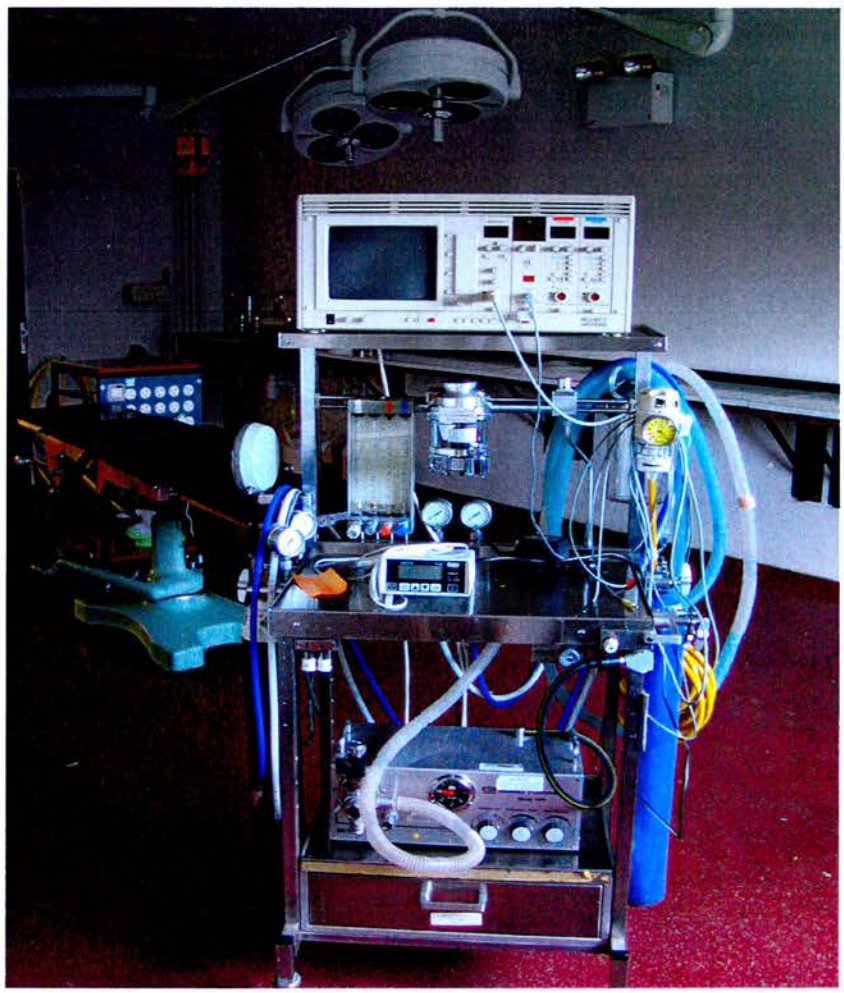

Figure 11

Pressure control ventilator used in maintenance of anaesthesia in the operating theatre at the Marshall building

Monitoring

A thermometer probe was inserted into the posterior pharynx. The temperature recorded was displayed on the multimodal monitor (Hellige GMB, Senomed, Freiburg, Germany) and used as a value for the core body temperature throughout the procedure. Active re-warming with an electrically heated blanket was attempted if the sheep's temperature fell below 35.5°C.

An area on each distal forelimb and one distal hindlimb was shaved and ECG electrodes attached (Blue sensor, Ambu, Rugmarken, Denmark) held by tape (Sleek, BSN medical, Lancashire, UK).

A lead 2 ECG output was monitored on the ECG monitor machine (Hellige GMB, Senomed, Freiburg, Germany). A pulse-oximeter (MicroSpan 3040, BCI International, Wisconsin, USA) was used to monitor blood oxygen saturation by a probe attached to the sheep's tongue.

Preparation for operation

The first operative procedure was carried out using sterile technique. The surgeon washed, gowned and gloved using standard sterile procedure. The lateral chest wall, axilla and upper forelimb of the right side of the sheep were cleaned with povidone iodine in spirit. Drapes were applied to cover as much of the sheep as possible to help maintain the sheep's body temperature and give a sterile surgical field while leaving access to the upper medial forelimb and lateral chest wall.

Bipolar diathermy (Malis Bipolar Coag. & Bipolar Cutter CMCII, Codman Inc., USA) was used throughout all surgical procedures to maintain haemostasis. Blood loss was kept to a minimum in order to maintain the animal's circulating volume and temperature.

An oblique incision was made from the lateral chest wall, across the axilla, to the postero-medial forelimb, proximal to the olecranon. The superficial pectoral muscle is a superficial layer of muscle in the upper forelimb underlying the skin. This was split transversely in the line of its fibres and then cranially and caudally to reveal underlying loose connective tissue which overlay the neurovascular bundle. The inferior border of pectoralis major was visible superiorly, and the serratus ventralis thoracis medially.

Once the loose connective tissue had been cleared by blunt dissection, the median nerve, brachial artery and ulnar nerve were obvious as they lay in the floor of the upper forelimb covered by a tight fascial layer. After division of the fascial layer, the median and ulnar nerves and brachial artery were visible in the floor of the proximal upper forelimb as represented by the diagram in figure 12.

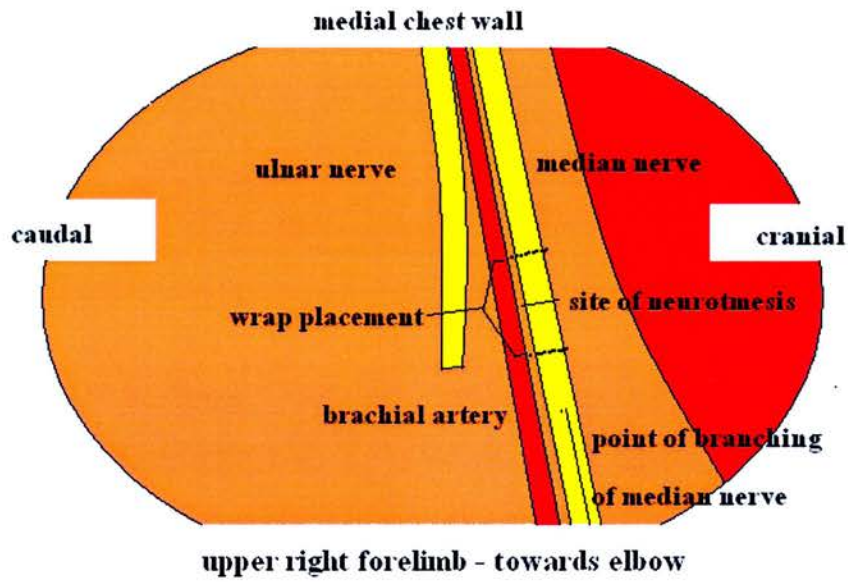

Figure 12

Diagram of the median nerve, brachial artery and ulnar nerve in the floor of the left proximal upper limb

During dissection of the median nerve an attempt was made to keep stretching to a minimum, preserve the adventia surrounding the epineurium and the extrinsic feeding vessels wherever possible, and mobilize as short a length of nerve as possible. The mobilized length at the time of neurotmesis was approximately 5 cm and during electrophysiological testing did not exceed 7 cm. Exposed nerves were kept moist with normal saline-soaked swabs and stretching of nerves was minimized by lifting them with

elastic rubber slings. The median nerve was gently dissected as far as its point of branching prior to entering the forelimb at the level of the elbow. The brachial artery lay immediately adjacent to the median nerve in the area of dissection and great care was taken not to damage the brachial artery.

The median nerve was divided using a Meyer neurotome, approximately 2 cm proximal to its distal site of branching. This preserved a portion of the median nerve distal to the site of repair which would be required during electrophysiological testing after regeneration. Repair was then undertaken by each of the four methods of repair.

Repair with epineurial sutures

An operating microscope (Wild Heerbrugge M600) was used to aid visualization during epineurial suturing. 9/0 polyamide (Nylon, Ethilon, Ethicon Ltd, Edinburgh, UK) and microsurgical instruments were used to complete the repair. The eyepieces were set to the correct interpupillary distance and the focus and zoom of the microscope viewing lens were centred prior to scrubbing for surgery. A sterile cover was placed over the whole microscope and once the median nerve was exposed, the microscope was positioned over the operation site and its position fixed by securing the x–y–z axis of the arm of the microscope. The foot controls were positioned for comfortable access. The output of the microscope was connected to a television monitor by way of a video recorder. This allowed the operation to be recorded onto video tape and to be viewed by all staff and observers present.

A rectangular piece of green coloured disposable drape 2 × 1 cm was placed underneath the nerve to provide a background contrast. Any clot present on the cut ends of the nerve was removed with the use of cotton 'Q tips'. Debris or clot at the site of repair

increases the fibrous tissue formation and fibrous tissue significantly delays growth of the regenerating neurones across the site of injury (Lundborg 1988b; Sunderland 1978). (In clinical practice the ends of the nerve often required initial debridement in order to produce a sharp, flat resection surface. This was not necessary in this study as division of the nerve by the Meyer neurotome produced a sharp-cut surface on each stump. Protrusion of the nerve ends owing to oedema (mushrooming) often occurred to some extent but was not marked). The magnification was adjusted as required between high power and lower power for the placing and knotting the sutures respectively (Nylon, Ethilon, Ethicon Ltd, UK). Around eight sutures were placed around the epineurium for each repair. The initial stitch was placed in the posterior wall as this was the most difficult site to access. Care was taken to place the sutures only in the epineurium while avoiding the perineurium of the fascicles and the fascicles themselves. The fascicular pattern of the proximal and distal stumps was matched as accurately as possible by using the blood vessels within the epineurium as markers to orientate the nerve stumps to their original configuration. Sufficient epineurial sutures were placed in order to hold the epineurium together. A tight opposition at the repair site was avoided as this could strangulate the axons in the nerve ends (Lundborg 1988).

The time taken for epineurial repair, between division of the nerve and the beginning of wound closure, was approximately thirty minutes.

Repair with controlled release glass wrap and Tisseel glue

Tisseel glue

Tisseel glue (Baxter Healthcare Ltd., Bioscience, Wallingford Road, Berkshire, U.K.) is a fibrin glue manufactured form human plasma. It is currently licensed for use in neurosurgery as a complement to surgical technique in achieving haemostasis and for the closure of dural tears when conventional techniques are not adequate.

It is supplied in four vials for which there is a specific mixing process. These vials contain:

1. Tisseel powder for sealer protein solution, human, vapour heated
2. Aprotinin solution, solvent for Tisseel powder, aprotinin—bovine (3000 kIU ml^{-1})
3. Thrombin powder for thrombin solution, human, vapour heated
4. Calcium chloride solution, solvent for thrombin powder Ca^{2+} (40 μmol ml^{-1})

The 'Fibrinotherm' is a specially designed heating and mixing aid for use with Tisseel glue. The vials were inserted into the appropriate cavities in the Fibrinotherm and the machine was switched on. When the temperature reached 37 °C, the red indicator light went out. The aprotitin solution was drawn up in a syringe and added to the Tisseel powder using sterile technique. The Tisseel powder vial was then re-inserted to the Fibrinotherm and mixed using a magnetically controlled mixing device, a process which took eight to ten minutes.

The calcium chloride solution was aspirated form its vial and added to the thrombin powder vial. This mixture was gently swirled until the thrombin powder had dissolved and was then replaced in the Fibrinotherm to be kept at 37 °C.

When it was time to use the glue, the solutions were drawn up into the 'Duploject Two' syringe. This is a double-barreled syringe with a 'Y' nozzle in which the two solutions are mixed during application (figure 13).

Figure 13

The Duploject syringe

Application of the CRG-wrap

The CRG-wrap (Giltech Ltd, Ayr, Scotland) was supplied in rectangular sheets of 6 × 2 cm and in sterile packaging. Prior to application of the warp around the divided nerve ends, it was folded twice to produce a wrap that was quarter its original length and four layers thick.

The divided ends of the nerve were positioned on the top of the folded CRG-wrap with as little a gap as possible between their ends. A small amount of Tisseel glue was applied to

each nerve stump as they lay on the wrap at a distance of around 0.5 cm from the cut ends. A small amount of Tisseel glue was then applied down the lateral edge of the wrap. The wrap was then folded to form a tube around the divided ends as illustrated in figure 14.

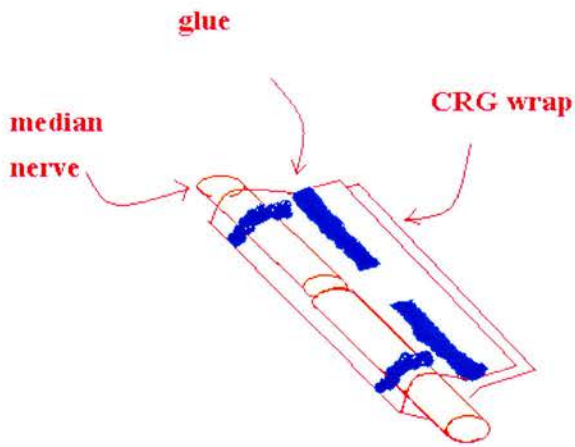

Figure 14

Diagram of CRG-wrap applied with Tisseel glue.

A stainless steel ligating clip (Ligaclip, Ethicon, Edinburgh, UK) was then applied to the edge of the CRG-wrap taking care to avoid contact with the nerve. This allowed clear identification of the site of repair so that dissection close to this area at the second operative procedure could be avoided.

The time taken between division of the median nerve and the completion of application of the wrap was around three minutes.

Repair with CRG-wrap and polycaprolactone glue

The polycaprolactone glue (Giltech Ltd, North Harbour Industrial Estate, Ayr, Scotland) was supplied in a sterile vial and, once drawn up in a syringe, was ready to dispense directly to the site of application. The method of application of the polycaprolactone glue was the same as that used with Tisseel glue. A Ligaclip was applied to the edge of the folded wrap. The time taken between division of the nerve and completion of application of the wrap was around three minutes.

Repair with CRG-wrap and sutures

CRG-wrap was folded twice and placed under the cut ends of the median nerve as before. An anchoring suture of 6/0 polyglactin (Vicryl, Ethicon Ltd, Edinburgh, UK) was placed through the layered wrap underneath the nerve approximately one centimetre from the cut end on each side and then through the epineurium on the underside of the nerve. The sides of the wrap were then folded to cover the site of the approximated nerve stumps to form a tube. Two further 6/0 polyglactin (Vicryl, Ethicon Ltd, Edinburgh,UK) sutures were placed on the upper surface of the folded wrap through its layers and into the epineurium of the enclosed nerve. The arrangement is shown in the diagram in figure 15.

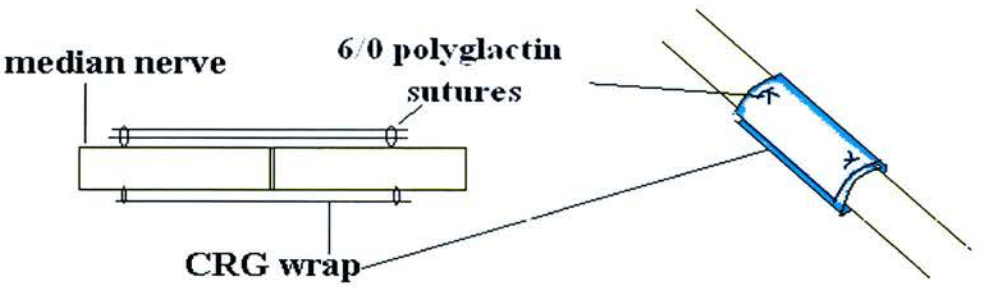

Figure 15

Diagram of the CRG-wrap secured in position with 6/0 polyglactin sutures

A ligating clip (Ligaclip, Ethicon Ltd, Edinburgh,UK) was attached to the edge of the wrap as in the other repair groups. The time taken between division of the median nerve and the completion of application of the wrap was around ten minutes.

Closure

The wound was washed out with 0.9 % saline solution and cleared of any haematoma. The divided edges of the superficial pectoral muscle and pectoralis minor were re-apposed with interrupted 2/0 polyglactin (Vicryl, Ethicon, UK) sutures. To do this without undue tension on the muscle, the leg was released from the arm rest. The skin was closed with a continuous sub-cuticular 3/0 polyglactin suture (Vicryl, Ethicon Ltd, Edinburgh, UK). The wound was cleaned with povidone iodine and saline and then dried. The sheep was given an intramuscular bolus injection into the lateral thigh of the non-steroidal anti-inflammatory Flunixin Meglumine (Finadyne Solution, Schering-Plough Animal Health, Welwyn Garden City, UK) (1 ml per 25 kg body weight), and 'Streptacare' (Animalcare Ltd, York, UK)(1 ml per 25 kg body weight) which contained

procaine penicillin (200 mg ml^{-1}) and dihydrostreptomycin (250 mg ml^{-1}). The sheep received another ear-tag on each ear with a code number that identified the type of repair received and the date of the procedure. A log was kept in the department of each tag number and the corresponding operative details.

Recovery

On transfer to the recovery pen, to prevent injury during recovery, the sheep were positioned prone on the floor with a bale of straw supporting them in an upright position against one wall. Most sheep were standing within two hours. They were allowed to eat as drink as they were able postoperatively and remained isolated in the recovery pen for three days. The wound was examined daily during this time and they received a daily bolus of intramuscular Streptacare (Animalcare Ltd, York, UK) (1 ml per 25 kg body weight). Sheep grind their teeth when in pain (bruxism) but none showed this sign of discomfort post-operatively.

ELECTROMYOGRAPHY AND TISSUE EXCISION

Anaesthesia

Anaesthesia was induced, maintained and monitored as in the first operative procedure. This second operation was a terminal procedure and there was no need for sterile technique though the sheep was draped to reduce heat loss and provide a clean area for experimental work.

The sheep was positioned on its back on the operating table and the forelimb of the side under examination was abducted to approximately 70° and secured to an armrest. The

forelimb was kept in a relaxed position as previous work has shown that *jitter* values increase if the muscle being examined is under tension (Trontelj & Stålberg 1992).

Temperature

Core temperature was measured by a thermistor placed in the larynx and the temperature of the muscles of the upper limb at the time of CV_{max} measurement was made using a Raytek infrared temperature recorder (Raynger MX2, Raytek, Milton Keynes,UK). This thermometer measured the amount of infrared energy emitted by a target object, and calculated the temperature of the objects surface.

Order of Tests

All the tests on one side were carried out first prior to changing to the other side. This was to reduce the total anaesthetic time of the procedure as constantly changing from one side to another would have lengthened the time of the studies significantly and also would have meant the dissected nerves would have been exposed for longer. The side in which the nerve repair had been carried out—the right side—was always operated on first in case the sheep died while under anaesthesia.

The tests were carried out in the following order:

1. *Transcutaneous stimulated jitter* (*TSJ*)
2. *Maximum conduction velocity* (CV_{max}) (m s^{-1})
3. *Minimum F wave latency* (F_{min}) (ms)
4. Isometric muscle twitch
5. Excision of nerve for morphometric analysis
6. *Wet muscle mass* (g)
7. Excision of nerve for tension testing

Electrophysiological apparatus—the Medelec

The Medelec Synergy EMG/EP (Oxford Instruments, Manor Way, Old Woking, Surrey, GU22 9JU, England) is a two-channel electromyograph which provides facilities for electromyography (EMG) and nerve conduction studies (including their production, measurement, display and storage). The Medelec was designed for clinical use and so generates reports with test results in Microsoft Word format with the possibility of displaying recorded traces if required.

The components of the Medelec are:

- a portable mainframe with a Windows 98 (Microsoft inc.) operating system
- a two-channel pre-amplifier
- a 12 inch monitor
- a footswitch with three control pedals
- two stimulator probes (A and B)
- a keyboard and mouse

These components are mounted on a trolley as shown in figure 16.

Figure 16

Photograph of the Medelec Synergy components mounted on the trolley

The Medelec was used to measure *transcutaneous stimulated jitter* (*TSJ*), *maximum conduction velocity* (CV_{max}) and minimum F wave latency (F_{min}). A USB memory pen (Cruzer mini, Sandisk plc) was used to transfer saved files of results from the Medelec Synergy to a *Hewlett Packard Pavillion zt 1121s* or *Acer Aspire 1355LC* laptop computer (both with Microsoft Windows XP operating system, Microsoft, inc.). *Synergy Reader*, which had been loaded onto the laptops, allowed Medelec Synergy files to be read and the data to be examined from electronic storage media.

Amplifiers

The amplitude of the action potentials recorded from single muscle fibres during *TSJ* measurements were approximately 200 μV, and during CV_{max} measurements, the amplitude of the compound muscle action potentials (CMAPs) were approximately 500 μV. Interference from the coupled potential of an alternating-current power line, if in the order of 1–2 V, is over a million times greater than the output from these biological sources. The potential being recorded from the muscle fibres therefore had to be selectively amplified. The Medelec contains a differential amplifier. This allowed selective amplification of the signal from the active electrode without amplification of background electrical, magnetic and thermal signals.

Differential amplifiers

A normal amplifier takes the potential difference recorded between two electrodes and amplifies it. A differential amplifier records the output from two electrodes and selectively amplifies the potential difference between them in relation to the ground electrode. Any potential difference from surrounding noise will be detected at both electrodes and therefore will not be amplified because it is equal and of opposite polarity. The combined output of a differential amplifier can be expressed as:

$$(V_A + V_C) - (V_B + V_C) = V_A - V_B$$

Where:

V_A, V_B = electrophysiological signals

V_C = common mode potential.

Common mode rejection ratio

The ratio of amplification between differential signals i.e. the signal being detected at the recording electrode, and signals common to both electrodes and the ground electrode is called the common mode rejection ratio (CMRR). This should ideally be >100 dB for physiological recording. The CMRR of the Medelec amplifier is 110dB (Oxford Instruments Medical Systems Division 2000).

Noise

Noise is the term used for unwanted background electrical activity recorded along with an electrode signal. Amplifiers have their own intrinsic noise which is due to switch contacts, resistors, transistors and thermal noise and integrated circuits (Kimura 2000a). The noise of the amplifier of the Medelec was < 0.7 μV r.m.s. (0.1 –10 kHz bandwidth) (Oxford Instruments Medical Systems Division 2000). Common causes of 50 Hz interference patterns in the theatre setting were fluorescent lights, diathermy, high impedance of recording electrodes due to broken wires, defective or poorly adherent ground electrodes, and recurrent biological discharge.

Impedance

Impedance in an alternating circuit (a.c.) is analogous to resistance in a direct current (d.c.) circuit. It determines the current flow for a given alternating voltage in a circuit. When connected in series, the total potential difference in a circuit equals the sum of the potential differences across each component in series, therefore:

$$V_{total} = Z_1 I + Z_2 I$$

Where:

V_{total} = total potential difference across circuit

Z_1 = impedance across component one

Z_2 = impedance across component two

I = current in circuit

If the input impedance of the amplifier is much greater than that at the needle tip, very little of the original voltage will be lost. It is beneficial therefore to have amplifiers with high input impedances and electrodes with low impedances. Higher electrode impedances increase the amplifier noise and increase external interference. For electrophysiological measurements, amplifiers should have input impedances (>5 MΩ) and electrodes low impedances (< 4 kΩ). The Medelec amplifier has an impedance of 1000MΩ (Oxford Instruments Medical Systems Division 2000). When using needle electrodes, the tissue itself and electrode wires add only negligible impedances compared with the needle tip and the input terminal of the amplifier. The potential difference (V)

at the points of the needle tip, input terminal of the amplifier and electrode wires depends on the impedance (Z) at each point.

Potentials may arise at the metal-fluid junction of the intramuscular needle electrode. The smaller the electrode tip, the higher the impedance. Inert metals have lower impedances and so metals such as stainless steel and platinum are used to minimize electrode noise (Kimura 2000). The concentric monopolar electrode used in the measurement of *TSJ* was made of stainless steel (personal correspondence with Medelec Systems, Oxford). The impedance of the electrodes was checked using the preamplifier when the circuit had been constructed and was below 4 kΩ.

Filters

The input signal to an amplifier can be further selectively amplified by limiting the frequency range that is amplified. Low-pass filters limit high frequencies and high-pass filters limit low frequencies.

Muscle acts as a low-pass filter; in other words, high frequency components of a signal are lost. When distant action potentials were detected by the concentric needle electrode they had a larger low-frequency component (recorded curves had a longer, flatter appearance). To increase the selectivity of recording from near muscle fibres, the amplifier's filter was set to reduce its response to low frequency signals, thus near fibres, recorded as high frequency signals, were amplified. With a low-pass filter of 500 Hz, a significant reduction of background noise is achieved, but the amplitude of the action potentials from near fibres is only attenuated by 10% (Stålberg & Trontelj 1994). This is especially important when using the concentric monopolar electrode because this type of electrode because of its larger recording surface area records a greater proportion of

signals from distal muscle fibres (Kimura 2000). The analogue filter also affects the peak latency of the recorded response because of phase shift. High frequency filtering increases and low frequency filtering decreases the apparent latency of peaks (Kimura 2000). The same filters were therefore applied in all groups when a particular recording was being taken.

Constant current versus constant voltage stimulation

It was possible to set the stimulating impulses from the Medelec to be constant current or constant voltage in their output. When using a constant voltage output the amount of current delivered to the tissues depends on the impedance of the skin, subcutaneous tissues and electrode. A constant current supply allows the same magnitude of current to be delivered to the nerve by altering the stimulating voltage according to the impedance of the tissues and the electrode. Either type of stimulating set-up can be used to provide a supramaximal stimulus to a nerve but by using a constant current stimulus, as was done in the present study, it is possible to assess nerve excitability by the level of shock intensity required (Kimura 2000).

The ground electrode

An area on the right anterolateral chest wall was shaved and cleaned with 100% alcohol and abrasive gel (Nu prep, D.O. Weaver and Co., 565-B Nuclaway, Aurora,Co-80011, USA). The ground electrode, a stainless steel disk 3 cm in diameter with a connecting lead, was sutured to this prepared area of skin. A layer of conductive electrode paste (Ten 20 Conductive, D.O. Weaver and Co. D.O. Weaver and Co., 565-B Nuclaway, Aurora, Co-80011, USA) was placed between the electrode and the cleaned skin—it was

essential to maintain complete contact between the electrode and the skin. The ground lead was then connected to the ground port on the two-channel pre-amplifier of the Medelec. It was important to check the ground electrode connecting cable for breaks in its insulation, poor contact with the skin or poor connection with the port on the pre-amplifier as these were all sources of noise. If the ground electrode was faulty there was an obviously unsteady baseline on recordings in the Medelec display window thus indicating 'noise'.

Transcutaneous stimulated jitter

Measurement of transcutaneous stimulated jitter

The region of a muscle which contracts with a minimal-intensity, short-duration stimulus is defined as the *motor point*. The terminal portion of the motor neurones enter the muscle and spread to supply individual motor units at the motor point (Kimura 2000). It was decided to stimulate the axons just proximal to the motor point of the muscle to avoid damage to the end plates and prevent mass activation of the muscle (Trontelj & Stålberg 1992). Unless atrophied, the flexor carpi radialis (FCR) was easily identifiable on the medial aspect of the forelimb by its central position, fusiform shape, and its action of flexing the carpus. Using the Medelec *Stimulator A* probe (figure 17) and the *motor nerve conduction velocity* programme in Synergy, a stimulating square wave pulse of 0.5 μs and a constant current stimulus of between 30–40 mA was applied to the area of skin overlying the median nerve in the proximal upper forelimb.

Figure 17

Photograph of the Medelec *Stimulator A* probe and two-channel pre-amplifier.

The maximally contracting region was visible and the skin over this area was marked with a blue skin marker. The overlying skin was closely shaved and cleaned with 100% alcohol and an abrasive cleaning gel (Nu prep, D.O. Weaver and Co., 565-B Nuclaway, Aurora, Co-80011, USA). The stimulating cathode, a stainless steel monopolar needle electrode (disposable subdermal needle electrode, Medelec accessories, Oxford instruments, Old Woking, UK) was inserted 0.5 cm distal to the putative motor point (to avoid stimulation or damage to the main branch of the median nerve as it entered the muscle belly). The anode, a similar monopolar needle electrode, was inserted into the tendinous part of FCR at its attachment to the medial epicondyle of the humerus (approximately 3 cm proximal to the motor point of FCR on the medial aspect of the forelimb). The electrodes were connected to the corresponding cathode and anode ports in the Medelec Stimulator A probe.

A supramaximal stimulus was delivered in order to ensure that the threshold EPP was being reached. The delivery of a supramaximal stimulus was ensured by observing the current required to produce maximal contraction of the FCR muscle fibres and then increasing this current level by 15–20%. A large current above threshold was not desirable because of the possibility of damage to the axons or direct stimulation of the muscle cells.

The concentric monopolar needle was connected to the DIN port 1 of the pre-amplifier. Square wave electrical pulses of 50 μs duration at a rate of 10 Hz were delivered to the muscle via the anode. A current of 1.90–3.00 mA and 2.00–5.00 mA, in normal and re-innervated FCR muscles respectively, was required to ensure a supramaximal stimulus.

The display was set with a full scale deflection (f.s.d.) of 10 ms and a voltage gain of 1 mV cm^{-1}. A high pass filter of 500 Hz and low pass of 10 kHz were used. This was important with the monopolar needle in order to decrease recordings from distant muscle fibres which were more often detected by the larger recording surface area of the monopolar electrode (Stålberg.E. & Trontelj 1994).

The recording concentric needle was introduced through the skin to the muscle in an oblique orientation and then gradually rotated through an angle of 90° while being slowly withdrawn. This had been found in previous studies to increase the ease of detecting action potentials (Lawson & Glasby 1998; Starrit 2004). The stimulating current was not applied via the anode until the concentric needle had been inserted into the muscle. This prevented damage to the muscle fibres and decreased the formation of haematomas.

Recording was initiated by sustained pressure on the right-hand footswitch for 1–2 seconds. A train of 100 stimulating pulses was applied and the single fibre action

potentials produced were recorded. The recorded action potentials were displayed on the left hand side of the Medelec display screen. Horizontal marking windows had to be placed to record measurements of the interpotential intervals (IPI) from the regions of the curve closest to the isoelectric baseline. This represented the point at which the recording surface of the needle was perpendicular to the wave of depolarization and so small movements of the needle during recording had less effect on the recorded action potential. The marking window was placed on the action potential recorded from the muscle fibre at the straightest, steepest portion of the curve and usually on the upward slope as recommended by Stålberg and Trontelj and Kimura (Stålberg.E. & Trontelj 1994; Kimura 2000).

The Medelec automatically calculated the value of jitter from the variation in the IPI between each recorded action potential using the equation:

$$MCD = \sum \left(\frac{(IPI_{n}) - (IPI_{n-1})}{n} \right)$$

where:

MCD = mean consecutive difference

IPI = interpotential interval

n = number of action potentials

The mean consecutive difference in times of transmission of nerve impulses measured by microneurography down one nerve fibre to innervation of one muscle cell has been shown to be less than 4 μs (Kimura 2000). Therefore a measurement of *TSJ* that was

< 5 μs was considered to come from direct stimulation of a muscle fibre and was not incorporated within the results.

Three recordings were taken from one site of insertion and then the position of the needle was moved to another area of muscle and twenty recordings of *jitter* were taken in each muscle. The Medelec automatically calculated the mean of the individual *TSJ* values.

Precautions taken in recording

Differentiation of single fibre potentials

As suggested by Kimura (Kimura 2000) a spike potential was accepted to be originating form one muscle fibre if it had a rise time of less than 300 μs and an amplitude of greater than 200 μV, had a straight rising or falling edge and, could be identified on the loudspeaker as a crisp, high pitched, clear sound. One slope of a double potential was sometimes used if it was possible to distinguish a clear, single, leading or falling edge which then became notched at one point along its slope, in which case, measurements of jitter were taken from the initial straight part of the curve.

The action potential recorded was chosen carefully to avoid imposition of one wave on another as this can cause a decrease in the measured jitter, at least from that of the muscle fibre with the larger value of jitter (Stålberg, Mihelin, & Trontelj 1992).

Bimodal Jitter

Thiele and Stålberg (1974) describe a bimodal distribution of single fibre action potentials occurring in approximately 1 in 20 recordings from normal muscle during SFEMG recording. When the mean IPI between these two potentials is small this may be caused by sub-depolarization of a second fibre by the immediately preceding action potential causing a changed propagation velocity, or, that the first fibre's action potential summates with the otherwise sub-threshold EPP of the second and causes a contraction. During re-innervation, the time delay between the two action potentials can be longer and may be due to uncertain conduction down a poorly myelinated nerve twig (Stålberg.E. & Trontelj 1994). Kimura (2000) suggests that both series of action potentials can be measured if they are separated by over 150 μs, but Thiele and Stålberg suggest only measuring from one or neither. In the present study, jitter was only calculated from one of the two action potentials.

Interference

Interference causes the slope of an action potential to be measured at varying points of its rising curve (Stålberg.E. & Trontelj 1994) leading to an artificially high value for jitter. To reduce interference during measurements the following measures were taken:

- All electrodes were cleaned with soapy water or alcohol and dried thoroughly in between sides and cases.
- The operating lights and diathermy were switched off.
- The leads of the stimulating, ground and electrocardiogram electrodes were kept away from the lead of the recording monopolar electrode.

- High voltage equipment in the vicinity e.g. freezers were turned off if there was evidence of a disturbed baseline prior to beginning recording.

The most common reason for an unsteady baseline was an abnormality in the grounding either due to poor apposition of the ground electrode with the skin of the sheep, a break in the insulation or wire of the ground or recording electrode or a poor connection between the electrodes and their sockets in the pre-amplifier.

Maintenance of concentric monopolar electrode

It was important to maintain a sharp point on the monopolar electrode to prevent damage to the muscle fibres upon the needles insertion. As suggested by Stålberg and Trontelj (1994), the point of the electrode was sharpened at an angle of 15° on an Arkansas stone and the opposite side to the beveled surface sharpened to create a plough shaped smooth tip. This was tested with a gauze swab or on the surface of a glove and even minor irregularities corrected. A magnifying glass was also used on occasion to examine the tip for irregularities.

Maximum conduction velocity

Measurement of maximum conduction velocity

After the measurement of *TSJ*, dissection of the chest wall and proximal upper forelimb was carried out to expose the median nerve as in the first operative procedure of neurotmesis and repair. There was wasting of the superficial pectoral muscle and an increase in fibrous tissue overlying the median nerve, brachial artery and ulnar nerve in all the groups that had undergone repair. The fibrous connective tissue overlying the

median nerve was carefully removed. An obvious plane existed between this fascia and the underlying median nerve, brachial artery and ulnar nerve. The proximal ends of the median nerve and ulnar nerve were easily recognizable (see figure 18). The ulnar nerve was dissected free from the brachial artery and divided.

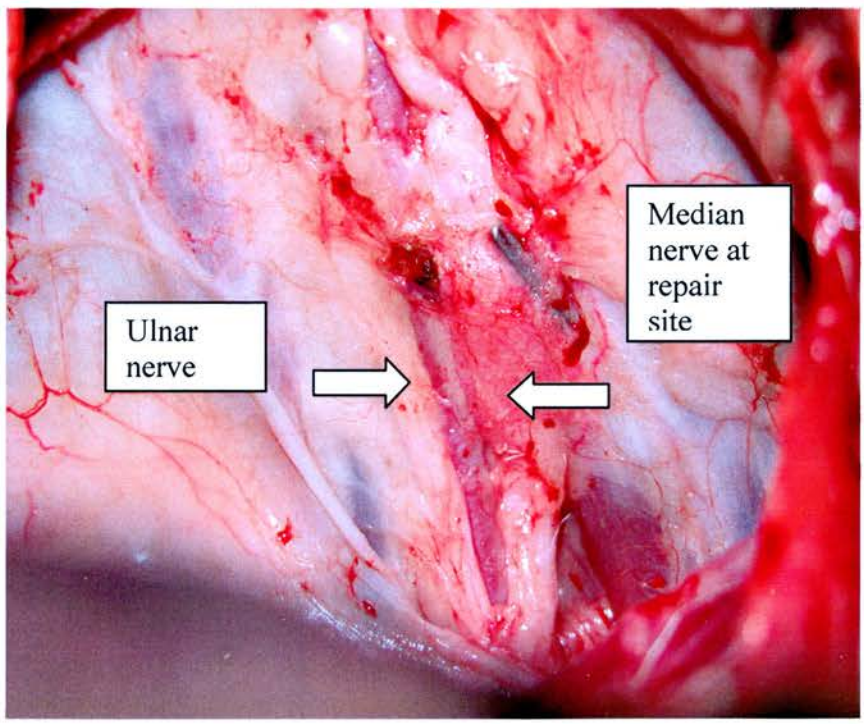

Figure 18

Photograph of operative site as seen after dissection to expose median nerve for nerve conduction studies

If there was any doubt about the continuity of the median nerve or the identity of the nerves, a fine bayonet nerve stimulator probe was connected to the Stimulator A probe of the Medelec and, using the *motor conduction velocity* programme, a constant current square wave impulse of 50 μs duration with a current in the range 0.8 mA and 5.0 mA was used to stimulate the proximal section of the nerves while the muscle contraction in the forelimb was observed. A contraction of FCR identified the stimulated nerve as the

median and confirmed that regeneration across the site of repair had occurred. Contraction of flexor carpi ulnaris (FCU) (a large muscle lying on the caudal side of the abducted forelimb and causing flexion of the wrist joint) identified the stimulated nerve as the ulnar nerve. The stimulating current used was limited to being just above threshold and a piece of rubber was placed under the stimulating cathode to prevent spread of the current from the intended site on the median nerve to the surrounding median, radial or ulnar nerves. The ulnar nerve was divided to prevent transmission of current down it.

The distal end of the median was now dissected from the surrounding connective tissue. The distal end was often covered by fatty tissue and various small vessels and could be difficult to localize. The brachial artery lay immediately caudal to the median nerve and could be palpated to help find the median nerve. A small transverse branch of the brachial artery with an accompanying vein often overlay the distal end of the medial nerve before the nerve dipped to enter the forelimb. These branches were divided and tied as they were of a reasonably large diameter and lay close beside the nerve. Strict haemostasis was maintained with bipolar diathermy (Malis Bipolar Coagulator and Bipolar cutter, Codman, Codman and Shurtleff, inc., Randolf MA 02368) to maintain the sheep's circulating volume and maintain a bloodless surgical field. Care was taken not to stretch the nerve or injure the brachial artery.

Two small rectangular sheets of rubber were placed under the median nerve both proximal and distal to the site of repair (figure 19). As long a length of nerve as possible was kept between these two regions when measuring the distance between the two points of stimulation. The rubber prevented transmission of the current to the surrounding muscles and nerves.

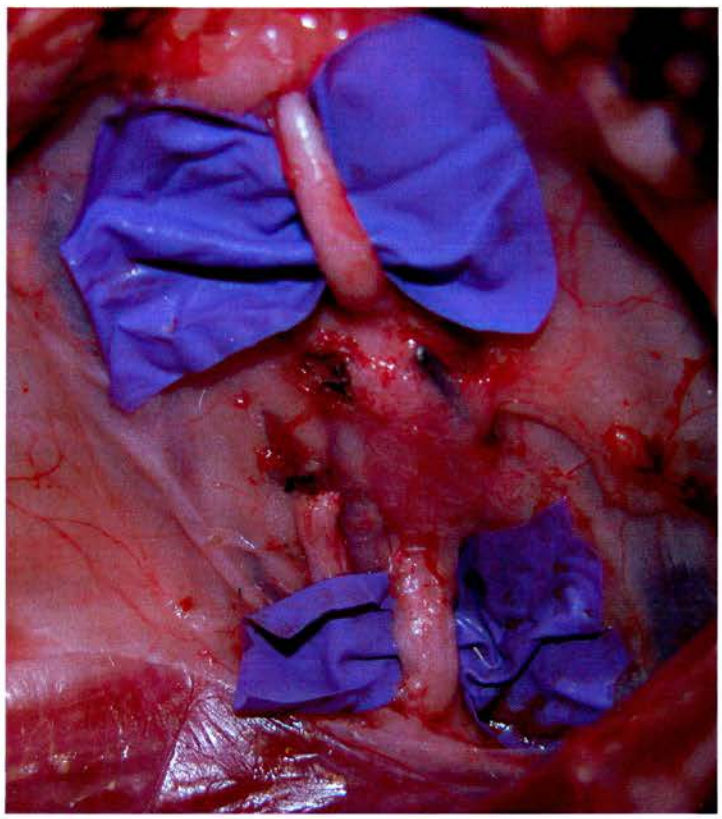

Figure 19

Photograph of dissected proximal and distal ends of median nerve in the axilla with rubber insulation in place and ulnar nerve divided. The brachial artery in visible on the left side of the median nerve and the divided ulnar nerve lies on the left side of the brachial artery.

A bipolar hook electrode was placed under the distal exposed end of the median nerve with the rubber insulation lying beneath. The length of nerve being stimulated was kept free from surrounding fluid. (Transmission of an impulse through fluid would be faster than conduction down the nerve. Current would therefore favour this pathway and transmission of the impulse would be conducted to another site in the nerve thus leading to inaccurate values for CV_{max}).

The hook electrode was held firmly in a fixed position by means of a clamp (designed by Brendan Hawes, Orthopaedic research department, Chancellor Building, Royal Infirmary Edinburgh) attached to a Layla retractor. The Layla retractor was fixed to the operating table. Care was taken not to stretch the nerve. (Both ischaemia and stretching of a nerve alters the function of axons and could have given falsely low results of maximum conduction velocity and increased minimum F wave values). Rubber insulation had been applied to the hooks of the electrode and a small hole cut on the inside surface of it as overlay the circular parts of the hook so that the electrode underneath was insulated except at the point of contact with the nerve. The electrode was connected to the Stimulator A probe of the Medelec. The cathode was connected to the distal hook and the anode to the proximal. The hook electrode was positioned on the median nerve distal to the repair site as seen in figure 20 (note also the divided median nerve to the right of the median nerve.

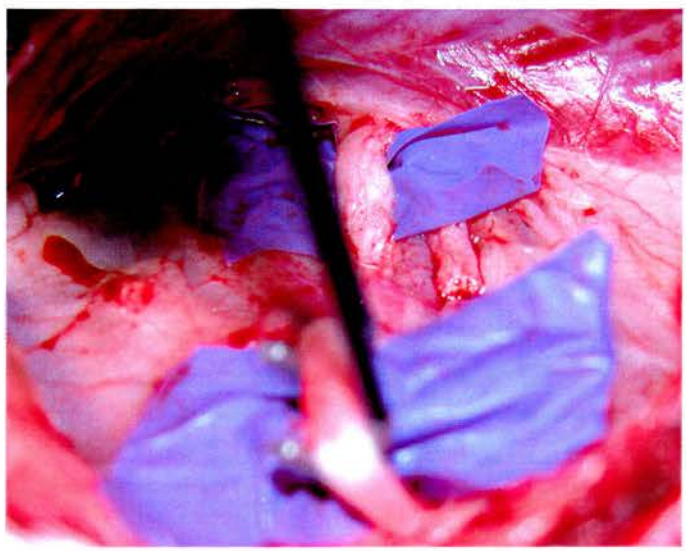

Figure 20

Photograph of the set-up for distal median nerve stimulation.

The position of the cathode was marked on the nerve using a fine-tipped blue skin marker. (One hook was the cathode, the other the anode. The cathode was positioned so that it was distal to the anode). Two surface 10 mm Ag / AgCl disposable disc electrodes (Meditec, S. Polodi torrible, Parma, Italy) were used to record CMAPs from FCR. Disk electrodes were chosen instead of needle electrodes as they give a less localized recording of a mass muscle response. Needle electrodes placed in a sub-dermal position over a muscle accurately, but selectively record the wave of depolarization passing perpendicular to their shafts (Kimura 2000). In this study it was important to measure accurately the wave of depolarization produced from the whole muscle upon stimulation of the median nerve. This was especially true in the repair groups because when regenerated neurones reinnervated muscle fibres, the normal arrangement of the motor unit is lost: instead of the muscle fibres in one motor unit being widely distributed throughout the muscle, they become grouped together.

The site of the motor point had been identified during the measurement of jitter but the motor point's position was marked again by stimulating the median nerve with the bayonet stimulator, observing the point of maximum contraction of the FCR muscle, and marking the skin over the area.

A small area was shaved approximately 2 cm proximal to the joint line of the knee where the FCR tendon ran, for the application of the reference electrode.

These areas were then cleaned with an abrasive cleaning gel (Nu prep, D.O. Weaver and Co., 565-B Nuclaway, Aurora, Co-80011, USA) and 100% alcohol. Electrode conducting paste (Ten 20 Conductive, D.O. Weaver and Co. D.O. Weaver and Co., 565-B Nuclaway, Aurora, Co-80011, USA) was applied to the surface of the disc electrodes.

The active recording electrode was positioned over the motor point and the reference electrode over the distal tendon of FCR. The disk electrodes were secured using 'Sleek' or zinc oxide tape which held them in closer apposition to the skin than suturing. The shorter the distance between the active and reference electrode the smaller was the stimulus artifact in the recorded signal. They were positioned approximately 3 cm apart, as recommended by Kimura (2000). EEG connecting wires (SPES Medica S.R.L., St. da Nuova Rivoltana, 53-S Pedrino diVignette, MI – Italy) connected the active and reference electrodes to the black and red input terminals respectively of the Medelec pre-amplifier. The ground electrode was in place as before.

The *Motor nerve conduction test* programme was selected from the Medelec Synergy software. Its settings were adjusted to:

- Sweep duration—20 ms (f.s.d.)
- High pass filter—500Hz
- Low pass filter—10kHz
- Pulse duration—0.1ms
- Stimulation rate—1 Hz
- Stimulating current range—0 to 25mA
- Gain—20mV

The stimulating current delivered by the hook electrode was gradually increased from zero until a CMAP with the maximum amplitude was obtained. To ensure a supra-maximal stimulus, a current 20–30 % larger than the current which produced a CMAP of maximum amplitude, was delivered. This required a current in the range of

0.18–0.80 mA when stimulating a normal nerve, and between 0.60–2.40 mA when stimulating a repaired nerve.

A point was now marked with blue dye as proximally as possible on the median nerve. The bayonet electrode was connected in place of the hook electrode to Stimulator A of the Medelec. The orientation of the cathode and anode points was not important when using the bayonet stimulator as it was possible to orientate it perpendicular to the length of the nerve because the tips of the anode and cathode lay within 3 mm of each other. The current was increased from zero as before to obtain a supra-maximal CMAP. This usually required a current of between 1.80–3.00 mA for a normal nerve and between 2.00–6.00 mA for a repaired nerve. The Medelec automatically calculated the latency difference between the two CMAPs.

The cursors placed by the Medelec indicated the start, maximum negative deflection, 2nd crossing of the isoelectric baseline, and maximal positive deflection. They often had to be manually placed to improve accuracy. As by convention, the latency was measured from the first negative deflection from the isoelectric baseline.

Often, a small positive deflection occurred prior to the negative deflection crossing the baseline. The causes for this were;

- Reversed connection of the active and reference electrodes to the pre-amplifier. (This was obvious and always corrected.)
- Poor positioning of the disk electrode leading to detection of contracting muscles surrounding FCR: It was necessary to reposition the active electrode to try and locate the motor point more accurately.

The position of the disk electrodes was altered to try and stop this occurring. If, after repeated repositioning of the electrodes this initial positive deflection persisted, the first marker was placed at the point at which the first negative deflection crossed the baseline as shown by the position the marker position in figure 21.

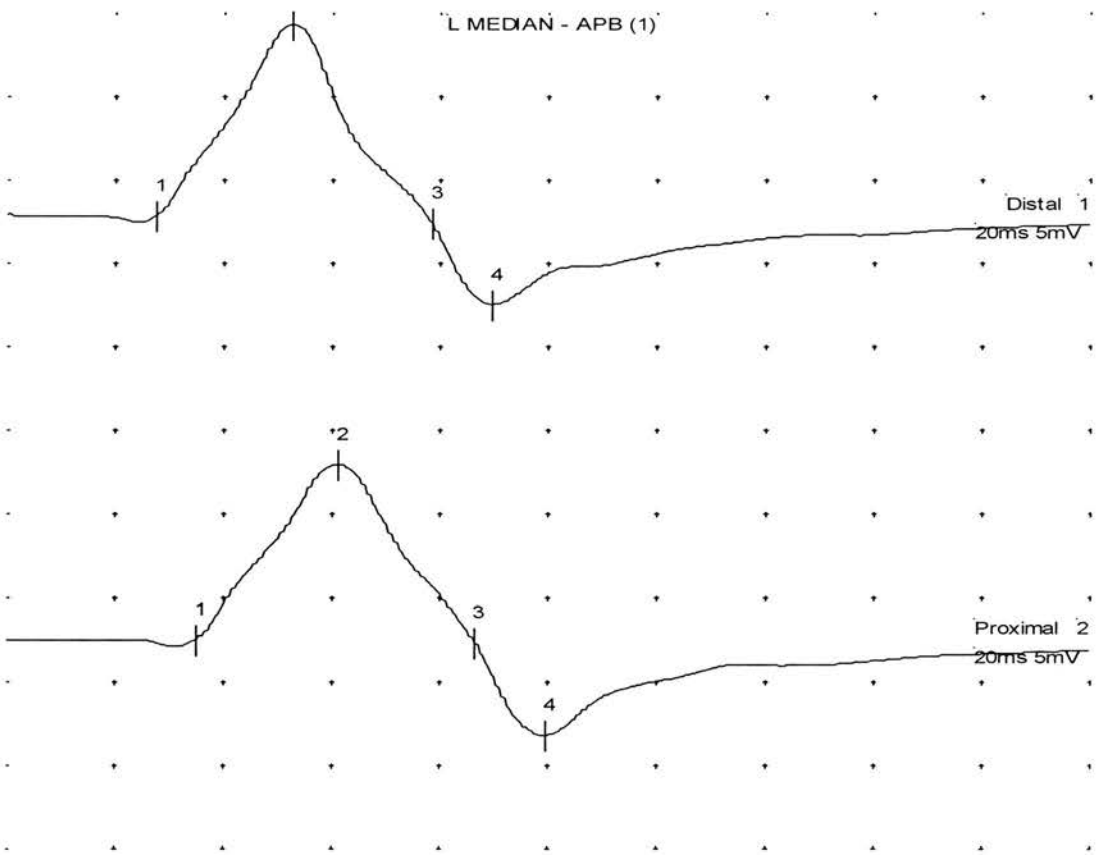

Figure 21

Traces showing the position of the placement of markers when the first displacement from the baseline is positive.

Compound muscle action potential shape

In the repair groups, the shape of the CMAPs obtained from distal stimulation was obviously different from the shape of the CMAPs obtained from proximal stimulation in the operated groups (figure 22) (a difference was also visible in the normal group and un-

operated nerves but was not so marked). Proximal stimulation often produced an action potential with multiple peaks. As the distance between the stimulating point and the recording point of the CMAPs increased, the delay in time between the action potential of the fastest and slowest conduction motor neurones reaching the muscle increased and hence produced more prolonged, multi-peaked, and lower amplitude CMAPs. Examples of CMAPs obtained on distal stimulation and proximal stimulation of the FCR muscle in a sheep who had received an epineurial repair are shown in figure 22.

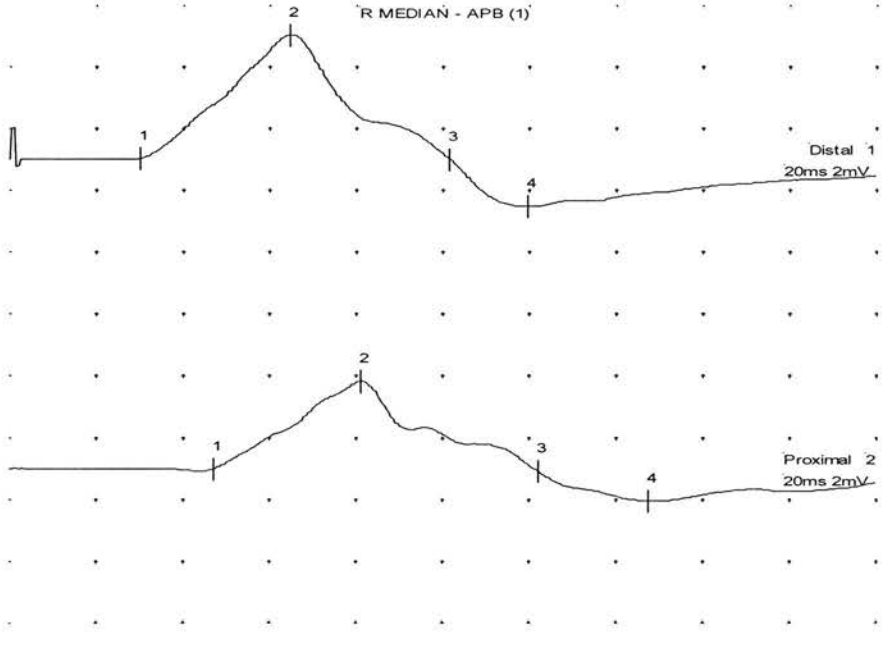

Figure 22

CMAPs measured from distal and proximal sites of stimulation of the median nerve seven months following epineurial repair.

Measuring the inter-cathode distance

The distance between the two cathodes was measured using a piece of silk or linen suture and cutting it to the length between the two marked stimulation points and then

measuring its length using a tape measure. This was accurate to approximately 0.1 cm. The suture adhered to the nerve by surface tension effect and allowed the measured length of the nerve to include curvatures in its course.

The measured distance between the two points of stimulation was entered in the results table of the Medelec programme. The conduction velocity was calculated automatically from the difference between the two latencies. For example, considering a median nerve stimulated at two points, S_1 (distal) and S_2 (proximal), the latencies of the CMAPs measured form these two stimuli were called L_1 and L_2 respectively (see figure 23).

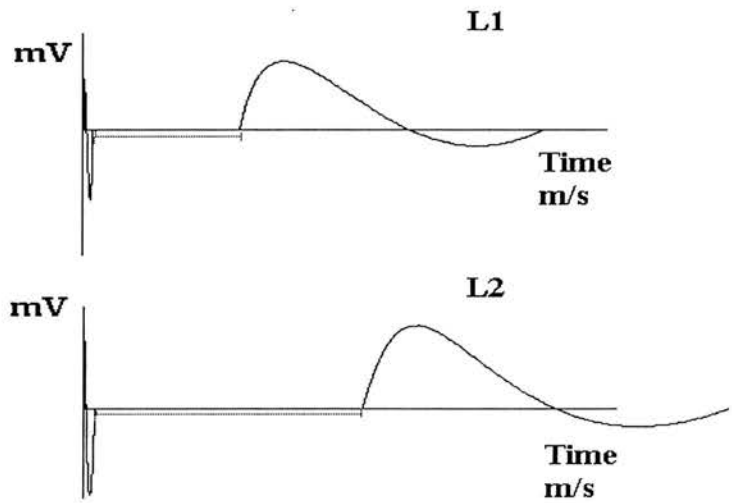

Figure 23

Diagram demonstrating the CMAP latencies from distal and proximal stimulation of two points along a peripheral nerve

The distance between the two points of stimulation was *D*. The maximum conduction velocity in the nerve was therefore calculated by the formula:

$$CV_{\max} = \frac{D}{(L_1 - L_2)}$$

Where:

CV_{max} = maximum conduction velocity (m s^{-1})

D = distance between points of stimulation on the nerve (m)

L_1 = CMAP latency from proximal point of stimulation (ms)

L_2 = CMAP latency form distal point of stimulation (ms)

The calculated maximum conduction velocity and distal latency were recorded in the results sheet and saved in the synergy file for that sheep.

The temperature of the exposed tissues in the axilla was now measured with the Raytek infrared thermometer (Raynger MX2, Raytek, Milton Keynes,UK) and recorded on the results sheet.

Motor latency (*M lat*)

The M wave is the first motor response produced by a muscle in response to stimulation of its supplying nerve, in this case the motor response of FCR on stimulation of the median nerve. The *M wave latency* (ms) was recorded during measurement of CV_{max} as time between stimulation of the nerve (at the distal site of stimulation) and the first negative deflection from the baseline of the CMAP. The *M lat* (ms) measurements could

then be used in the calculation of *peripheral latency* (ms) which will be described after the subject of the *F wave*.

F wave

Physiology

The *F wave* was first described by Magladeny and McDougal who recorded it from intrinsic foot muscles leading, presumably, to its name 'F wave' (Kimura 2000). The F wave is a late response produced by recurrent orthodromic transmission of an initial antidromic transmission of a stimulus along an α-motoneurone (illustrated in figure 24).

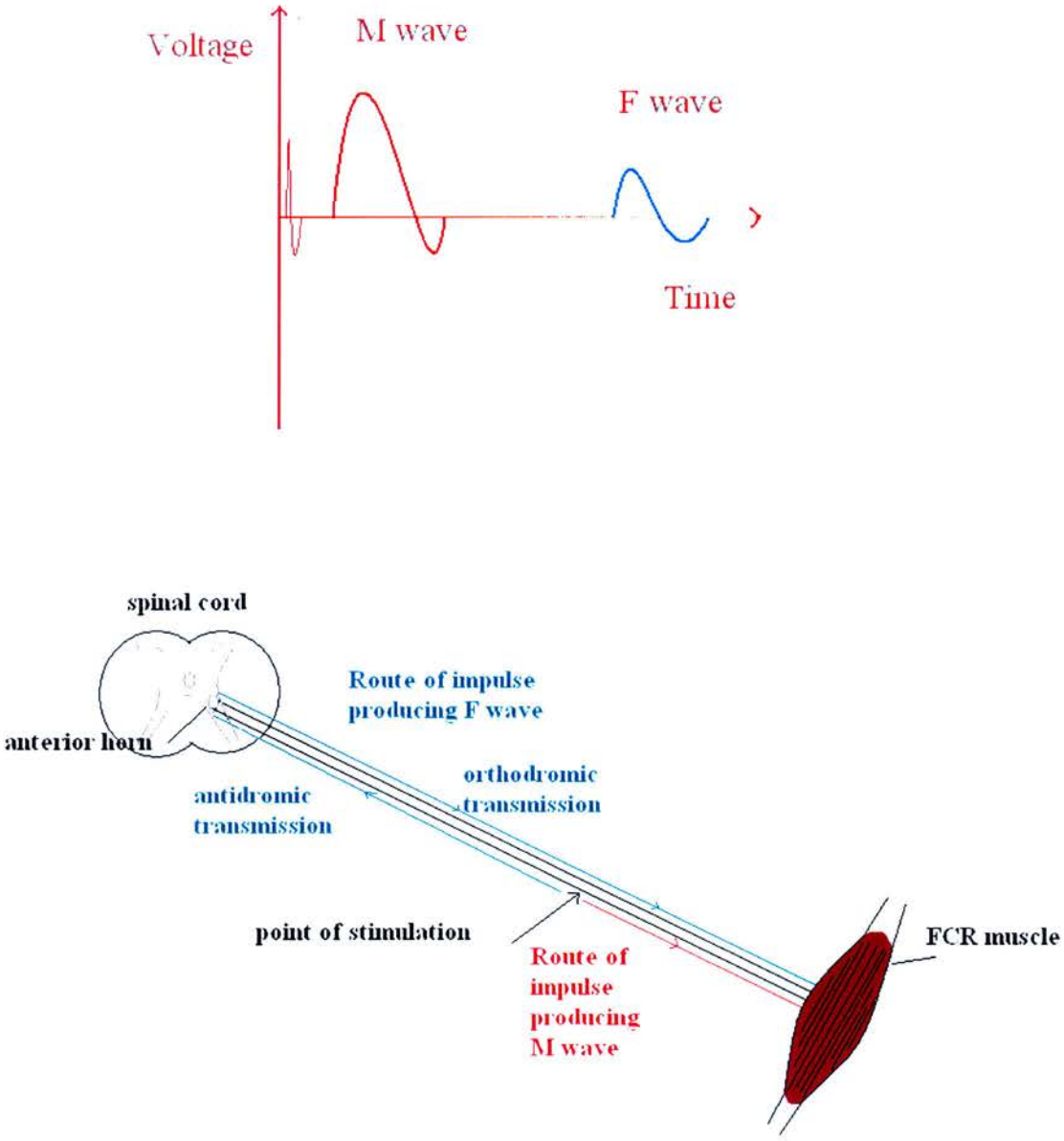

Figure 24

Pathway illustrating the production of an F wave

The diagrams in figure 24 illustrate the pathway of conduction that causes production of an F wave. Because the action potential which produced an F wave travels first towards the spinal cord, measurement of F wave latency can be used to measure conduction velocity in the proximal section of the motor pathway. This was of benefit to assess the speed of conduction in the region of the motor nerves proximal to the repair site.

F min

The minimum F wave latency (F_{min}) recorded was used for comparison between groups in the results. The fastest conducting fibres should produce an F wave with the shortest latency. This measurement was thought to be the best for making comparisons between the groups of the regeneration of the motor axons.

F wave conduction velocity

The speed of conduction in the proximal section of a nerve has been found by many authors to be faster than that of the distal segment (Sunderland 1978).

Using the values for F min, the distance from the point of stimulation on the nerve to the spinal cord, and the motor latency, the speed of conduction in the fastest motor neurones of the F wave was calculated using the equation:

$$Conduction\ time_{(proximal)} = \frac{(F - M - 1)}{2}$$

Where:

F = F wave latency (ms)

M = M wave latency (ms)

The reason for subtracting '1' from '$F - M$' in the formula above is because animal and human studies have shown that the shortest refractory period allowing the conduction of an orthodromic action potential after arrival of the antidromic action potential in a spinal α motoneurone is approximately 1.0 ms (Kimura 2000).

The F wave conduction velocity can then be calculated from the formula:

$$FWCV = \frac{(2D)}{(F - M - 1)}$$

Where:

$FWCV$ = F wave conduction velocity (m s^{-1})

F = F wave latency (ms)

M = M wave latency (ms)

D = distance between point of stimulation on peripheral nerve to spinal cord (mm)

Measurement of F waves

The measurement of the F wave was made directly after the measurement of CV_{max}. The hook electrode was still in position at the distal end of the median nerve with the rubber insulation underlying it. The hook electrode was reconnected to the Stimulator A probe of the Medelec and this time the anode was connected to the proximal fork of the hook electrode and the cathode to the distal. The Ag / AgCl disk electrodes were kept in the same position as when measuring CV_{max}. The *F wave* programme was selected from the Medelec Synergy test menu.

The settings chosen were as follows:

- Pulse width—0.05 ms
- Rate of stimulation—0.5 Hz
- High pass filter—500 Hz
- Low pass filter—10 kHz
- Sweep duration—50 ms (f.s.d.)
- Stimulating current—0 to 25mA

A supramaximal response was elicited as with CV_{max} measurements. On pressing the 'Aquire' button on the mainframe of the Medelec, a train of ten pulses at a frequency 0.5 Hz were delivered. The Medelec automatically recorded the M wave and F wave responses (see figure 25). Minimum, maximum and mean F wave latencies for the train of ten stimulating pulses were automatically calculated.

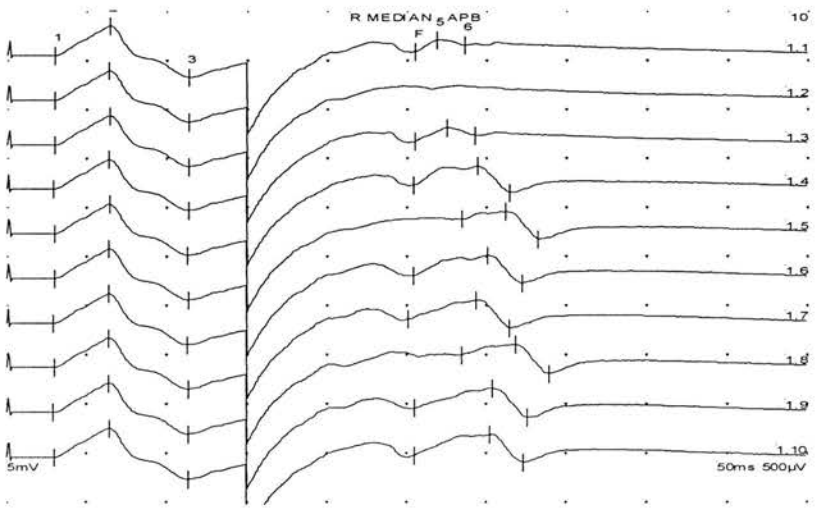

Figure 25

Copy of the display from a train of ten stimulating pulses and the M wave and F wave responses elicited and marked by the Medelec from a nerve repaired by epineurial suturing.

If no F wave was elicited, the level of stimulus was checked to ensure it was supra-maximal. The pulse duration of the stimulus was changed by increasing it from 0.05 to 0.1 ms. Again a supramaximal stimulus was given. This did not result in the production of F waves.

If the sheep seemed to be very deeply anaesthetized, the delivery of halothane was decreased by approximately 0.25% (e.g. from 2.5% halothane to 2.25%) while ensuring that the sheep's level of anaesthesia did not become 'light'. In one out of four such attempts an F wave was then recorded.

The F wave does not occur with every supramaximal stimulus to an α-motoneurone. Kimura (2000) states that, 'In normal subjects, F wave frequency varies, with a mean of 79 percent, and most responses occur only once during a rain of 200 stimuli.'

F wave production could have failed for several reasons:

- Failure of the axon hillock to repolarize prior to the arrival of the spike potential generated in the somadendrite membrane
- Excessive depolarization (e.g. during voluntary muscle contraction) of the somadendrite membrane leading to early generation of the spike potential causing it to arrive at the axon hillock again prior to the axon hillock's repolarization
- Failure of the antidromic action potential to enter the cell body owing to blocking at the axon hillock or more distally in the cell body
- Collision of the F wave and M response owing to a short distance between the point of stimulation of the α-motoneurone cell body (e.g. in the axilla in humans)(Kimura 2000)

- Suppression of spinal α-motoneurones by halothane and nitrous oxide (Freidman, King, & Rampril 1996; Rampril & King 1996)
- Failure of antidromic propagation of the action potential owing to damage to the peripheral nerve which follows dissection (Lundborg 1988)
- Failure of antidromic propagation of an impulse owing to stretching at the site of hook electrode placement (Lundborg 1988)

The reason for the less frequent production of F wave on the operated side was not fully understood. The normal side was the second side to be operated on and the question of whether the time under anaesthesia or a drop in peripheral temperature could influence the production of F waves. The average values for peripheral temperature were 33.0 °C and 32.8 °C for the right (operated) and left (un-operated) sides respectively. This minor difference is unlikely to have had any influence F wave production.

Peripheral latency

Using the measurements of *F min* and *M lat*, the time for an impulse to travel from the anterior horn of the spinal cord, where the cell bodies of the motor neurones are positioned, to the muscle fibres of FCR, can be calculated.

The peripheral latency (*P lat*) (ms) is then calculated by the formula:

$$P\ lat = \frac{\left(F_{\min} + M\ lat - 1\right)}{2}$$

The peripheral latency gives a measure of the time taken for transmission along the whole nerve from the spinal cord to the FCR muscle. This measure is therefore useful as a measure of conduction velocity in the whole length of the peripheral nerve.

Central conduction latency

Damage to peripheral nerves has been shown to alter the arrangement of cell body connections in the anterior horn of the spinal cord (Myles, Gilmour, & Glasby 1992). It was attempted to measure the central conduction latency by stimulating the motor cortex of the sheep over the region corresponding to F_z, the position over the precentral gyrus, in the 10-20 system used in the human (Delisa et al. 1994). Corkscrew electrodes were positioned in the scalp at 1–3 cm lateral to F_z point and an external stimulator (Digitimer Stimulator Model DS7) with a high voltage supply was connected and triggered to deliver a 100 V square wave pulse of 100 μs duration. This failed to produce a response. A second method using a high output magnetic coil placed over the area of the precentral gyrus was then undertaken. Again, there was no response in the muscle twitch and so the measurement of central conduction latency was not pursued further.

ISOMETRIC TWITCH TENSION

The force generated by a muscle on contraction can be used as an objective measurement of the muscle's capacity to do work. The measurement of isometric twitch contraction is a reliable method of testing muscle function as it is easier to accurately measure a force produced than a change in length of the muscle (Kettle 2003; Starrit 2004).

Peak Isometric twitch tension measurement

After the measurement of F wave latency, the forelimb was removed from the arm rest and the ground electrode detached from the Medelec pre-amplifier. The olecranon was exposed through a 6 cm longitudinal skin incision. The soft tissues and periosteum were

excised from the olecranon. An electric drill was used to make a vertical hole in the olecranon perpendicular to its medial surface and a 6 cm cortical, self-tapping screw was inserted. While drilling this hole, it was important for an assistant to hold the forelimb abducted at an angle of 90° to the vertical. Holding the limb in this manner prevented the screws bending when they inserted into the olecranon fixation device (shown in figure 26).

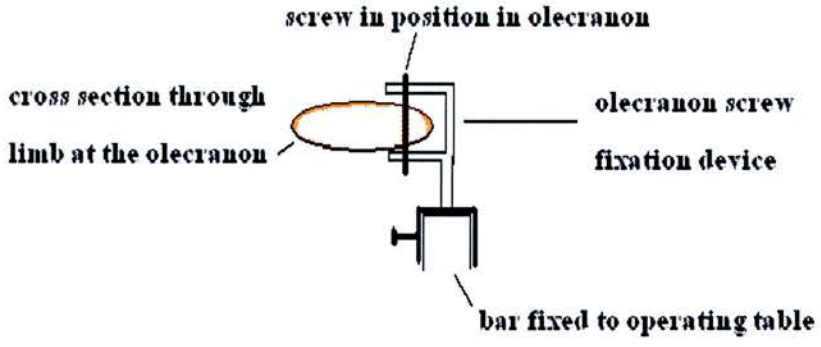

Figure 26

Diagram of the olecranon fixation device in cross section

The tendons of flexor digitorum superficialis (FDS) then had to be prepared. FDS is supplied by the median nerve. It arises from the medial epicondyle of the humerus and has a long tendinous distal portion which inserts into the volar surface of the second phalanx (May 1970). The tendons were easily accessible in the forelimb and could be attached to the force transducer to pull the arm of the transducer in the normal line of the muscle's action.

A longitudinal incision was made in the midline of the posterior lower forelimb from the posterior carpal bones to the skin overlying the second phalanx. The double tendon of

FDS was dissected from its attachment to the second phalanx. The FDS tendon lay superficially and was usually covered by a fine network of veins. The epimyseum and connective tissue attached to the tendons was divided at the proximal end towards the carpal bones. No dissection was carried out proximal to the distal muscle fibres of the superficial and deep bellies of FDS. Using a 2/0 silk or polyglactin tie, the distal end of the FDS tendon was looped back on itself and the suture tied to form a loop of tendon at its distal end. A 1/0 linen tie was then threaded through this loop and knotted to from a series of loops with slip proof knots resembling a chain.

The vertical screw through the olecranon was then inserted into the olecranon screw fixation device which was fixed to a horizontal bar which, in turn, was fixed to the table. The limb was taped around the phalanges distally to a horizontal bar which was fixed to a rigid stand as shown in figure 27.

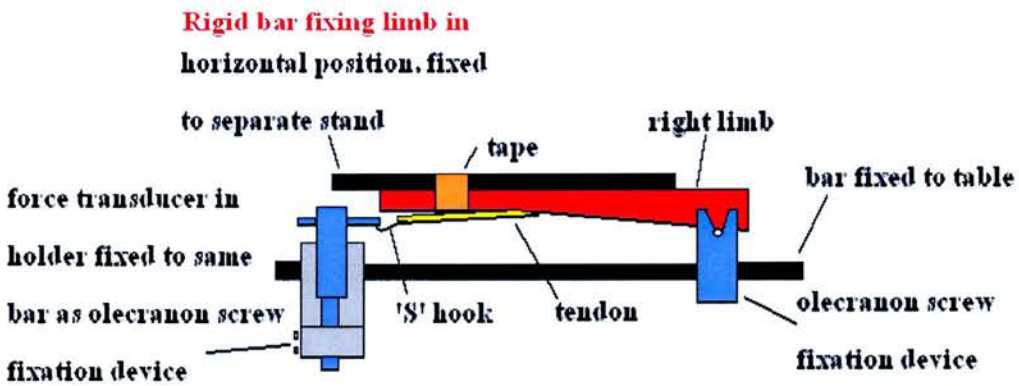

Figure 27

The limb was fixed in position by securing it to two rigid bars. The force transducer and the olecranon screw fixation devices were rigidity secured to the same bar which was fixed to the operating table. The limb was secured to a separate bar which was firmly attached to a rigid vertical stand which was fixed to the ground.

A Grass FT10E (Grass Telefactor, Warwick, RI, USA) tension transducer was rigidly fixed to another specially designed holder which attached to the same horizontal bar as shown in figure 27.

One of the linen loops was hooked over the 'S' hook of the tension transducer (Grass FT10E tension transducer, Grass Telefactor, Warwick, RI, USA).

Alignment

Force is a vector. The force transducer only records the force in the direction of pull of the arm of the transducer. It was therefore important to align the forelimb such that the line of pull of FDS was the same as the arm of the tendon transducer and in the same direction as the pull of the muscle *in vivo*.

The output from the tension transducer was passed through a PII strain gauge amplifier (Grass Telefactor, Warwick, RI, USA). This analogue signal was then digitized by an analogue-digital converter (Pico ADC 212, Picotech Ltd.). This signal was then input to a laptop computer (Hewlett Packard (hp) pavilion zt1121s). The Picosoft software enabled the laptop to function as an oscilloscope (figure 28). The digitized twitch tension curves were displayed on this screen, saved, and then opened in Microsoft Excel (Microsoft, inc.) as a text file.

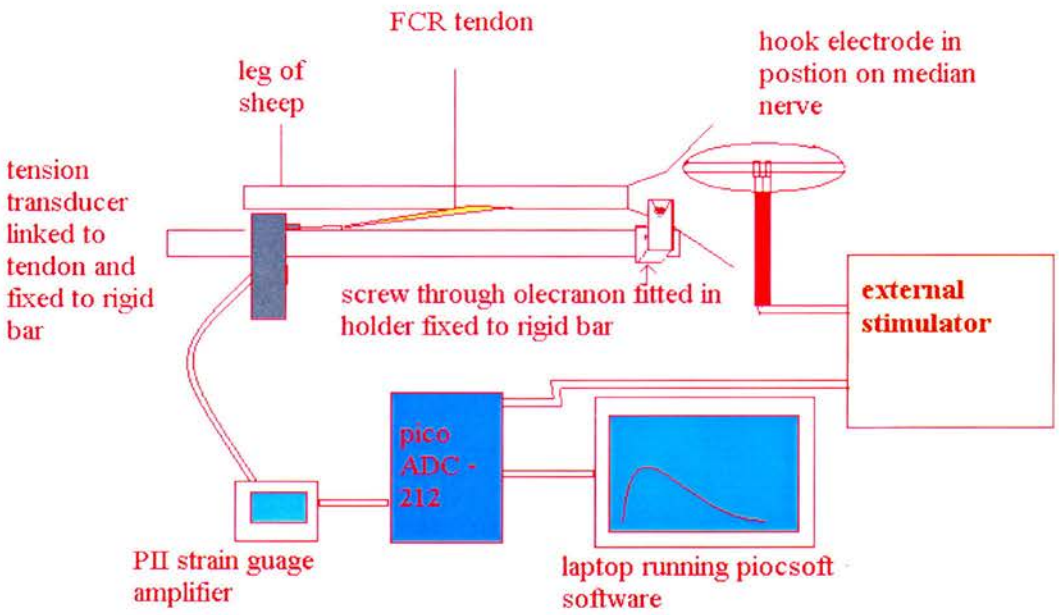

Figure 28

Diagram of the setup used in the measurement of the isometric twitch tension of the FDS muscle

Determining the initial tension applied to the muscle

Muscle contains a contractile (active) component and an elastic (passive) component. The total tension developed in a muscle during an isometric twitch is equal to the sum of the passive and active elements. The force generated by a muscle at a fixed length varies according to its degree of elongation from its resting length. Because of the elastic nature of components (connective tissue, sarcolemma, blood vessels, and nerves), when a muscle is stretched beyond its resting length, the passive tension increases. There is a point of stretch beyond which the maximum force of contraction produced by a muscle will decrease. This occurs when the elongation is such that the overlap between the thick (actin) and thin (myosin) filaments decreases.

The length of a muscle at which its maximum isometric twitch tension is produced is close to its resting length. Shortening velocity decreases as the load on a muscle increases. Muscles produce a maximum shortening velocity with no load. Because of this variation of maximum isometric twitch tension with the stretch of a muscle beyond its resting length, every effort had to be made to ensure that each muscle was stretched by the same initial load.

The length of the FDS muscle bellies from their origins near the medial epicondyle of the humerus, to their tendinous junctions adjacent to the carpus, was measured. The muscle was linked to the force transducer by the 'S' hook. A series of test measurements with the muscle stretched to various initial lengths showed that a maximum isometric twitch was produced when the resting length of the muscle was increased by 5%.

The tension associated with a 5% increase in the muscles resting length gave a reading of 0.22 V on the Grass PII strain gauge amplifier. Every time a new muscle was attached to the tension transducer the muscle was lengthened until the same initial reading of 0.22 V was produced on the strain gauge amplifier.

The median nerve divides before its entry into the proximal forelimb into two branches; a smaller inferior branch, the musculocutaneous nerve; and a larger superior branch, the main median nerve (Ashdon & Done 1984). To be sure that the main branch of the median nerve alone supplied the FDS muscle, the maximum isometric twitch tension of FDS was tested in two sheep by stimulating the large main branch of the median and then both branches together. There was no difference in the peak isometric twitch tensions obtained and so it was accepted that the large main branch of the median nerve was the

only supply to the FDS muscle and so this branch alone was stimulated in all subsequent experiments for isometric twitch tension measurement.

A problem was encountered with one sheep which had a fixed flexion contracture of 90° at the knee on the right forelimb. It was not possible to release the contracture surgically. This meant that it was not possible to get a straight line of pull between the line of action of the muscle and the tension transducer during isometric twitch tension measurement. An isometric twitch curve was therefore not measured for this sheep.

The stimulating bipolar hook electrode was positioned on the large branch of the median nerve distal to the site of previous repair. The electrode was held in place by a Layla retractor and clamp which was then attached to the operating table by a clamp on the Layla retractor. The leads of the hook electrode were attached to the output of the external stimulator (Digitimer Stimulator model DS7, Welwyn Garden City, Hertfordshire, England) which was set to supply a stimulus of approx 100 V per square wave impulse.

The time base of the oscilloscope selected was 50 ms per division, the voltage display '± 1.0 V', the input current to 'channel A' was set to 'DC' with 'channel B' set to, 'off', and the trigger set to 'single' and 'rising'. The stimulator source was set to 'external'. Recording began when the received input from the ADC-212 rose above 0.0 V.

The output from the tension transducer was in volts (V). It was necessary to convert this output in volts into the corresponding force in newtons (N). Three pairs of springs were supplied with the tension transducer. These controlled the amount of movement of the transducer's arm per unit of force applied according to their Young's modulus.

$$Young's\ modulus = \frac{stress}{strain}$$

$$= \frac{(force/area)}{(elongation/original\ length)}$$

The red springs were chosen because the entire range of forces produced in the experiments could be accommodated by the range of movements made by the transducers arm.

A calibration curve had been plotted for each spring by hanging weights of a known size from the transducer arm and plotting the d.c. output in volts (V) against the force applied in newtons (N). For the red set of springs the force applied to the transducer arm related to the d.c. output of the transducer according to the equation:

$$Force(N) = Voltage\ output_{tensiontransducer}(V)/1.6155$$

Analysis of isometric twitch

From each isometric twitch curve recorded, the variables calculated were:

- Maximum isometric twitch tension (N)
- Maximum rate of change of force (dN/dt) (N s^{-1})
- Time to peak tension (ms)
- Time to $R_{½}$ (ms)
- Work done in contraction to time $R_{½}$ (time tension integral) (J)
- Time tension index (J s^{-1})

Maximum isometric twitch tension (PN) (N)

This is a value for the maximum force that is able to be produced by the muscle twitch. Denervation results in a decrease in the myofibrillar component of muscle (Grieve et al 1991; Sunderland 1978).

Maximum rate of change of force (dN/dt_{max}) ($N\ s^{-1}$)

This corresponds to the rate at which crossbridges form in the muscle, and may be related to the type of muscle fibres present (i.e. fast-twitch or slow-twitch) and also to the maturity of the reinnervation. It is possible for de-innervated muscle fibres to be reinnervated anywhere along their length by any type of motor neurone (Sorbie & Porter 1969). If a fast-twitch muscle fibre is reinnervated by a nerve that usually supplies a slow-twitch muscle, the reinnervated muscle fibre behaves like a slow-twitch muscle. Therefore, if the rate of change of force is decreased, this may be because more slow-twitch fibres have regenerated or because the reinnervation of the muscle is not fully completed.

Time to peak tension (PT) (ms)

When a small voluntary contraction occurs, motor units with slower contraction times and greater resistance to fatigue are recruited first. With stronger voluntary contractions, motor units with faster contraction times and less fatigue resistance are recruited. The high voltage stimulus delivered directly to the nerve during twitch tension analysis in the present study is likely to be the equivalent of a strong voluntary contraction. If more slow-twitch than fast-twitch fibres have regenerated there will be a longer time to peak

tension. Partial denervation leads to longer contraction times and decreased twitch tension

Time to $R_{½}$ ($R_{½}$) (ms)

Ideally one would measure the total contraction time but contractions tend to tail off and there is not an easily definable end to them, or if there is, it is often longer than the display duration. In previous work, the value for the time to half relaxation has been used as a defining point from which to make measurements of the *relaxation time* and *total work done in contraction* (Grieve et al 1991; Kettle 2003; Starrit 2004b).

After denervation, the enzyme activity of myosin ATP-ase decreases, leading to a prolongation of contraction and therefore a long $R_{½}$. With reinnervation, muscles tend to regain their previous fast properties (if innervated by a fast twitch neurone) but this may not be complete (Grieve et al 1991). A prolonged $R_{½}$ could therefore be evidence of ongoing denervation or, re-innervation by nerves usually supplying slow twitch muscle fibre.

Work done in contraction to time $R_{½}$ (TTIG) (J)

The area under the force / time graph for a muscle contraction equals the ability of the contracting muscle to increase the potential energy of a mass by lifting it against gravity, i.e. the amount of energy the muscle can transfer to another object (Kettle 2003; Lenihan et al 1998; Starrit 2004).

Time tension index (TTI) ($J\ s^{-1}$)

The time tension index is calculated by dividing the total work done to time $R_{½}$ (J) by the time $R_{½}$ (ms) and gives a value for the average work done in the muscle throughout the contraction, i.e. the number of fibres recruited for contraction on average throughout the twitch (Carter et al. 1998).

The peak voltage output (mV), time to $R_{½}$ (ms), any initial offset from a baseline of zero, and the time to peak voltage (ms) were marked on the recorded oscilloscope curve. These values were recorded on the results sheet. The whole curve was then copied into Microsoft Excel as a text file.

Analysis of the curve

The values of force produced and time up to time $R_{½}$ were copied into Datafit (Oakdale engineering, 23 Tomey Rd, Oakdale, PA 15071, USA), in order to find the curve with best fit by regression analysis. Differentiation was then applied to calculate the maximum rate of change of force (dN/dt_{max}) of the contraction.

Invariably, the tenth order polynomial curve was the best fit. A graph of force against time for the input data and the fitted tenth order polynomial curve was produced. Using the values of the tenth order polynomial curve; the maximum force of contraction (PT), the maximum rate of change of force (dN/dt_{max}), and the area under the curve (J), were calculated.

WET MUSCLE MASS

After denervation, striated muscle undergoes atrophy, degeneration and fibrosis.

In atrophy, the fibre diameter decreases and the sarcoplasm is lost. Myofibrils become irregular, lose their parallel arrangement, fragment, and disappear. Lysosomes appear among the fibrils. Mitochondria decrease in size and number and then disappear. The basic structure of the muscle fibre remains. Based on experiments carried out on the Australian opossum, Sunderland reported that limb muscles may survive denervation for 485 days without progressing to degeneration. In the FCR of the opossum, after 224 days, 78% of the muscle had undergone degeneration. Sunderland also reported that the size of the fibres decreased at a greater rate than the mass of the muscle and attributed this to an increase in the surrounding fibrous tissue (Sunderland 1978).

Connective tissue forms 10–25% of normal muscle (Weiss & Edds 1946). After denervation there is a relative increase in connective tissue. Some authors have reported an increase in collagen fibres and connective tissue. Sunderland (1978) described that a change appeared first in the perimyseum, with an increase in the number of fibroblasts; then in the endomyseum, with peak of cellularity (fibroblasts). He found that the amount of fibrin deposition was not consistent. The amount of fibrosis present in denervated muscle was found by Bowden and Guttman (1944) not to be solely dependant on the duration of denervation. The transformation of muscle fibres into fatty tissue is not necessarily related to the duration of denervation (Sunderland 1978).

In the present study, when reinnervation had completely failed due to dehiscence of the nerve repair, it was noted that there were considerable adhesions between the FCR and the underlying muscle bellies of FDS (see figure 29).

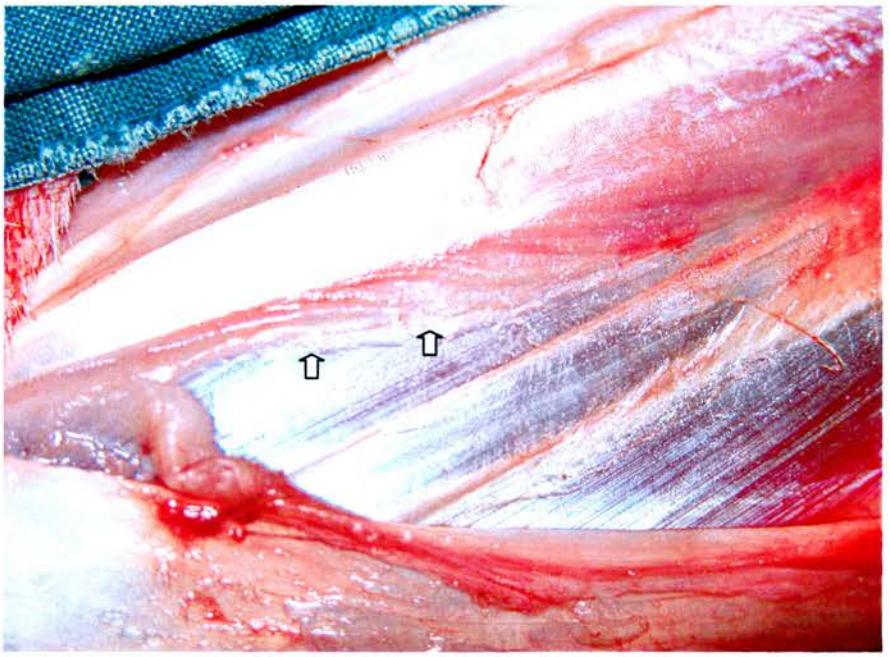

Figure 29

Photograph demonstrating adhesions (arrows) from FCR to the underlying FDS muscle following failed epineurial suture repair.

Measurement of Wet Muscle Mass

The sheep was given a lethal intravenous injection of pentobarbitone. The muscle bellies of flexor carpi radialis (FCR) was excised bilaterally. Distally, the FCR muscle belly was divided at its junction with its tendon and proximally, it was removed directly from the medial epicondyle as it has only a very short tendinous attachment at that site. The excised muscles were weighed immediately on scales (Mettler AE 163) that measured to an accuracy of 0.0001 g. When recording the results, because of the possible errors in the amount of muscle excised, the mass was considered significant to 0.01 g. Muscles excised from a sheep in the epineurial repair group are shown in figure 30.

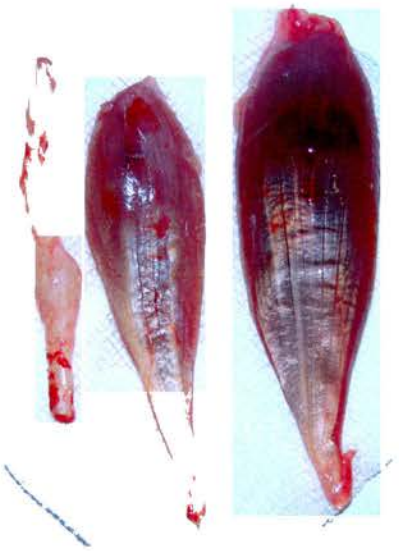

Figure 30

Photograph of the excised FCR muscles from a sheep following a successful epineurial repair

MORPHOMETRIC ANALYSIS

The distribution of fibre size in mixed nerves is markedly bimodal (Aitken et al 1947) with peaks at approximately 7 μm and 16 μm. Sensory and motor fibres make up both groups (Aitken et al 1947). Motor fibres in humans range in thickness between 2 μm and 20 μm. and can be divided into two groups. One group has diameters ranging from 10–17 μm with a peak of the distributions between 14–15 μm. This, the larger group of motor fibres, provides 70% of the innervation to a normal muscle. The second group have a range of diameters between 2 μm and 8 μm with a peak in the distributions between 5 μm and 6 μm and provide the rest of the motor innervation to a normal muscle (Sunderland 1978).

When neurones regenerate the normal bimodal distribution is lost. After nerve regeneration, there is a shift in the size of neurones within the regenerated nerve towards the left of the spectrum (i.e. smaller, more thinly myelinated fibres) (Guttmann & Saunders 1943; Lawson & Glasby 1998). There is a loss of the peak normally corresponding to the large diameter, fast conducting fibres of the A-α and A-β motor fibres as well as the type Ia, Ib and II sensory fibres (Lawson & Glasby 1998; Lawson & Glasby 1995) which correspond to the neurones of muscle spindles and tendon organs (Lawson & Glasby 1995).

Ultimate fibre diameter depends on the formation of appropriate peripheral connections e.g. motor axon to muscle fibre (Aitken et al 1947; Aitken & Thomas 1962) and on the timing of the repair (Aitken et al 1947). After nerve division and suture there is a marked increase in the number but decrease in size of nerve fibres in the regenerating nerve end (Aitken et al 1947). As regeneration continues, the number of nerve fibres decreases as the nerve diameter and axon diameter increases.

Preparation and fixation of the nerve specimen

After the completion of the isometric twitch tension measurement, a 1–2 cm length of nerve distal to the site of repair was cut from the median nerve. The fatty and connective tissue was excised from around the nerve. This prevented uneven penetration of the fixation solutions (Aitken et al 1947). The section was placed on a piece of labeled card and then immediately in a solution of 2.5% gluteraldehyde (Agar Scientific Ltd, Essex, UK) in 0.1 M sodium cacodylate buffer for one hour at room temperature. This caused the specimen to stiffen. The specimen was then removed from this solution and placed on a sheet of dental wax. Using an Olympus SZ 40 dissecting microscope and

microsurgical forceps the ends of the specimen were trimmed with a razor blade (these ends were then discarded) and the remaining specimen cut transversely into 1 mm sections. These sections were replaced into the 2.5% gluteraldehyde (Agar Scientific Ltd, Essex, UK) buffer solution and left for approximately twenty hours. The specimens were then washed in three washes of 10% sucrose buffered with sodium cacodylate (30 minutes for each wash on a rotating rack) and then placed on a standing rack for three hours in a 0.1% solution of osmium tetroxide (Agar Scientific Ltd, Essex, UK) in 0.1 M sodium cacodylate buffer. The osmium tetroxide buffer was then removed and the specimens were washed in three washes of 10% alcohol solution for twenty minutes at a time while on a rotating rack. The specimens could then be left in 10% alcohol overnight. It is known that shrinkage due to this fixation and dehydration process is unlikely to be more than 10% of the original volume (Boyd & Davey 1968).

The specimens were then placed in Araldite for 36–48 hours at room temperature and then arranged into moulds. Care was taken to orientate the specimens so that their cross-sectional surface was parallel with the end of the mould. (When using the microtome, this allowed the specimens to be inserted directly into the holding block without the need for first mounting them in a separate block.) The sections of the mould were then filled with Araldite and placed in the oven for a minimum of 72 hours at 60°C. The Araldite polymerized forming a solid block.

Creating slides

The specimen was mounted in the holding block and excess Araldite trimmed using a microscope to enhance vision of the specimen and a razor blade to cut. A Reichart U3 microtome (C.Reichart, Austria) was used to cut 0.75–1.00 μm ultra-thin sections. The

specimen was trimmed using a glass knife. Any irregularities in its cutting edge could lead to damage to the section. The cut specimens were floated on a water bath and transferred to slides using a fine metal probe. The slides were then placed on a heated tray to evaporate excess water. One set of approximately four sections was stained with toluidine blue dye. A few drops of the stain were placed on the specimen, enough to cover it completely, and observed until a green halo was seen around the rim. Although this did not occur in a specific time, it had been found by previous fellows (Lenihan 2002) to be the most reliable method of avoiding over staining and has since been used as a staining technique. The slide was then washed in tap water with a very slow flow and allowed to dry.

Toluidine blue (Wolman 1971) stains tissue nuclei, the cytoplasm of some cells and the Nissl substance of neurons orthochromatically, giving a blue colour. Other tissues such as connective tissues stain metachromatically, giving a purple or red colour (Kiernan 2003; Vowles & Francis 2002).

Systematic randomized sampling

It has been shown that examination of 200 neurones is adequate to represent the distribution of diameters in a whole nerve (Mayhew 1988; Mayhew 1990). Mayhew examined various techniques of sampling a portion of nerve fibres from the total number of fibres in multifascicular and unifascicular nerves (Mayhew & Sharma 1984a; Mayhew & Sharma 1984b) in order to find a technique that gave an accurate value of the mean axon and fibre diameter of the axons in the whole nerve without measuring every neurone. He demonstrated that by dividing a cross-sectional specimen of multifascicular nerve into 100 equal squares and measuring the axon and fibre diameters in every 16th

square, a derived result for the mean axon and fibre diameters and myelin sheath thickness was obtained which varied by only 4% from the results obtained when every neurone was measured. The time taken using the sampling method was however less than one tenth of that required when every nerve fibre was measured (Mayhew & Sharma 1984a). Mayhew concluded that this method of *systematic randomized sampling* was efficient and accurate compared with measuring every fibre. The same technique was used in the present study.

The specimens were approximately 2 × 3 mm in diameter on the slides. Microscopy was performed using the Jenamed Variant microscope (Carl Zeiss, East Germany). Initially a 3.2 × objective lens with a 10 × eyepiece lens and an eyepiece graticule with a grid of 5 × 5 mm, 0.5 mm pitch (NE10A, Pyser-sgi Ltd, Kent, UK) was used to visualize the nerve.

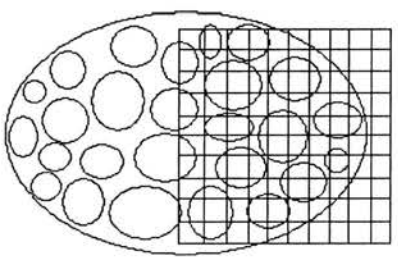

Figure 31

Diagram of image seen under microscope at 3.2 × objective lens power with graticule image superimposed as seen when viewing slide on microscope.

By noting the position of the graticule in relation to the fascicles (see figure 31), every 16th square seen through the grid was then viewed at higher magnification (100 × objective lens using oil immersion) and photographed using a camera (Kestrel 25

compact TV camera) mounted above the microscope. A diagram of the set up of the microscope, camera and networked computer (with AIS software) is shown in figure 32.

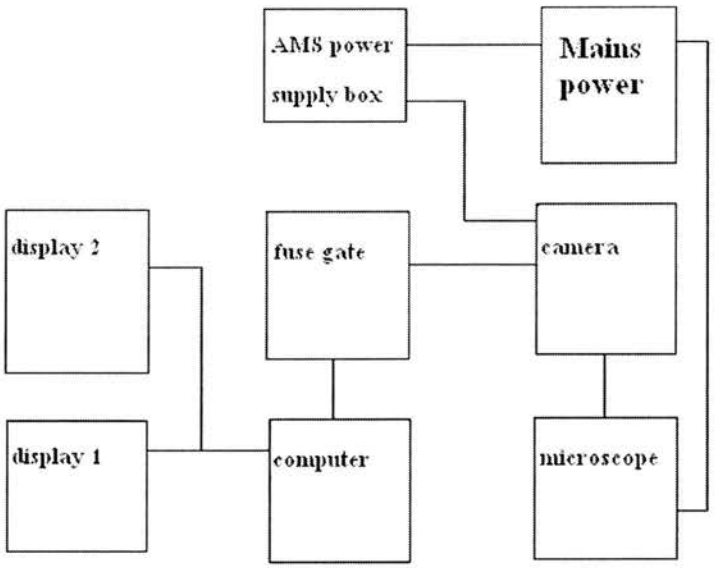

Figure 32

Set up of equipment used to photograph nerve sections and store them as TIFF files on network.

The images were saved in tagged image file format (TIFF) and were retrieved on a distant computer at a later time. About ten images were stored for each specimen.

Measurement of axon and myelin sheath diameter

The images were viewed using the *Analytical Image Station (AIS)* software version 3.0 Rev 1.3 (Imaging research Inc., Brock University, St. Catherine's, Ontario, Canada, L2S 3A1) on a Compaq professional workstation 6000). AIS enabled the measurement of the sizes of images imported in TIFF format and the automatic calculation of the mean and standard deviation of the measured distances. The measurements were taken across the outer points of the myelin sheath at the narrowest point. This was because if fibres were

cut obliquely in cross section their shape would appear elliptical. The shortest diameter of the ellipse would be closest to the diameter of a perfectly transverse section. By selecting the 'region' (e.g. axon or sheath) being measured prior to the placement of the cursors across it, the AIS programme automatically groups the measurements made and if requested, will calculate the mean of the measurements as well as the maximum and minimum values, and the standard deviation of the sample.

Every myelinated fibre in the field was measured except those that bordered the left and upper edges of the field (as per accepted protocol), or those that were very elongated or were very irregular in outline suggesting that a node of Ranvier had been traversed. The shortest vector that crossed the centre of the fibre was always measured. At least 200 nerve fibres were measured in each section. The recorded measurements were transferred to a Microsoft excel spreadsheet (Microsoft inc.) and used to calculate the g-ratio and create histograms of fibre and axon size.

MECHANICAL PROPERTIES OF THE NERVE

Two sets of nerves were tested from each of the repair groups with both the normal and repaired side being tested so that a comparison could be made. This was felt to be sufficient as early tests on several sets showed that the nerves did not tend to break at the site of repair and in fact, most of the repaired nerves broke at a higher stress than the normal nerves.

Methods

Sunderland and Bradley (1961) comment that it was more difficult than expected to prevent slippage of the nerve specimens from their holding sutures and that if great care

was not taken, much greater elongation than expected could be recorded. To prevent slippage of the nerves and any holding sutures during testing, a new method of holding the nerve specimens was designed. Two holding blocks were manufactured that could be fixed on a tensile test machine (Instron, Zwick / Roell 2005, Southern Avenue, Leominster, Herefordshire, HR6 0DH).

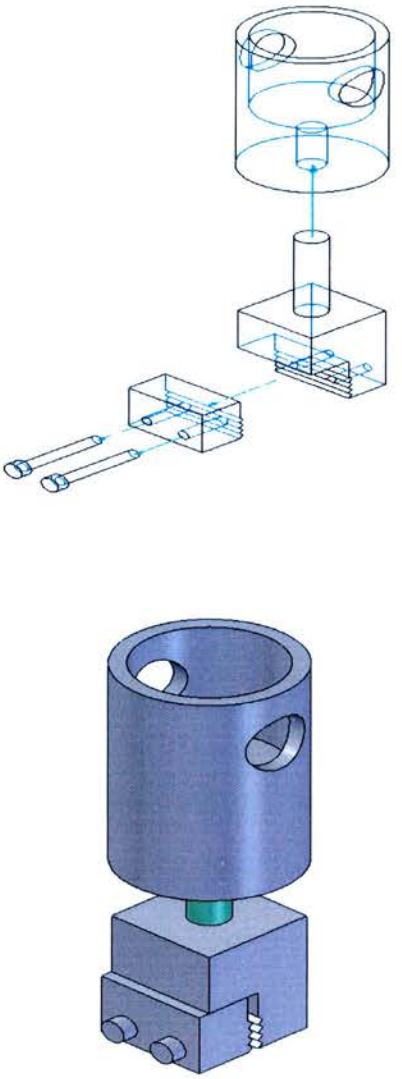

Figure 33

Holding blocks for nerve specimens (reproduced by permission of Mr Brendan Hawes)

The holding blocks were designed to have serrated edges as shown in figure 33. These were filed so that the nerves would not be severed on their edges. The blocks were produced by the medical physics workshop, Teviot Place, University of Edinburgh, Edinburgh. A photograph of the setup of the nerve holding blocks connected to the tensile test machine is shown in figure 34.

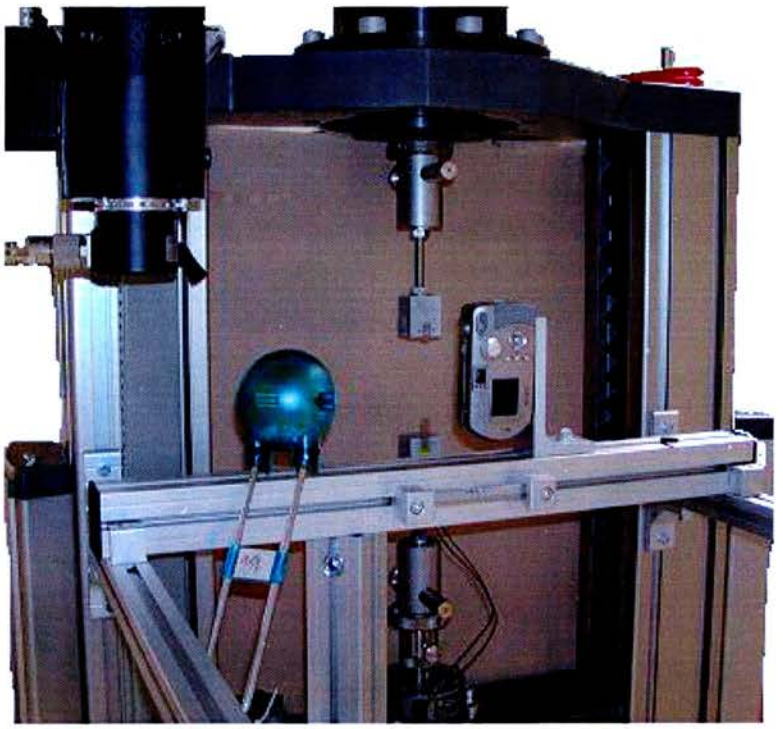

Figure 34

Photograph of the tensile test machine with the holding blocks attached and the digital camera (Cybershot, Sony) in a fixed position for recording a video of the stretch testing

By setting up a digital camera (Cybershot, Sony, MPEG movie VX, Smartzoom DSC-P92, 5.0 Megapixels. 3 x optical zoom) with a video recorder facility it was possible to record the site of breakage of each nerve specimen.

The Instron was linked to a Dell Optiplex CUX 260 PC (Dell, UK) which ran the software 'TestXpert'. This programme allowed control of the Instron to cause a certain rate of stretch of a material while recording the stress (force per cross sectional area), strain (elongation per unit initial length) and Young's Modulus (stress per unit strain, a measure of a materials stiffness) of the material under testing.

Fixation of nerve within blocks

Several variations of preparing and positioning the nerve in the blocks were attempted before a method was found which prevented slippage of the nerve specimens (seen in figure 35) from between the blocks.

Figure 35

Photograph showing excised segments of the repaired and normal median nerves from the CRG-wrap repair + Tisseel glue group

All surrounding loose connective tissue from the distal ends of the nerve specimen was removed. The epineurium was then divided longitudinally and the fascicles spread like a

fan from both upper and lower sides. The ends of the nerve and the surface of the serrated blocks were then painted with isopropyl alcohol (Catalyst-C, M-line Accessories, Vishay Measurements Group, Stroudley Rd, Basingstoke, Harts, RG24 8FW) to remove any surface oil and increase the speed of bonding with the superglue. A small amount of cyanoacrylate adhesive (M-bond 200 adhesive, M-line accessories, Vishay Measurements group, Stoudley Rd) was then placed on each of the serrated surface of the holding blocks. The nerve was then placed perpendicular to the grooves on the surface of the holding blocks and its distal end was turned over by approximately 2 mm to create a bulge which lay just beyond or within serrated edges. The blocks were then placed over each other enclosing the nerve end, and the bolts tightened to secure them.

The nerve in one holding block was attached to the upper arm of the Instron. The second block was then attached to the lower arm of the Instron and the nerve inset as before. The distance between the two blocks was measured using electronic calipers and recorded as the initial length of the specimen. The width of the narrowest portion of the nerve was also measured in two perpendicular diameters. The narrowest portion of the nerve was chosen as this was thought to be the region that was most likely to correspond to the breaking point. The same force would be applied to the whole length of the nerve. The stress would be the greatest therefore at the point of minimum surface area and estimation of the stress at this level would give an upper limit for the stress applied at each length of the nerve. The surface area in the middle of the nerve was measured before any force was applied. As the force exerted on the specimen increased, the diameter of the specimen decreased. The ultimate breaking stress was probably much higher than the values which have been estimated from the surface area measured.

The settings on TestXpert were customized to give an initial separation speed of 100 mm min^{-1} until reaching a preload of 2 N. The speed of stretch was then programmed to continue at 50 mm min^{-1}. Yoshimura et al stretched the tibial nerves of rabbits at rates of 5 mm min^{-1}, 50 mm min^{-1}, 500 mm min^{-1}. As the rate of stretching increased, they found that there was an increase in the total elongation before breakage and an increase in the tensile strength. A fixed rate of elongation was therefore maintained during measurements on all the nerve specimens (Yoshimura et al 1989).

The test was programmed to stop when a 90% decrease in the maximum force had occurred.

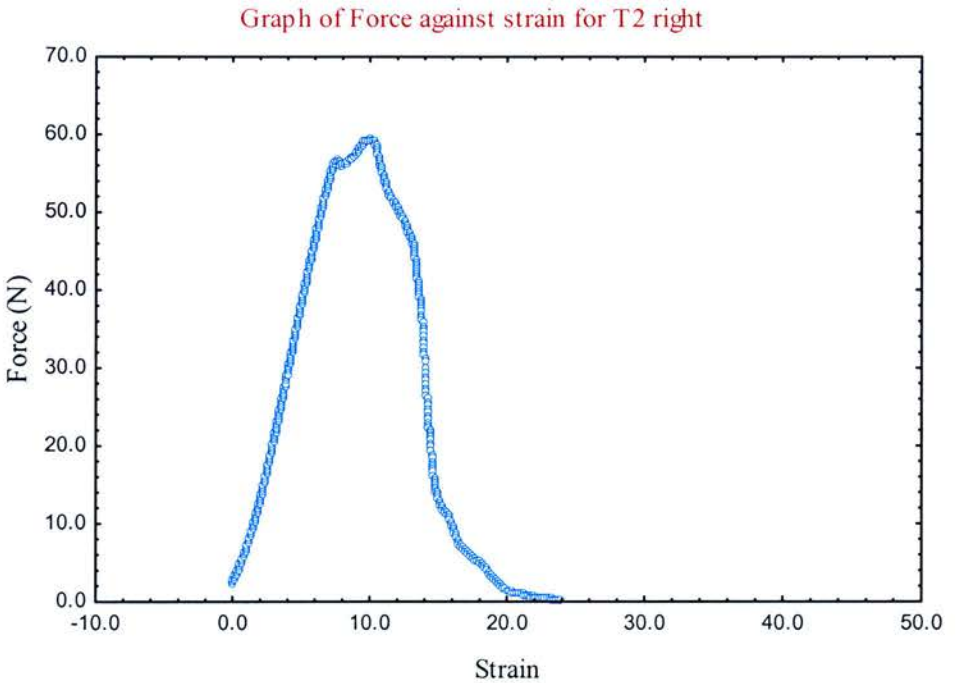

Figure 36

Graph of force against strain obtained on tensile testing of a nerve repaired by CRG-wrap + Tisseel glue.

Two sets of nerves were tested from each group (except normal controls). The results were saved then imported into Microsoft Excel (Microsoft inc.) spreadsheet (using

commas as delimiting factors). The data was then copied into Datafit (Oakdale Engineering Ltd, Oakdale, USA) and graphs were plotted of force against strain (as in figure 36).

The values considered from each set of data were:

- *Ultimate stress*; the unit of force per cross-sectional area at tensile failure
- *Ultimate strain*; the amount of elongation divided by the initial specimen length at the point of tensile failure
- *Young's Modulus*; which gives a measure of the material stiffness. A difference in this value between operated and normal nerve specimens could suggest that the composition of the perineurium and epineurium of regenerated nerves was somewhat different from that of the normal specimens.
- *Work done to failure*; the work to tensile failure was calculated by integration of the area under the force / elongation curve
- *Normalized work to failure*; this was calculated by dividing the work to failure by the initial length of each specimen and allowed comparison between specimens by correcting for minor variations in the initial lengths of the specimens (Borschel et al. 2003).

Immediate tensile strength of repairs

By applying the same tensile force to the repairs immediately after completion it was hoped to establish the immediate tensile strength of the repair. The most important factor in this is of course was the occurrence of dehiscence in the *in vivo* repairs.

One of each type of nerve repair was carried out (two sheep were used in total and repairs were carried out on both upper limbs). Immediately following insertion of the CRG-wrap by each of the three methods or by epineurial suturing, the repair site of the median nerve was excised between the most proximal and distal accessible points. The specimen was placed in a moist environment in a plastic container. The specimens were attached to the nerve holding blocks as before and attached to the Instron (Instron, Zwick / Roell 2005, Southern Avenue, Leominster, Herefordshire, HR6 0DH). The settings were changed to account for a much lower breaking stress and breaking strain. The settings on *TestXpert* were customized to give an initial separation speed of 10 mm min^{-1} until reaching a preload of 0.1 N. The speed of stretch was then programmed to continue at 10 mm min^{-1}. The breaking stress and strain for the four samples was recorded.

The effect of freezing on the tensile strength of nerves

A literature search revealed no information on the effects of freezing on the tensile strength of nerves. In the initial group of tensile tests on the regenerated nerves, the nerves had always had a period of time in a freezer at -11°C. Although all groups were the same it was decided to use the pieces of median nerve that were freshly excised for the last experiment to obtain figures for the breaking stress and strain of unfrozen, fresh nerves.

The nerve ends were prepared as before and attached to the nerve holders. The settings on the materials tensile testing machine were changed to a preload of 2 N, initial speed of 100 mm min^{-1}, and a speed of stretch of 50 mm min^{-1}.

The stress / strain curves for all the tests above were recorded and the corresponding data exported as text files into Microsoft Excel (Microsoft inc.) for further analysis.

STATISTICAL METHODS

In the planning stage of the project, it was important to ensure that the results obtained would have sufficient power that it could be said that it was unlikely that the any differences found between the groups could have come from the same population of animals and just resulted by chance.

Statistical error

There are two main types of statistical error that can arise from poor planning of group size in a study:

- Type I error: The erroneous rejection of a true hypothesis
- Type II error: The erroneous acceptance of a false hypothesis

When testing the null hypothesis of, 'there is no difference in results between the experimental groups' in this study, an acceptable degree of risk of a type I error was considered to be 5%, i.e. $\alpha = 0.05$. Or put another way, a 95% probability that the results confirming a true null hypothesis are representative of those that would occur in any population of similar sheep was considered acceptable. The probability of detecting a type II error (β) is determined by the 'statistical power' of a study. A 10% risk of the erroneous acceptance of a null hypothesis was considered acceptable in this study. The power was therefore required to be 0.9. (Power $=1-\beta$, where β = the probability of detecting a type II error).

To calculate group size, the *Power analysis* module of Statistica (Statsoft, Tulsa, USA) was used with these values of α and β along with previously obtained results after median nerve repair in sheep following neurotmesis and repair by nerve graft or CRG-wrap. (Values for the mean maximum conduction velocity in the median nerve of sheep six months following neurapraxia, axonotmesis and neurotmesis, with repair by nerve graft, controlled release glass wrap and epineurial suture obtained by Starrit (2004) were used to give a value of what the expected difference could be between the groups in this study). The figures for CV_{max} and *wet muscle mass* of FCR were found by Starrit to vary significantly according to the degree of median nerve damage and so were appropriate to use in the calculation.

A one way analysis of variance (one way ANOVA) using the means and standard deviations of each different repair group and the overall standard deviation (Σ) (calculated using the 'Basic Statistics' function in Statistica) was used to calculate the Root Mean Standardized Effect (RMSSE). This allowed power to be plotted against group number as shown in the graph in figure 37.

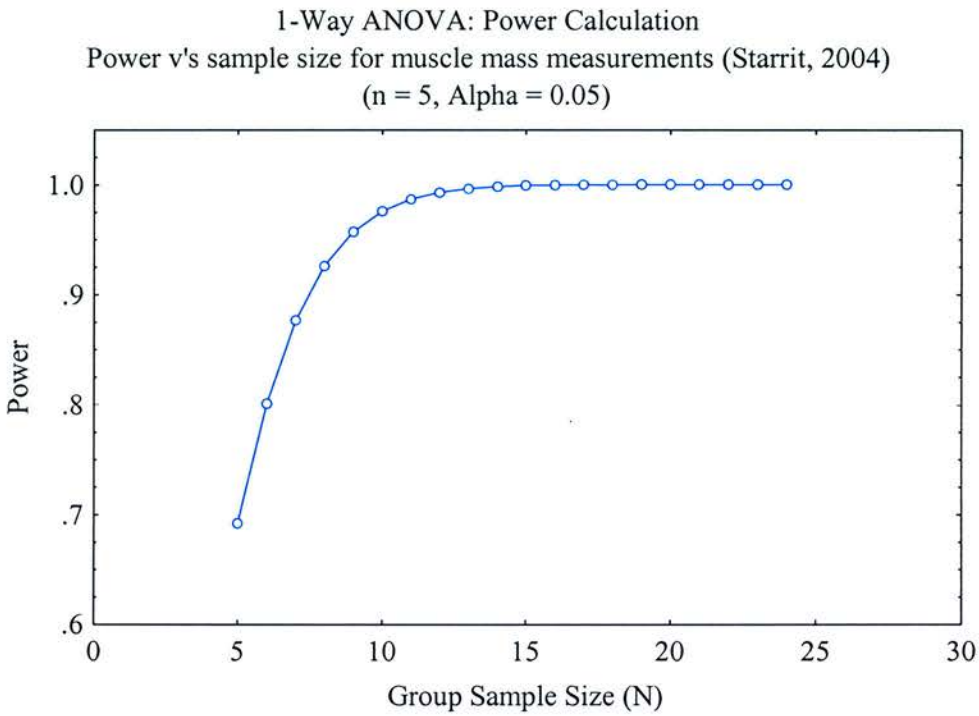

Figure 37

Graph of power versus group sample size based on muscle mass measurements (figures from Starrit 2004)

As can be seen from the graph in figure 37, a group size of nine would be required to give a power of 0.9 for one way ANOVA on wet muscle mass measurements from the operated limb only. It was expected that the differences in the values between our groups would be smaller as the type of injury inflicted was the same and the method of repair only differed on some occasions by the type of glue used. Also considered was the possibility of death of an animal within a group and so a group size of twelve was thought to be reasonable and not out with Home Office guidelines (HMSO 1986).

Analysis of results

The statistical methods employed had been used in the peripheral nerve research group for the appraisal of models of nerve repair in similar sized groups of animals (Fullarton et al. 2000; Fullarton et al. 2002; Fullarton et al 1998).

The data from each stage of the experimental work was inserted into one Microsoft Excel spreadsheet. The extreme left hand column contained the identification details of the sheep e.g. 'T1' identified the first sheep in the CRG-wrap + Tisseel glue repair group. A further column towards the left-hand side of the data sheet then recorded the group (the independent variable or grouping variable) to which each result belonged. The columns to the right of this recorded each measurement (the dependant variables) for that one sheep, for example; axon diameter, g-ratio, CV_{max}, etc. for both the right (red) and left (green) sides along with the ratio (black) of the right to the left sides. A section of the table is shown below in table 1.

Sheep	Opdate2	Weight	EXPT	Temp(°C)	TSJ	TSJ	TSJ
C1	17/03/2004	43	Control	38.2	7.96	10.49	0.76
C2	25/03/2004	42.5	Control		8.34	11.79	0.71
C3	31/03/2004	36	Control		9.21	10.12	0.91
C4	01/04/2004	45	Control	38.4	11.61	13	0.89
C5	05/04/2004	43	Control	39.5	9.39	9.46	0.99
C6	06/04/2004	55	Control	38.4	10.43	9.21	1.13
C7	13/04/2004	37	Control	38.4	10.16	10.33	0.98
C8	14/04/2004	38	Control	38.9	12.99	10.94	1.19
C9	15/04/2004	45	Control	38.4	9.89	11.5	0.86
C10	20/04/2004	37	Control		8.87	11.19	0.79
C11	21/04/2004	38	Control	38.1	12.74	11.16	1.14
C12	22/04/2004		Control	39.1	13.06	9.44	1.38
S1	30/06/2004	40	Epineurial	37.2		10.52	0
S2	30/06/2004	62	Epineurial	37.5	13.05	10.88	1.20
S3	05/07/2004	55	Epineurial	34.3	15.93	10.65	1.50
S4	05/07/2004	65	Epineurial	38.3	11.67	11.26	1.04

Table 1

Section of results table showing results from right side in red and left side in green and ratio of right over left in black

When all the results had been recorded in the table it was imported into Statistica (Statistica 7.0—Statsoft Inc.,2300 East 14th Street, Tulsa, O.K. 71404, U.S.A.). Outliers were identified and rejected by plotting *'half-normal' probability plots* in which the selected dependant variable is plotted in a scatterplot against the values 'expected from the normal distribution within the same mean and variance' for each dependant variable. The 'half-normal' probability plot only shows the positive values of the normal probability plot on the *y-axis*. An ellipse encompassing the 95% confidence intervals for the data was drawn around the points.

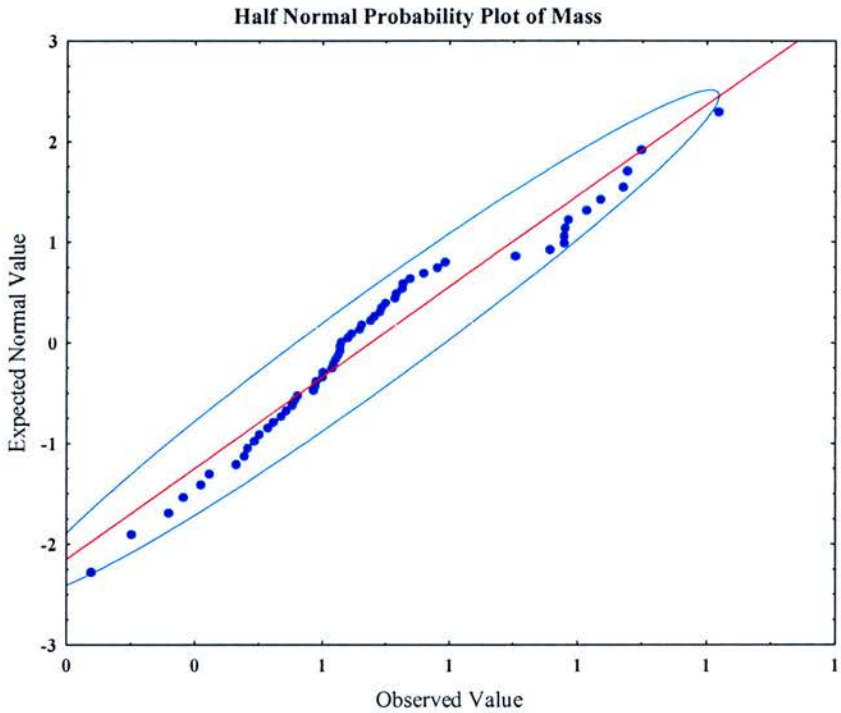

Figure 38

Half-normal probability plot of mass values

Each dependant variable was plotted in turn in this way. Any point lying outwith this ellipse (see figure 38) was considered an outlier and the value removed from the results table. This 'weeded data' was then used to determine the residuals of that variable. The residuals were re-plotted as normal probability plots and the *Shapiro-Wilk W test* applied to determine whether the weeded data were normally distributed. The distribution of the residuals was considered more important than the raw data, and the residuals often fitted a normal distribution when the raw data did not. Transformation of the raw data in this manner was useful as it decreased the need to use less sensitive non-parametric tests (Petrie & Sabin 2000).

Normal probability plots

The values of the independent variable are rank ordered. *Z* values (standardized values of the normal distribution) are computed based on the assumption that the data come from a normal distribution. The *Z* values are plotted on the y-axis against the observed values on the *x-axis*. In normally distributed data, a straight line plot is formed as in figure 39. The fit of the computed line was then tested by applying the *Shapiro-Wilk W test*. If the *W statistic* was significant ($p<0.05$), the hypothesis that the data is normally distributed was rejected.

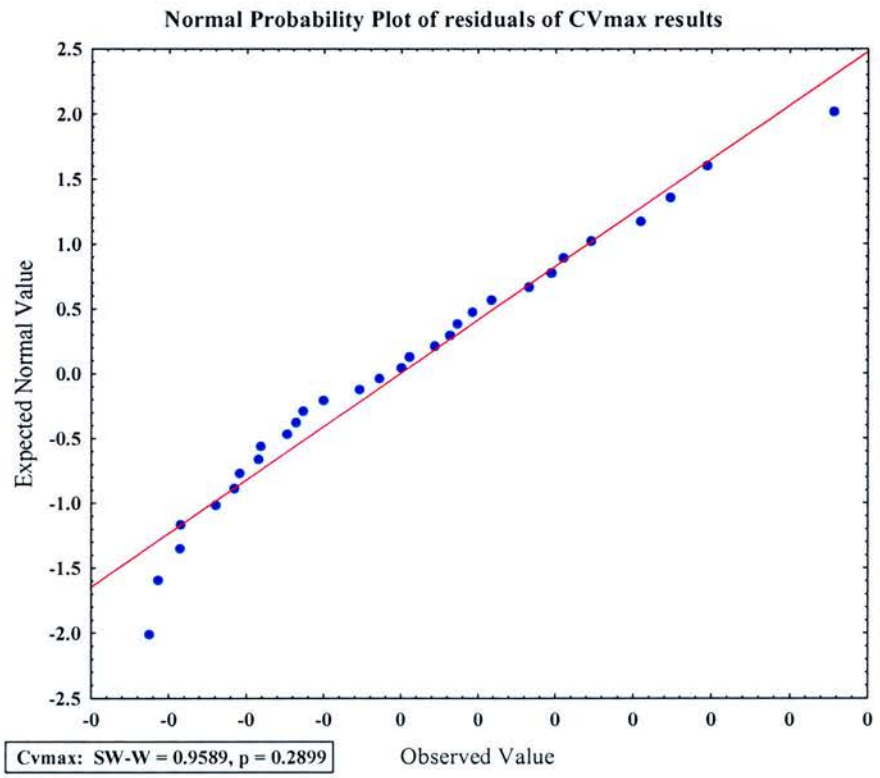

Figure 39

Normal Probability graph of residuals of CV_{max} values with results from Shapiro-Wilk W test

If the variables had a normal distribution, a *one way ANOVA* was used to test the null hypothesis that the different samples in the comparison were drawn from the same distribution or a distribution with the same mean. If the P value was < 0.05, there was less than 5% chance that the null hypothesis was correct, i.e. a $> 95\%$ chance that the means of the groups analysed did come from different populations. By applying a *Student's t test* then to the variables individually it was possible to find out between which groups the difference in the means existed.

Various tables and graphs were then used to display the results.

CHAPTER 3 – RESULTS

Handling characteristics of the wrap

The wrap creased sharply when folded and did not collapse or lose its form when wrapped around the nerve stumps. It remained in a cylindrical form when secured with glue or sutures as shown in the photographs of the wrap *in vivo* in figures 40, 41 and 42.

Figure 40

Wrap in place around divided nerve stumps; secured in place by 6/0 polyglactin macrosutures

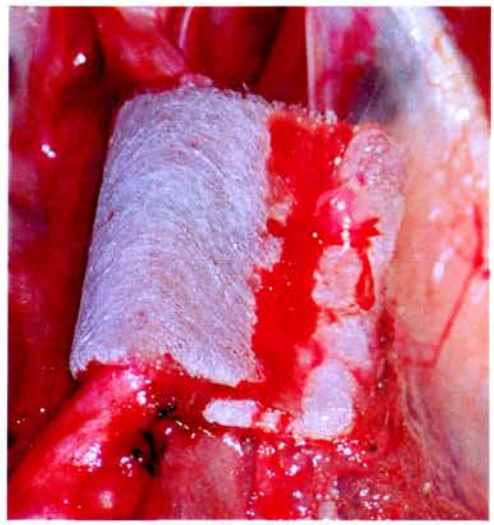

Figure 41

Wrap in place around divided nerve stumps; secured in place by Tisseel glue

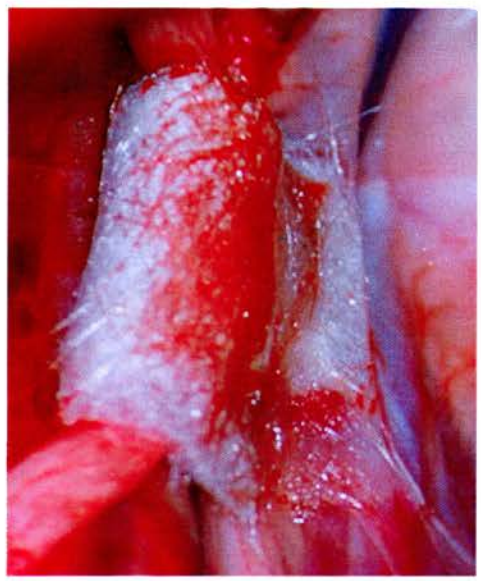

Figure 42

Wrap in place around divided nerve stumps; secured in place by polycaprolactone glue

When the wrap was in contact with blood it did not become friable, tacky or swollen. The CRG-wrap adhered, by surface-tension effect, to the tissue on which it was placed, e.g. muscle, but could still be repositioned easily by lifting it with forceps. The nerve stumps, when placed on the wrap also tended to adhere to a slight extent to the wrap's surface. This adherent property of the wrap made securing the wrap in position easier as there was no sliding of the wrap or of the nerve stumps from the positions in which they were placed during the application of glue or sutures.

Macrosutures, if placed wrongly, could be removed and replaced without causing damage to the wrap.

Time to complete repairs

It took the author an average time of twenty-five minutes to place the six to eight epineurial sutures required for each microsurgical epineurial suture repair. A completed microsurgical repair is shown in figure 43.

Figure 43

A completed microsurgical epineurial repair

In contrast, it took me only three minutes to complete a nerve repair using the wrap with Tisseel or polycaprolactone glue, and twelve minutes to complete repair with the wrap and macrosutures.

Epineurial suturing was the most difficult method of repair to learn and carry out. Securing the wrap with macrosutures was more difficult than using glue and there was the added concern that the uppermost macrosutures could have been placed deep to the epineurium of the nerve.

Clinical Condition of the Sheep

Early post-operative period

No sheep developed a wound infection post-operatively. All sheep were able to walk one to two hours after surgery but limped and avoided full weight-bearing on the right forelimb for three to four days after surgery. After these first few days, most sheep no longer obviously limped when walking or running but commonly continued to weight-bear on the left forelimb when stationary. Some sheep developed a bald, rough patch of skin on their anterior chest wall. This patch was produced because they tended to rest on their anterior chest while grazing and is not seen in normal healthy sheep.

Contractures

Five sheep developed contractures of the knee of the right forelimb. Four of these sheep were of a breed called 'Finn' and the other sheep was a 'mixed breed'. The contractures they developed ranged from 15°–90°. The contractures began, at the earliest, ten weeks

after nerve division and repair, and at the latest, six months after nerve division and repair. The contractures continued gradually to worsen. Three of these sheep, including the sheep with the most severe contracture which had a fixed flexion deformity of 90°, had undergone repair with the wrap and polycaprolactone glue. The results of twitch tension testing in this sheep were inadmissible because it was not possible to attach the flexed limb to the apparatus in the correct manner. Despite attempted release of the ligaments around the knee, the contracture could not be freed. One of the other two sheep which developed contractures was from the wrap and Tisseel group and the other was from the wrap and macrosuture group. There was not a dehiscence of the nerve repair in any of the sheep which developed contractures and all the sheep in which dehiscence of the nerve repair occurred did not develop contractures.

General health

The mean mass of the sheep was 53.9 kg (range 37–72 kg). All the sheep except one kept well during the seven months between the first and second operations. The exception was a sheep which died while being fasted and isolated during the twenty-four hours prior to its second operation. The cause of death was not certain. Isolation and starvation are the two most stress-inducing conditions for sheep and it was suggested by the animal handlers in the unit that a cardiac event may have led to its death. After the death of this sheep, all sheep were penned with one other sheep and allowed water to drink in the twenty-four hours prior to anaesthesia. No adverse events occurred during anaesthesia after implementing this change in pre-operative management.

Fibrosis

While dissecting in the upper forelimb to expose the original repair site it was observed that there was more fibrosis in the area surrounding the site of repair in the wrap and polycaprolactone group than in the other groups. This was a subjective observation.

In the polycaprolactone group, seven months after repair, there remained an area of firm tissue which had the shape of the original wrap (see figure 44 and 4th image in figure 45).

Figure 44

Two examples of sections from the repair sites in the wrap and polycaprolactone group

When this tissue was cut, strands of a white material were found within it which looked like remnants of the wrap. There was no macroscopic evidence of the wrap at the repair site at the time of the second operation in the other two wrap repair groups. Photographs of excised segments of nerve from the repair sites are shown below in figure 45.

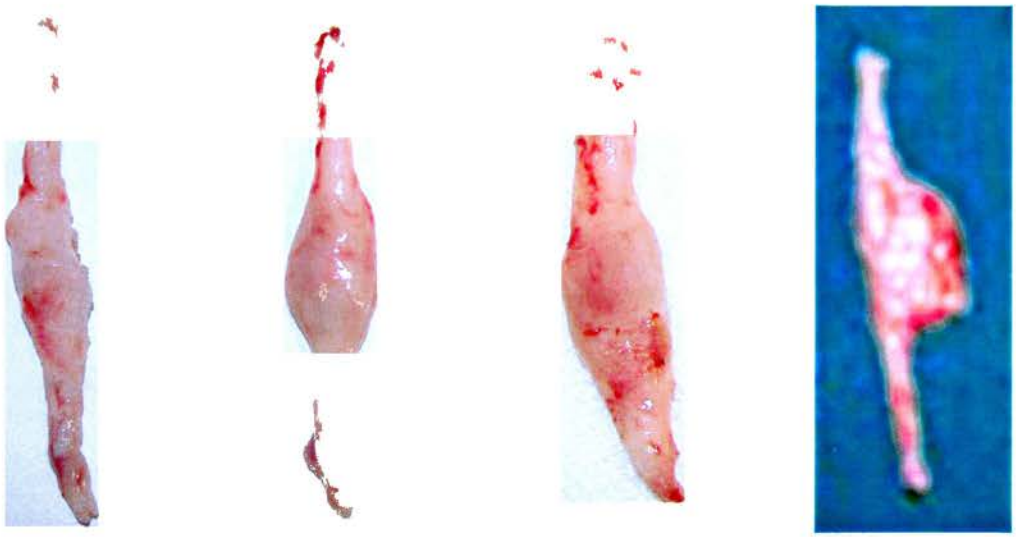

Figure 45

Sections of the repaired median nerve excised from the upper forelimb seven months after repair. The repair groups from which they came from were the epineurial suture, CRG-wrap + macrosuture, CRG-wrap + Tisseel and CRG-wrap + polycaprolactone respectively (from left to right). The outline of remnants of the wrap is clearly seen in the CRG-wrap + polycaprolactone specimen.

Dehiscence

Dehiscence of the nerve repair occurred in two repairs in the epineurial suture group and one repair in the CRG-wrap + polycaprolactone group. In one other sheep in the polycaprolactone group no contraction of FCR could be elicited by stimulating the repaired median nerve proximal or distal to the site of repair. Morphometric examination of the median nerve distal to the site of repair did however reveal that regenerated axons were present in the distal part of the nerve. Measurements of *TSJ*, CV_{max} and F_{min} were not possible in these four cases.

Management of data

The results from the right limb (operated) for each variable were divided by the results from the left limb (normal). The ratios produced were used in all statistical analyses. The benefit of using this technique was that differences in the age, sex, health and mass of the animals would not have had an impact on the variation of the results, i.e. within group variation was excluded.

Identification of Outliers

The ratios of the results of each variable were plotted on half-normal probability plots in Statistica (Statsoft, Tulsa, U.S.A). An example of one of these plots is shown in figure 5 below. Observed values were plotted on the *x*-axis against the expected normal value for a normal distribution of the same mean and variance on the *y*-axis. In the graph in figure 7, the ellipse represents confidence intervals of 95% for the spread of the data. The outlying points, e.g. the point with an observed value of 1.62 in figure 46, were outlying values and were excluded from the results.

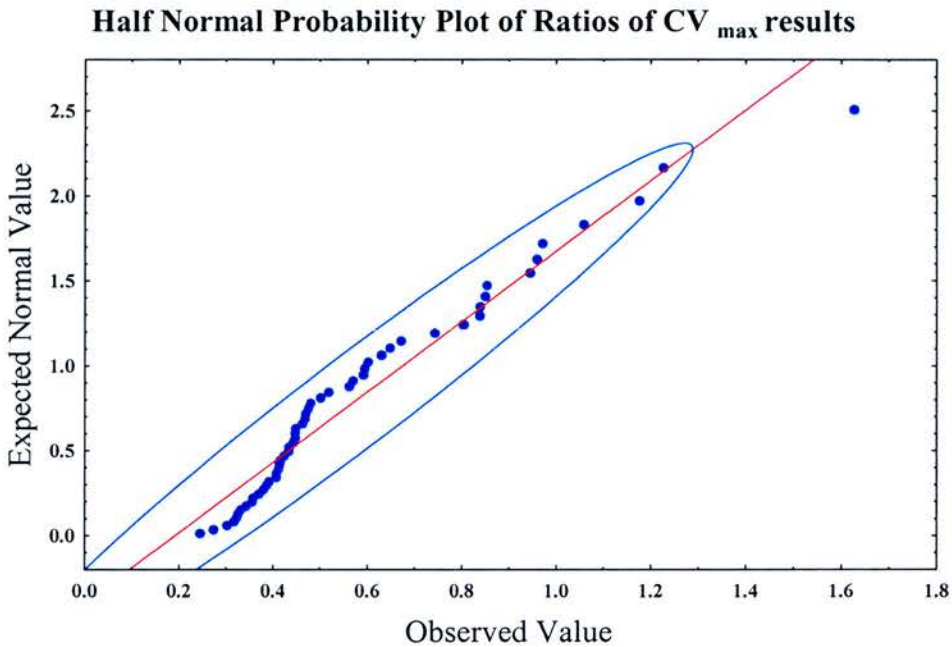

Figure 46

Half-normal probability plot of the ratios of CV_{max} results. The point that is outside the ellipse was considered an outlier and excluded from the results. The ellipse represents 95% confidence intervals for the distribution.

Normality of Distribution

Residuals (the difference between an actual value and the mean of the group) of the weeded data were calculated using Statistica. These residuals were plotted on normal probability plots as shown in figure 47 and the *Shapiro-Wilk W test* applied. If the *W* statistic produced by the Shapiro-Wilk W test was not significant ($p > 0.05$), the null hypothesis that the data were normally distributed was accepted.

Fibre Diameter

The *P*-value of the *W* statistic was <0.05 when one variable, fibre diameter, was tested. The normal probability plot for calculated residuals of the data of fibre diameter is shown below in figure 47. The *P*-value for the *W* statistic was 0.0017.

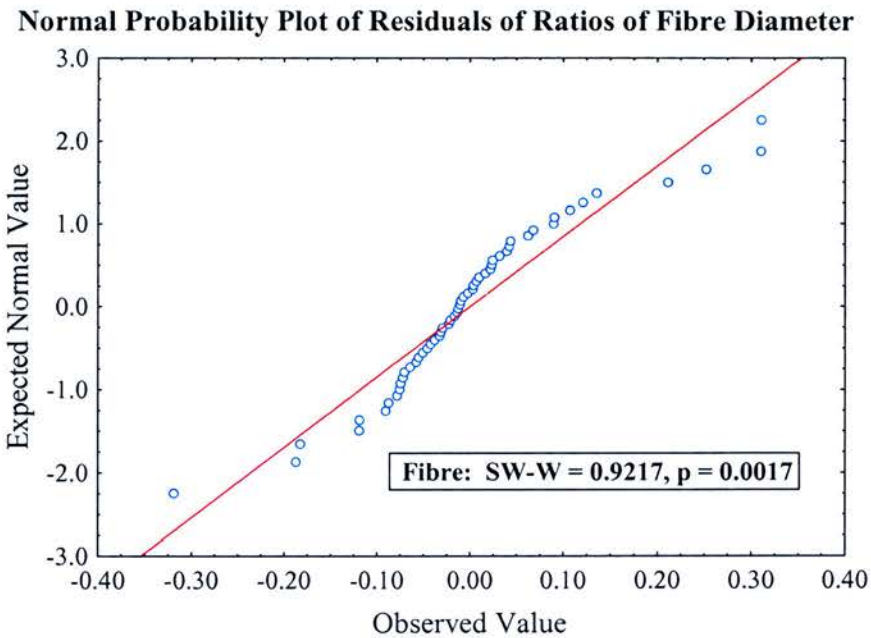

Figure 47

Normal probability plot of the residuals of the ratios of fibre diameter results. The plotted results deviate from the line representing a normal distribution of the residuals.

Three extreme values were removed from the data to determine the effect this would have on the *W* statistic. The graph produced after the removal of these three values is shown in figure 48. The *P*-value of the *W* statistic after the exclusion of these extreme results increased to 0.062 therefore indicating a normal distribution of the remaining data.

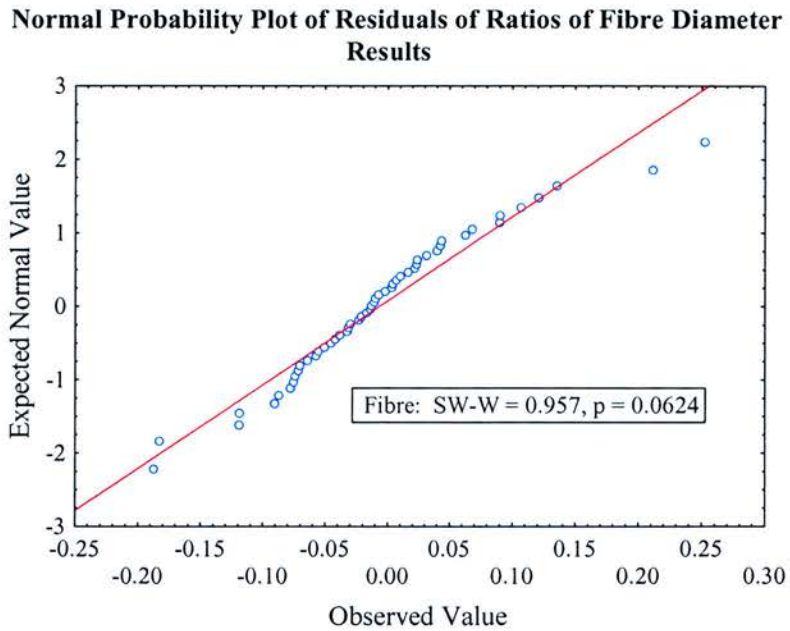

Figure 48

Normal probability plot of the residuals of the ratios of fibre diameter results with three extreme values excluded. The *P*-value for the *W* statistic is now 0.06 and no longer significant. The ratios for fibre diameter were therefore considered normally distributed with these values removed.

All three of these extreme values came from results in the control group. The range of axon and fibre diameter (μm) was the largest in the control group (see photographs of the nerve sections in the morphology section in pages 193–197; figures 77–86, and the bivariate histogram of fibre diameter in figure 66).

A scatterplot of the residuals of the ratios of the results in all the groups is shown below in figure 49. This demonstrated again that the spread of residuals was greater in the control group. It can be seen that the spread of the residuals of the control group (cases 1–12) was greater than in the repair groups (cases 13–57).

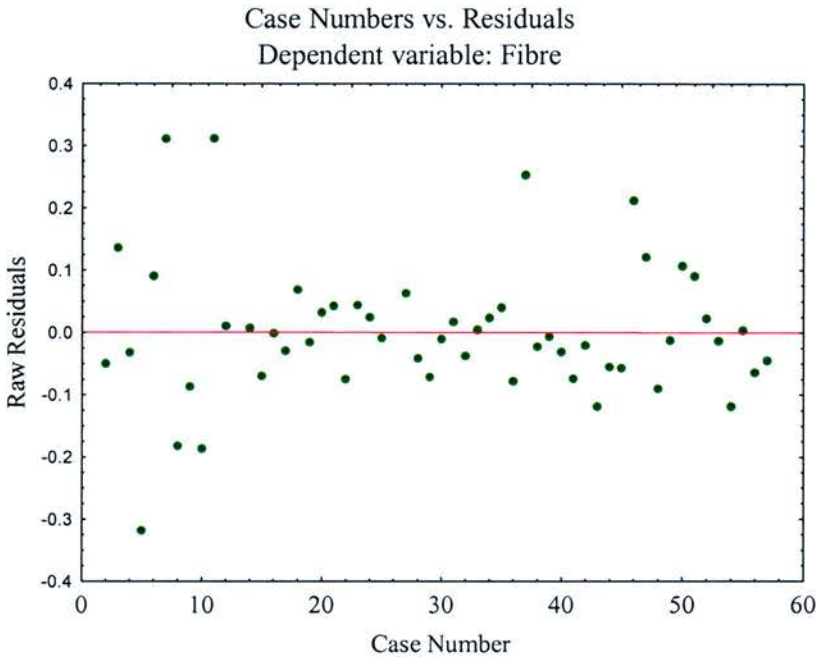

Figure 49

Scatterplot of the residuals of the ratios of fibre diameter according to case number. The control group included the case numbers 1–12; the epineurial suture group, case numbers 13–23; the wrap and macrosuture group, are case numbers 24–35; the wrap and Tisseel group, case numbers 36–46; and the wrap and polycaprolactone group, case numbers 47–57.

Explanation for wide spread of residuals in the control group

In each nerve section, 200–300 myelinated fibres were measured. A normal sheep median nerve contained a total number of 13, 800 myelinated fibres [this figure was calculated by counting the total number of fibres in one fascicle (600) of a normal nerve and multiplying this figure by the estimated number of times a fascicle of this size would be represented in the total surface area of neural tissue in the nerve section (23 times on this occasion)]. The variation in the calculated mean from a sample of 200 fibres from the true mean of all the fibres would be largest in the control group because the total

number of fibres per unit of nerve area was highest in this group and the range in the size of the fibres was the greatest.

The ratio of the results of mean fibre diameter between the right and left sides in the control group should have been around 1.0. After consideration of the cause of the wide range of the residuals in this group it was thought acceptable to exclude the three extreme values and so accept that the results of fibre diameter were normally distributed.

One way ANOVA (*F* test)

The ratios of all variables were therefore accepted as being normally distributed and were subjected to *one way ANOVA* to determine the probability that the ratios in each group could have come from the same population. If the *F* statistic produced by one way ANOVA was significant at the 5% level, the null hypothesis that the results of each group came from identical populations was rejected.

Box and whisker plots clearly display the means of the ratios (the points); the standard error of the means (the boxes); and 1.96 × standard error of the mean (the whiskers). They were therefore plotted to demonstrate the ratios of the results of each test.

Post hoc analysis

If it had been determined using one way ANOVA that the mean and variance of each group did not come from the same population, Scheffé's test was therefore applied to pairs of groups to determine where differences lay. Scheffé's test compares two groups at a time and so a table of results is produced for each variable when five groups are compared. For each variable to which Scheffé's tests was applied to the results, a table displaying; the *P*-values of the test statistics, the mean and the standard error of the ratios, and the

sample size number for each group will be shown. If the result of Scheffé's test was significant, i.e. the *P*-value of the test statistic was less than 0.05, the null hypothesis that the results from the two groups came from populations with the same mean and variance was rejected.

RESULTS - BY VARIABLE

Transcutaneous stimulated jitter (TSJ)

Excluded results

After the completion of electrophysiological testing in a sheep, the FCR muscle was excised. It was possible to see the entry marks on the fascia covering FCR caused by the needle electrodes used in the measurement of *TSJ*. On a few occasions, the needle insertion marks were not seen in the fascia overlying FCR but were in the fascia of flexor carpi ulnaris which lies adjacent to FCR *in vivo*. This happened on four occasions, always in the repair groups because FCR had become wasted and more difficult to identify. The results of *TSJ* from these sheep were excluded from the data. This, along with the exclusion of results after dehiscence and the removal of outliers, is the reason why the group sample size in the repair groups had been reduced to nine.

The ratios of the results of *TSJ* in each group are shown in the box and whisker plot below (figure 50). The *F* statistic produced by one way ANOVA for the results of *TSJ* was significant ($p < 0.05$) and so Scheffé's test was applied. The *P*-values obtained by Scheffé's tests are displayed in the table in table 2.

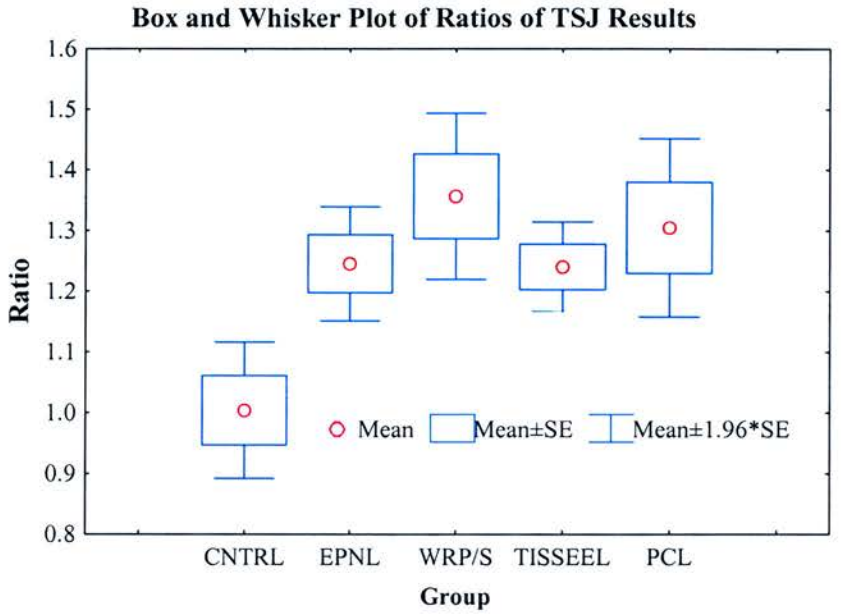

Figure 50

Box and whisker plot of ratios of the results of *TSJ* in each group

	CNTRL (1.00) {0.057}	**EPNL (1.24) {0.048}**	**WRP/S (1.36) {0.040}**	**TISSEEL (1.24) {0.038}**	**PCL (1.30) {0.075}**
CNTRL [11]		0.087	0.003	0.098	0.017
EPNL [9]	0.087		0.790	1.000	0.974
WRP/S [9]	0.003	0.790		0.764	0.985
TISSEEL [9]	0.098	1.000	0.764		0.966
PCL [9]	0.017	0.974	0.985	0.966	

Table 2

The *P*-values of Scheffé's test for the results of *TSJ*. The means of the ratios (in round brackets), the standard error of the means of the ratios {in braces}, and the sample size [in square brackets] is shown for each group. The *P*-values which were significant (<0.05) are highlighted in red.

The null hypothesis that the mean and variance of the ratios in the control group compared with the epineurial repair group and the wrap + Tisseel glue group came from identical populations was accepted at the 5% level. In contrast, the null hypothesis was rejected when comparing the results of the wrap + polycaprolactone group and the wrap + macrosuture group to the control group because the *P*-values of Scheffé's test were < 0.05. When comparing the repair groups with one another the *P*-values were > 0.05 and therefore it was accepted that ratios of these groups came from populations with the same mean and variance.

Power of TSJ results

A graph of the power of the results of TSJ against group number when $\alpha = 0.05$ is shown below in figure 51.

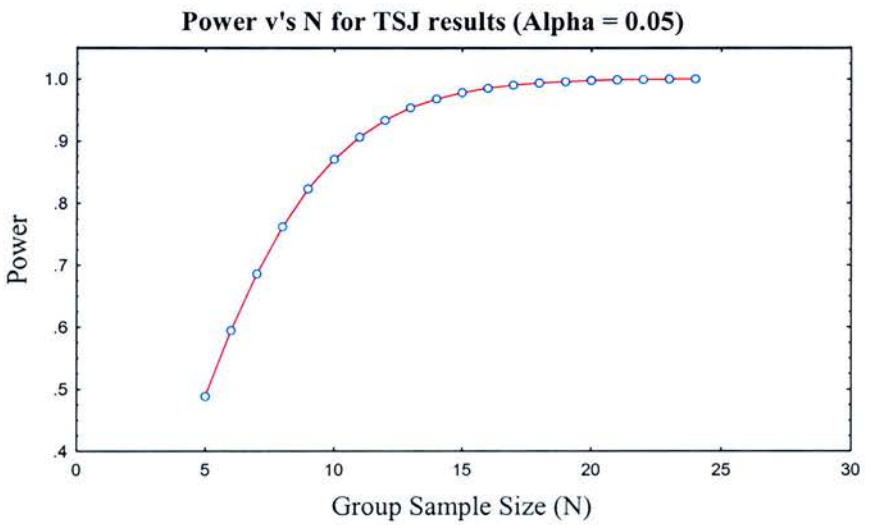

Figure 51

Power against group sample size for the results of one way ANOVA of TSJ results. The group sample size in the present study was nine therefore the power of the results of one way ANOVA was 0.85.

The group sample size for *TSJ* in the present study was nine and so the power of one way ANOVA was 0.85 ($\alpha = 0.05$).

Maximum conduction velocity

The *F* statistic of one way ANOVA for the results of CV_{max} was significant at the 5% level. The null hypothesis that the ratios of the groups came from populations with the same mean and variance was therefore rejected.

When comparing the repair groups with one another, the *P*-values of Scheffé's test were greater than 0.05 and so the null hypothesis that these results came from populations with the same mean and variance could not be rejected. When comparing each of the repair groups with the control group Scheffé's test was significant and so the null hypothesis was rejected at the 5% significance level.

Figure 52 shows a box and whisker plot of the ratios of the results of the maximum conduction velocity in each group. The large variation between the ratios of the control group and the repair groups highlights that the maximum conduction velocity in the repaired nerves was much lower than the maximum conduction velocity in the normal nerves. The means of the ratios are shown for each group in the table in table 3.

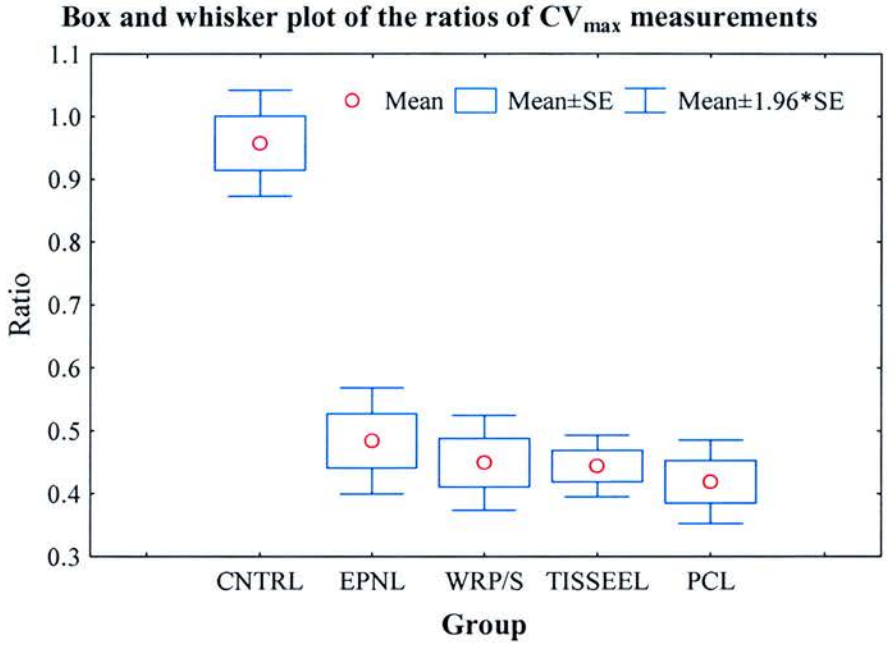

Figure 52

Box and whisker plot of the ratios of the results of the maximum conduction velocity measurements.

	CNTRL (0.96) {0.043}	**EPNL (0.48) {0.043}**	**WRP/S (0.45) {0.038}**	**TISSEEL (0.44) {0.025}**	**PCL (0.44) {0.034}**
CNTRL [11]		0.000	0.000	0.000	0.000
EPNL [10]	0.000		0.979	0.966	0.836
WRP/S [11]	0.000	0.979		1.000	0.988
TISSEEL [11]	0.000	0.966	1.000		0.994
PCL [10]	0.000	0.836	0.988	0.994	

Table 3

The *P*-values of Scheffé's test on the ratios of CV_{max} in each group. The means of the ratios (in round brackets), the standard error of the means of the ratios {in braces}, and the sample size [in square brackets] is shown for each group. The *P*-values which were considered significant (<0.05) are highlighted in red.

Power

The graph in figure 53 shows a plot of power against group sample size (N) for one way ANOVA on the ratios of the results of CV_{max}. The sample size in each group was 10 or 11 and therefore the power of one-way ANOVA was approximately 1.0 (α = 0.05). In the discussion, further power calculations will be carried out to determine the potential usefulness of this test in clinical practice.

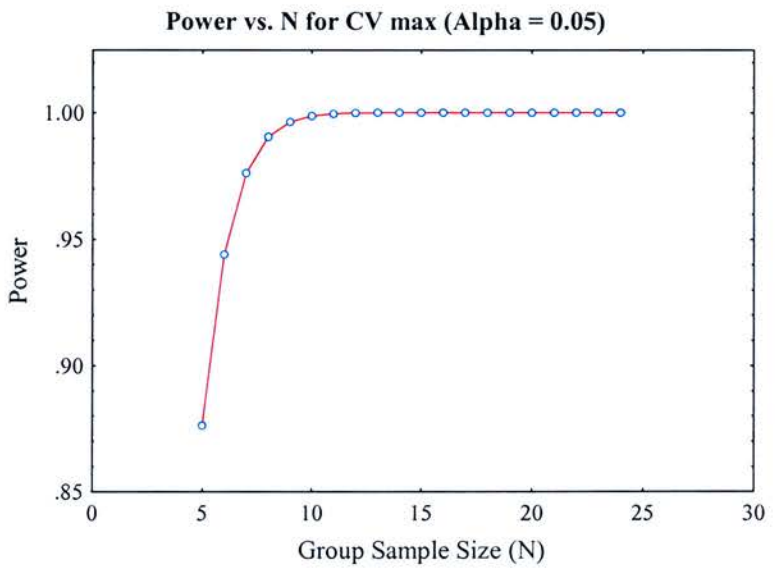

Figure 53

Change in power with group sample size for one-way ANOVA test. The group sample size number in the present study was eleven giving the test results of CV_{max} a power of approximately 1.0, i.e. there was approximately a 100 % possibility that a false null hypothesis would be rejected.

Motor latency

The F statistic of one-way ANOVA for the results of motor latency was significant at the 5% level and therefore the null hypothesis that the ratios in the five groups came from

populations with the same mean and variance was rejected. Only one result of Scheffé's test was significant at the 5% level. This was the comparison of the wrap and polycaprolactone group to the control group. The null hypothesis that the results of these two groups came from populations with the same mean and variance was therefore rejected at the 5 % significance level (p = 0.001) but the null hypothesis for all other comparisons was accepted.

A box and whisker plot of the ratios of the motor latency results in all groups is shown in figure 54. The *P*-values of Scheffé's test along with the mean and standard error of the ratios, and group sample size is shown in table 4.

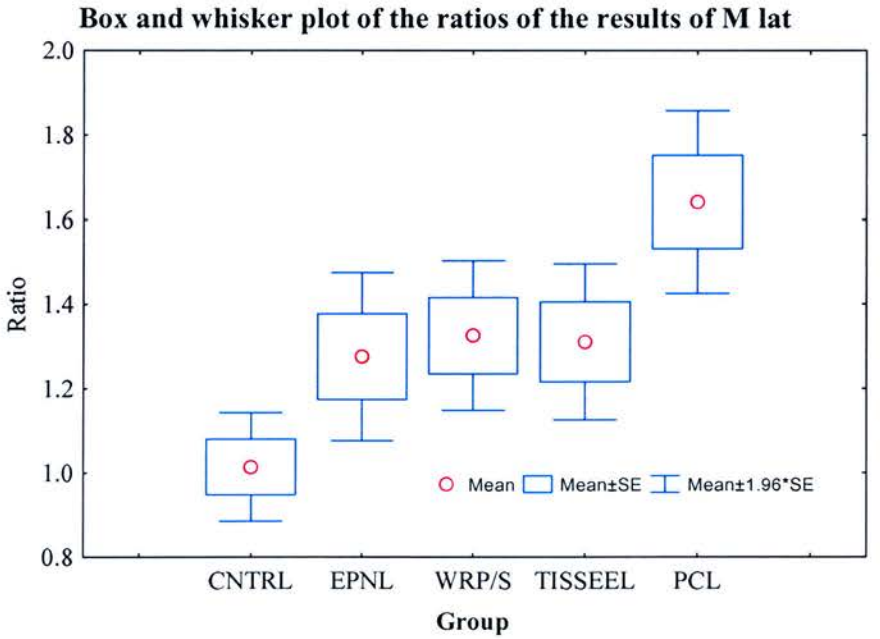

Figure 54

Box and whisker plot of the ratios of the results of motor latency in each group. The mean ratio of the wrap and polycaprolactone group is much higher than the mean ratio in the other groups.

	CNTRL (1.01) {0.066}	EPNL (1.28) {0.102}	WRP/S (1.33) {0.091}	TISSEEL (1.31) {0.095}	PCL (1.64) {0.110}
CNTRL [10]		0.442	0.265	0.290	0.001
EPNL [10]	0.442		0.998	0.999	0.134
WRP/S [10]	0.265	0.998		1.000	0.254
TISSEEL [11]	0.290	0.999	1.000		0.192
PCL [10]	0.001	0.134	0.254	0.192	

Table 4

The *P*-values of Scheffé's test for the ratios of *M lat*. The means of the ratios (in round brackets), the standard error of the means of the ratios {in braces}, and the sample size [in square brackets] is shown for each group. The *P*-values which were considered significant (< 0.05) are highlighted in red.

Power

The power of one way ANOVA was plotted against group size number. The group size was ten in the present study giving a power of 0.9 for one way ANOVA ($\alpha = 0.05$).

Minimum F wave Latency (F_{min})

There were few bilateral measurements of F waves obtained in the sheep in the repair groups. F waves were produced less frequently in the operated groups compared with the control group. However, in the operated groups, F waves were recorded more frequently on the operated side (89% of the operated limb) compared with the un-operated side, (41% of the limbs).

The scatterplot below shows the ratios of the measurements of F_{min} that were made according to the sheep case number. The number of F_{min} values recorded in each group (n) is shown in brackets within the legend.

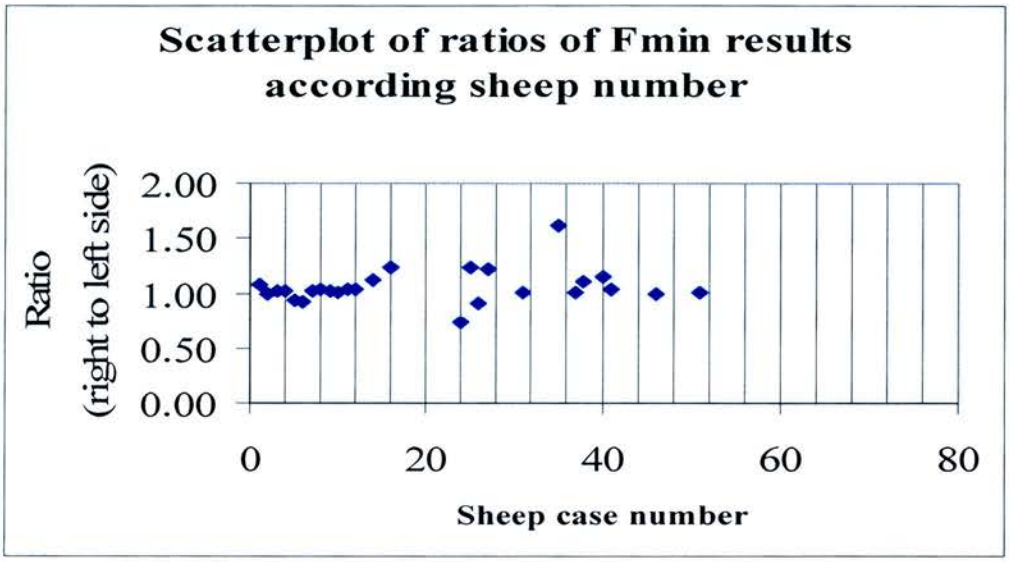

Figure 55

Scatterplot of the ratios of the results of F_{min} measurements according to sheep case number. The control group included sheep case numbers 2–13 (n = 12); the epineurial suture group, sheep case numbers 14–25 (n = 5); the wrap and macrosuture group, sheep case numbers 26–37 (n = 5); the wrap and Tisseel group, sheep case numbers 38–48 (n = 5); and the wrap and polycaprolactone group, sheep case numbers 49–60 (n = 1).

The results of F_{min} did not agree with the results of CV_{max}. F_{min} on the right side in the repair groups would have been expected to be much higher than in the control group thus producing a much larger ratio than 1.0. It can be seen from the scatterplot of the ratios in figure 55 that this was not the case.

It was decided that the results of F wave analysis were not accurate and could not be used in the present study because of the inconsistency in the ability to record F waves and because the latencies of the F waves recorded did not agree with the results of CV_{max}.

Peripheral latency

Peripheral latency was calculated from the results of F_{min} and motor latency. Because the results of F_{min} were considered unreliable, the peripheral latency results were not used in the present study.

Twitch tension testing

Box and whisker plots for the ratios of the results for all the variables calculated from the curves of force (N) against time (s) produced by an isometric twitch are shown below in figures 56–61. There was no significant difference at the 5% level in the means and variance of the results between the five groups for the ratios of peak force of contraction (N), time to peak force (ms), half relaxation time (s), rate of change of force (N s^{-1}), time tension integral (N s), time tension index (N). The ratios of the results are shown in box and whisker plots in figures 56–61.

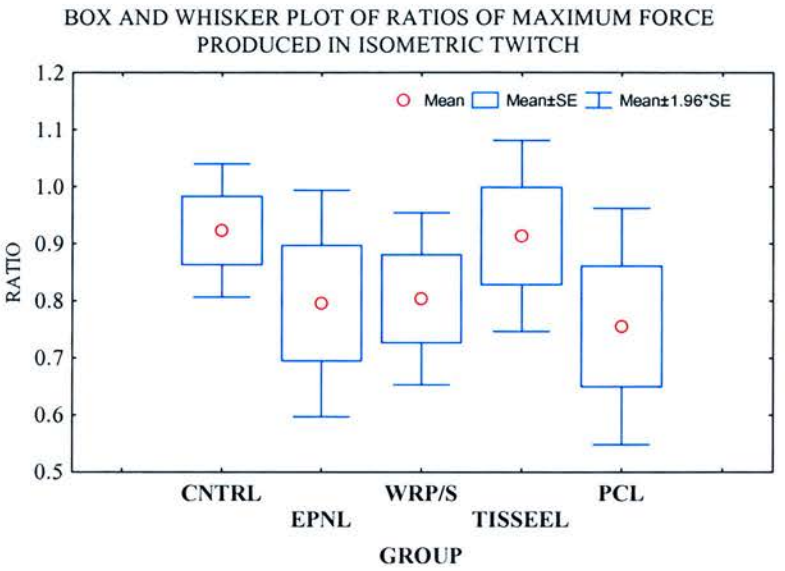

Figure 56

The ratios of the results of the peak force produced during an isometric twitch contraction

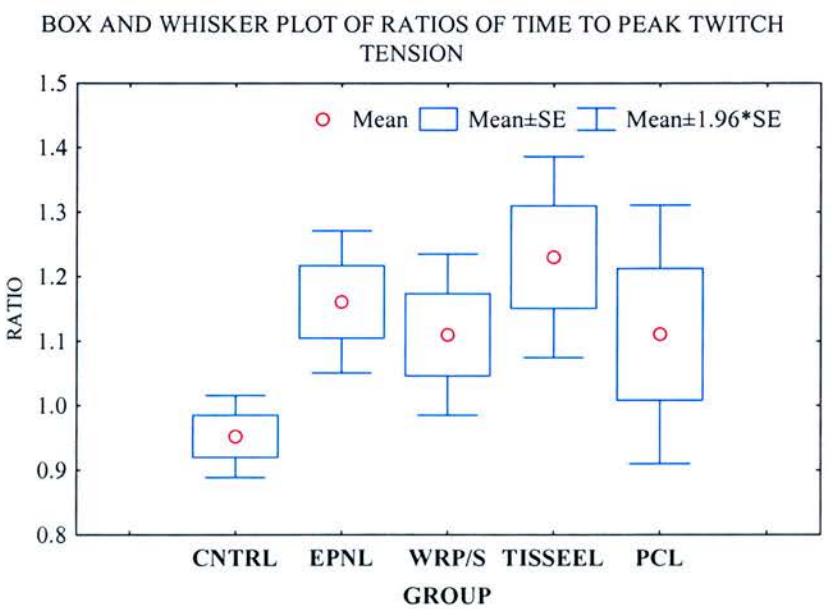

Figure 57

The ratios of the results of time to peak force of muscle contraction

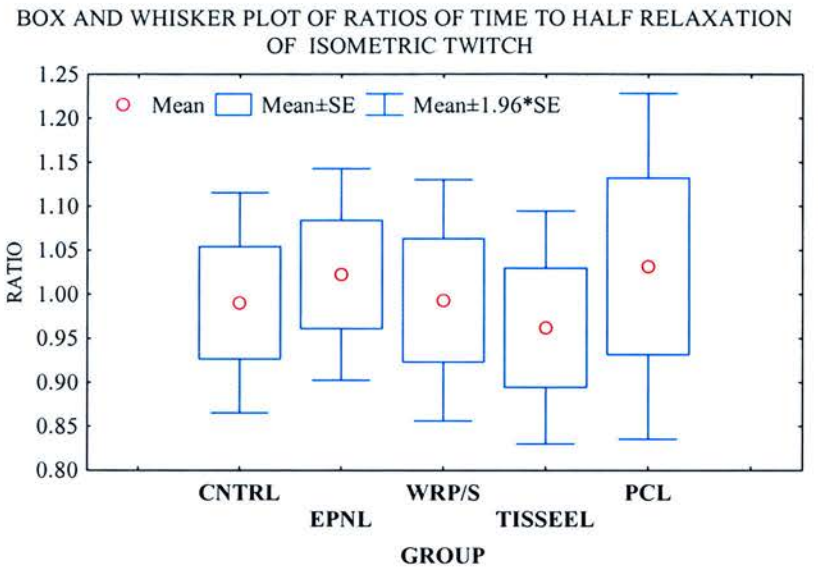

Figure 58

The ratios of the results of time to half relaxation (R½) of isometric twitch

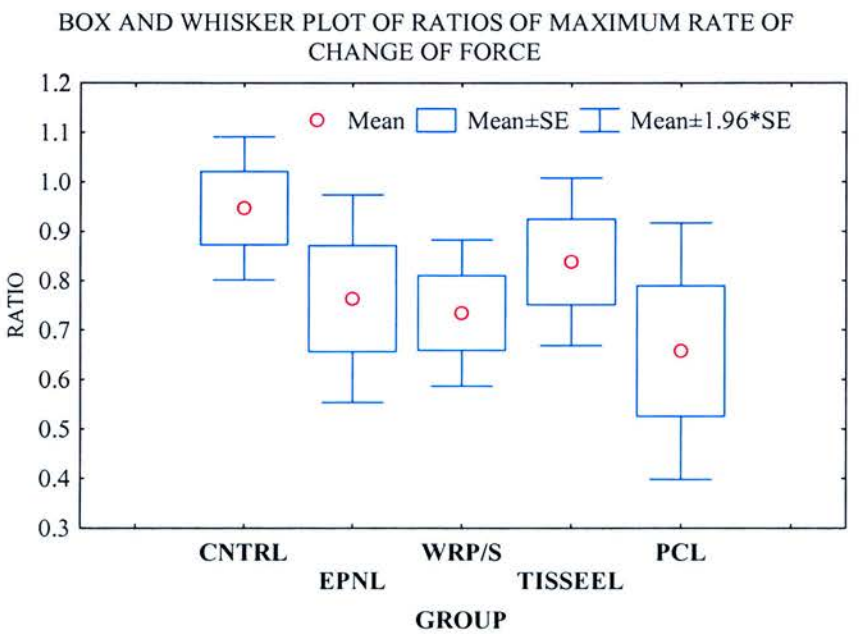

Figure 59

The ratios of the results of measurements of maximum rate of change of force during an isometric twitch contraction

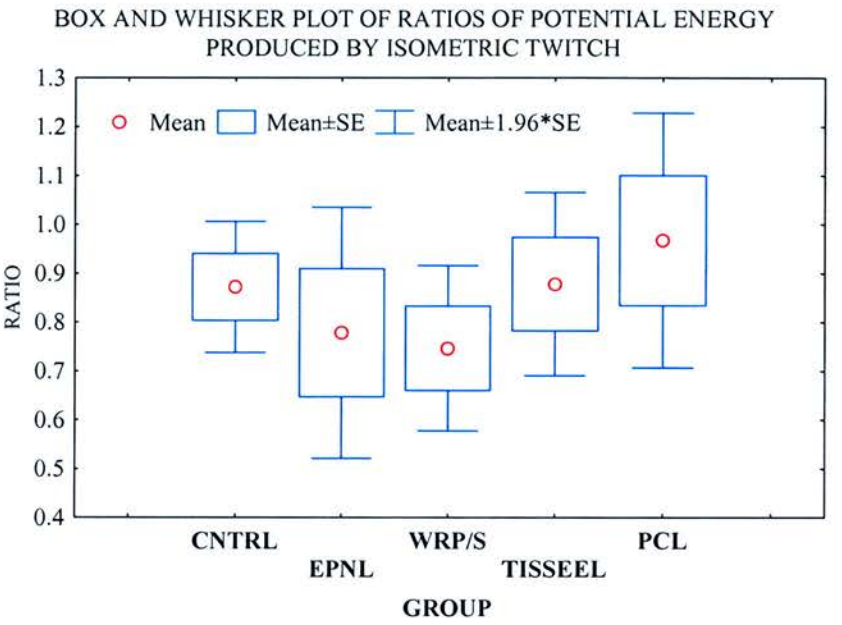

Figure 60

The ratios of the results of total potential energy produced by FCR muscle during one isometric twitch

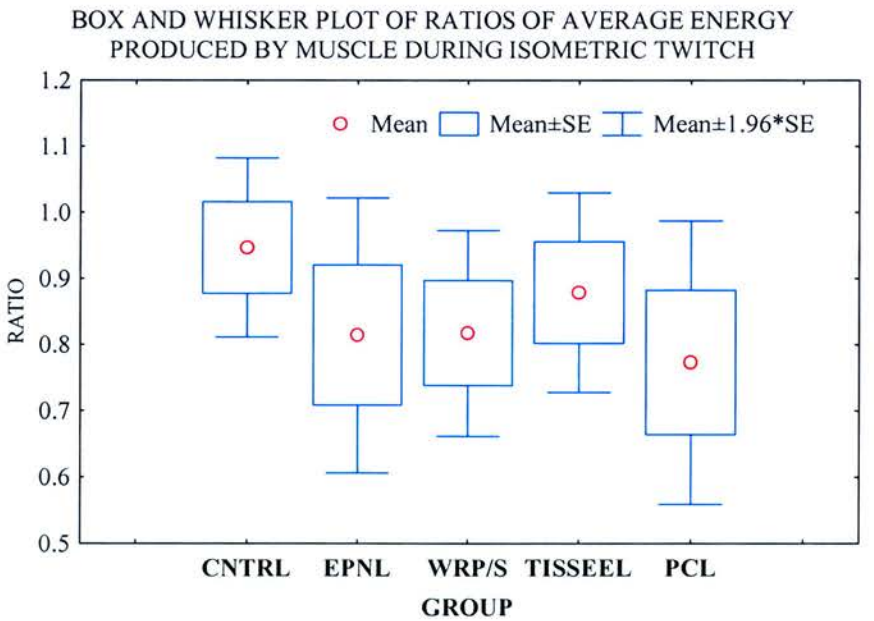

Figure 61

The ratios of the results of average energy produced during an isometric twitch

Wet Muscle Mass

The *F* statistic produced by one way ANOVA was significant at the 5% level for the results of wet muscle mass (g). A box and whisker plot of the ratios of the results of is shown in figure 62 and the *P*-values of Scheffé's test on the results are shown in table 5 along with the means of the ratios, standard error of the means, and group sample size for each group.

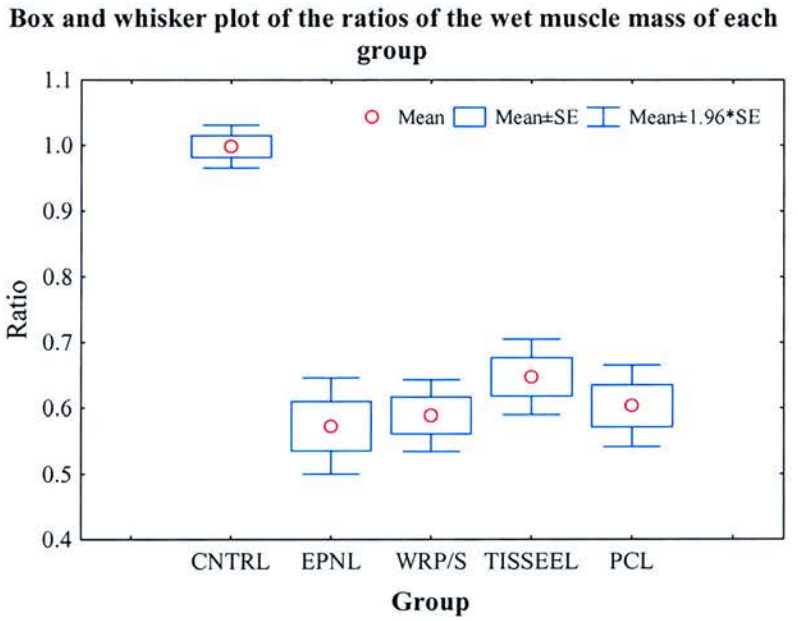

Figure 62

Ratios of the results of *wet muscle mass* in each of the groups. The results of Scheffé's test when comparing the ratios in the control group to the repair groups were significant ($p < 0.05$) but were not significant when comparing the repair groups to one another.

	CNTRL (0.998) {0.017}	EPNL (0.573) {0.037}	WRP/S (0.589) {0.028}	TISSEEL (0.647) {0.029}	PCL (0.603) {0.032}
CNTRL [10]		0.000	0.000	0.000	0.000
EPNL [11]	0.000		0.997	0.537	0.969
WRP/S [12]	0.000	0.997		0.729	0.998
TISSEEL [11]	0.000	0.537	0.729		0.893
PCL [11]	0.000	0.969	0.998	0.893	

Table 5

The *P*-values of Scheffé's test for the ratios of *wet muscle mass* in each group. The means of the ratios (in round brackets), the standard error of the means of the ratios {in braces}, and the sample size [in square brackets] is shown for each group. The *P*-values which were considered significant (<0.05) are highlighted in red.

The results in the table above suggest that the wet muscle mass in the repair groups was smaller than in the control groups (with the FCR having approximately 40% less mass on the repaired side). When comparing the control group to the repair groups, the *P*-values of Scheffé's test were less than 0.05 and so, below this significance level, it could be said that the means and variance of the ratios in these groups did not come from the same population. The null hypothesis of Scheffé's test was not rejected when comparing the ratios of the results of the repair groups to one another. The *P*-values of these tests were greater than 0.05.

Power

The power of the one-way ANOVA test is plotted below in figure 63 as power against group sample size number (N).

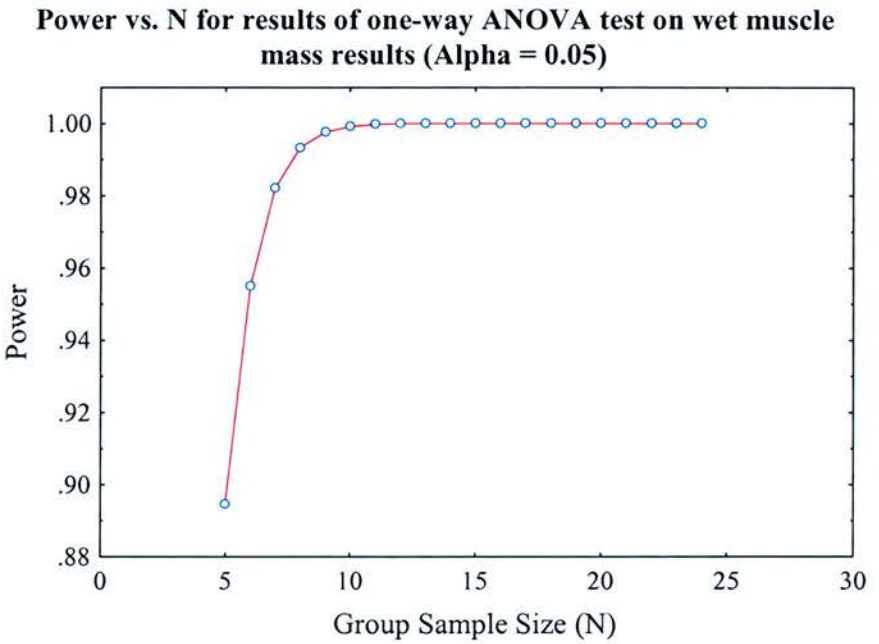

Figure 63

Power against group sample size number for one-way ANOVA on ratios of wet muscle results. The group size was eleven in this study thus the likelihood of rejecting a false null hypothesis was approximately 1.0.

The power of *one way ANOVA* for wet muscle mass in the present study, as taken from the graph in figure 63, was approximately 1.0 ($\alpha = 0.05$).

Morphometry

The measured fibre diameters (μm), axon diameters (μm), myelin thicknesses (μm), and calculated g-ratios are presented as separate histograms for each of the groups. The ratios of the cumulative results of the right and left sides for each group are presented as box and whisker plots. Bivariate histograms were included to give a more direct comparison of the distribution of values of each variable between the groups. The *F* statistics calculated in one-way ANOVA were significant at the 5% level for the results of fibre

diameter, axon diameter and myelin thickness. *Post hoc* analyses using Scheffé's tests were therefore carried out on the results for these three variables but not for g-ratio results where the *F* statistic for one way ANOVA was not significant at the 5% level.

Fibre diameter

The mean and variance of the ratios of the mean fibre diameter for each group are shown in the box and whisker plot in figure 64.

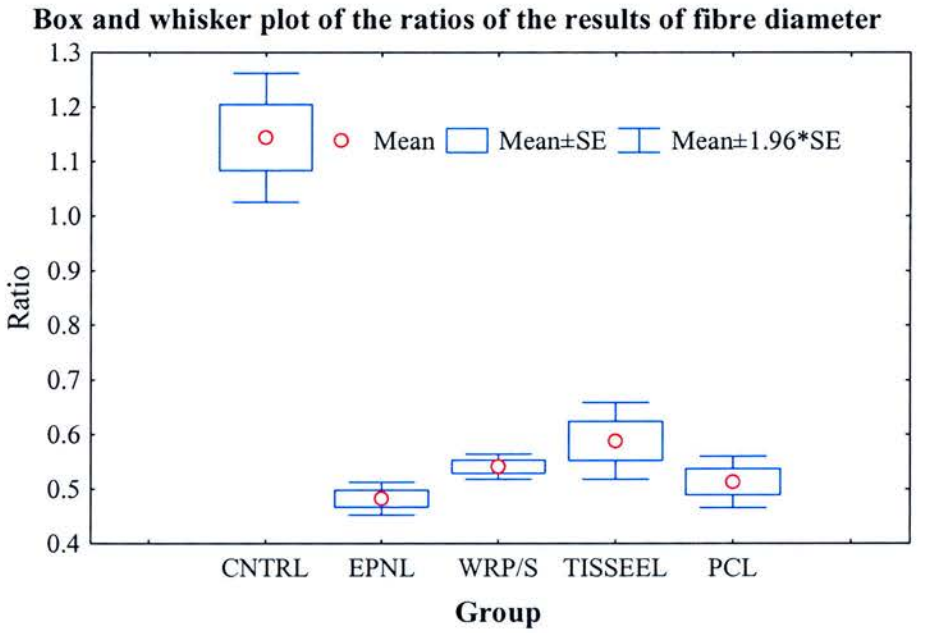

Figure 64

Box and whisker plot of the ratios of the results of mean fibre diameter. The results of Scheffé's tests were significant when comparing the control group with each of the four repair groups but not when comparing each of the repair groups with one another.

The *P*-values of Scheffé's tests for the variable fibre diameter are shown in table 6. The null hypothesis that the ratios in the control group and the ratios in the repair groups came from populations with the same mean and variance was rejected at the 5% significance

level because the *P*-values of Scheffé's tests were less than 0.05. This null hypothesis could not be rejected when comparing the ratios of repair groups with one another.

The power of one-way ANOVA for fibre diameter was approximately 1.0 ($\alpha = 0.05$).

	CNTRL (1.15) {0.060}	**EPNL (0.48) {0.015}**	**WRP/S (0.54) {0.012}**	**TISSEEL (0.59) {0.036}**	**PCL (0.51) {0.024}**
CNTRL [11]		0.000	0.000	0.000	0.000
EPNL [10]	0.000		0.847	0.359	0.984
WRP/S [11]	0.000	0.847		0.919	0.987
TISSEEL [11]	0.000	0.359	0.919		0.669
PCL [11]	0.000	0.984	0.987	0.669	

Table 6

The *P*-values of Scheffé's tests for the ratios of the results of *fibre diameter*. The means (in round brackets) and the standard error of the mean {in braces} of the ratios are shown in the top box of each results column, and the sample size [in square brackets] is shown in the first box of each row of results. The *P*-values which were considered significant (<0.05) are highlighted in red.

The histograms that follow show the distribution of the measured values of fibre diameter (μm) in each group. The contrast in the sizes of fibre diameter in the repaired and normal nerves in each group can be seen in the histograms in figure 65.

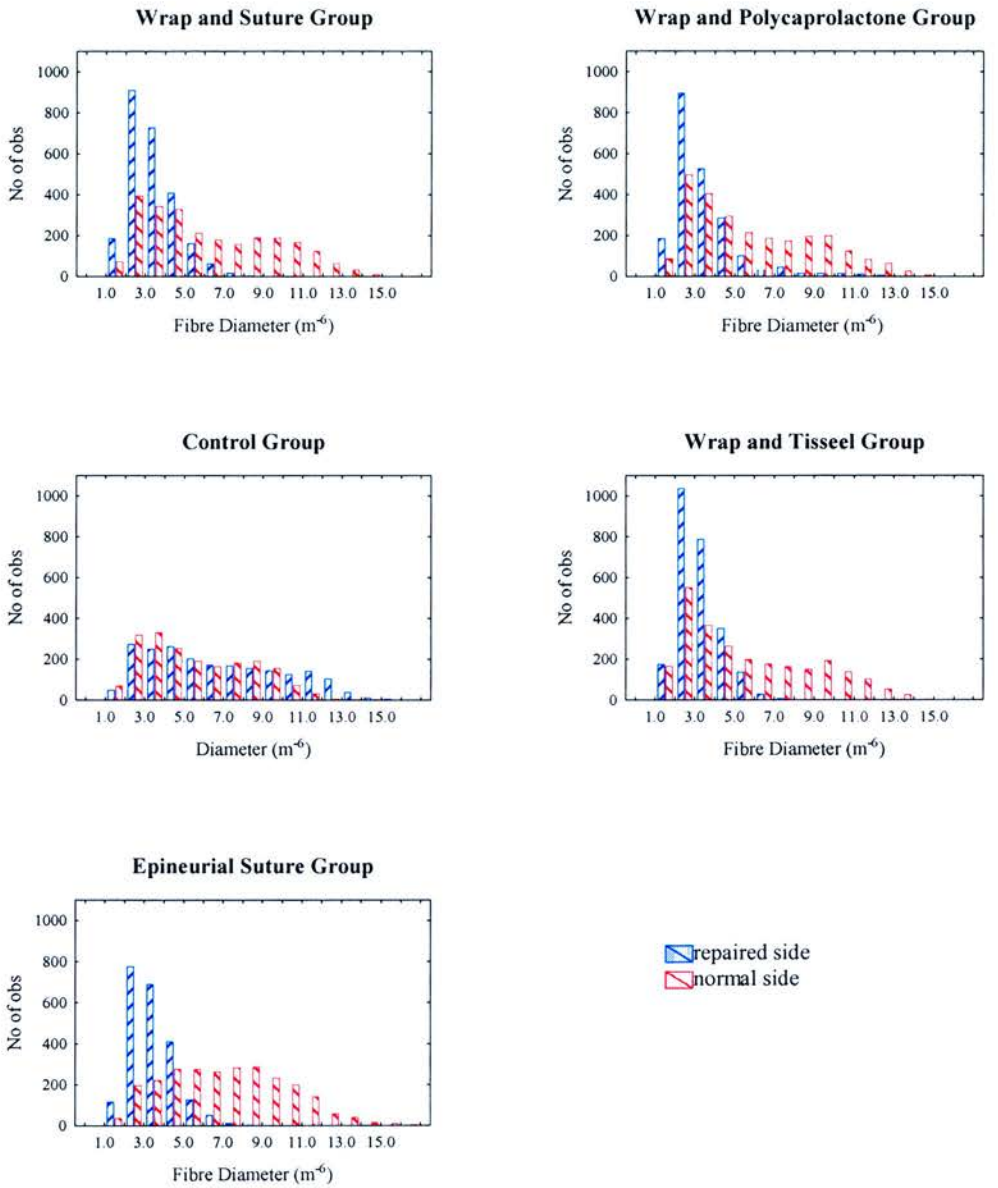

Figure 65

Histograms of the fibre diameter (μm) measurements in each group. The loss of the bimodal distribution and a shift to the left of the diameters in repaired nerves has been demonstrated in previous studies by Glasby et al (1990), Hems & Glasby (1992) and Starrit (2004). The bimodal peaks of fibre diameter occur at 2.0–4.5 μm and 7.5–11.0 μm in the normal nerves and the unimodal peaks in the repair groups occur between 1.8–3.5 μm.

The change from a bimodal to a unimodal distribution of fibre diameter and a shift to the left in the mean and median fibre diameter has previously been described by Glasby et al (1992), Hems & Glasby (1992) and Starrit (2004). In the present study, the bimodal peaks of fibre diameter in the normal nerves occurred at 2.0–4.5 μm and 7.5–11.0 μm, and the unimodal peak in the repaired nerves occurred between 1.8–3.5 μm. The distribution in the fibre sizes in the five different groups is shown in the bivariate histogram in figure 66.

Bivariate Histogram of fibre diameters

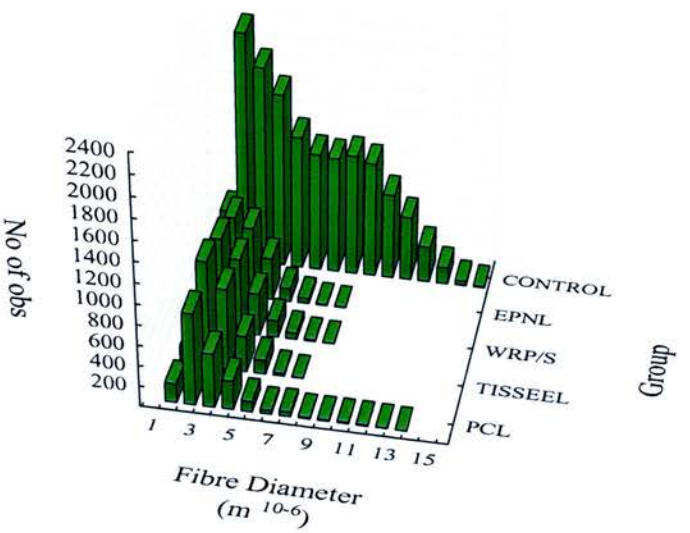

Figure 66

Bivariate histogram of fibre diameter (μm) measurements in all groups. All the data for the unoperated (left) limbs and the control group are displayed cumulatively as the 'Control' column. In the repair groups, there is a shift to the left in the mean fibre diameter and a loss of the bimodal distribution of fibre size that is found in normal nerves ('control' column).

Axon diameter

A box and whisker plot of the ratios of the results of axon diameter in each of the groups is shown in figure 67. Histograms of the measurements of the axon diameters for the right and left sides in each group are shown in figure 68 and a bivariate histogram in figure 69.

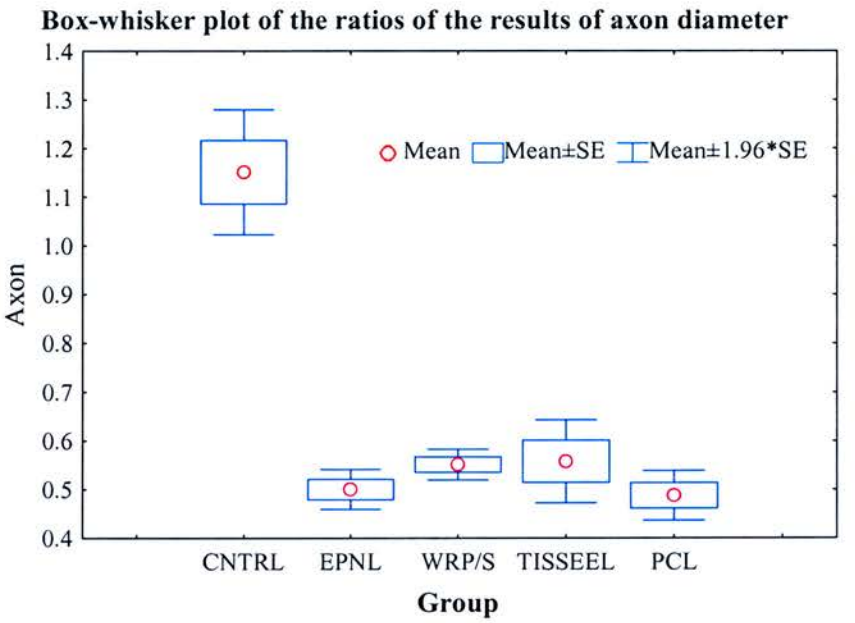

Figure 67

The ratios of the results of the axon diameter measurements. The F statistic calculated by one way ANOVA was significant ($p < 0.05$). The power of the one-way ANOVA test was 1.0 ($\alpha = 0.05$).

The P-values obtained by the use of Scheffé's test are shown in table 7. There was a significant difference at the 5% level between the means and variance of the control and repair groups. The results of Scheffé's tests, when comparing the repair groups with one another, were not significant at the 5% level and therefore the null hypothesis that the

results from the repair groups came from populations with the same mean and variance was accepted.

The power of one way ANOVA for the results of axon diameter in the present study was approximately 1.0 ($n = 11$; $\alpha = 0.05$).

	CNTRL (1.15) {0.065}	**EPNL (0.50) {0.021}**	**WRP/S (0.55) {0.016}**	**TISSEEL (0.56) {0.043}**	**PCL (0.49) {0.026}**
CNTRL [10]		0.000	0.000	0.000	0.000
EPNL [10]	0.000		0.924	0.887	1.000
WRP/S [10]	0.000	0.924		1.000	0.835
TISSEEL [11]	0.000	0.887	1.000		0.779
PCL [11]	0.000	1.000	0.835	0.779	

Table 7

The *P*-values of Scheffé's test for the ratios of the results of *axon diameter*. The means of the ratios (in round brackets) and the standard error of the mean of the ratios {in braces} are shown in the top box of each results column, and the sample size [in square brackets] is shown in the first box of each row of results. The *P*-values which were significant (< 0.05) are highlighted in red.
The *P*-values of Scheffé's test were such that the null hypothesis was rejected when results of the control group and the four repair groups were compared but not rejected when the repair groups were compared to one another ($\alpha = 0.05$)

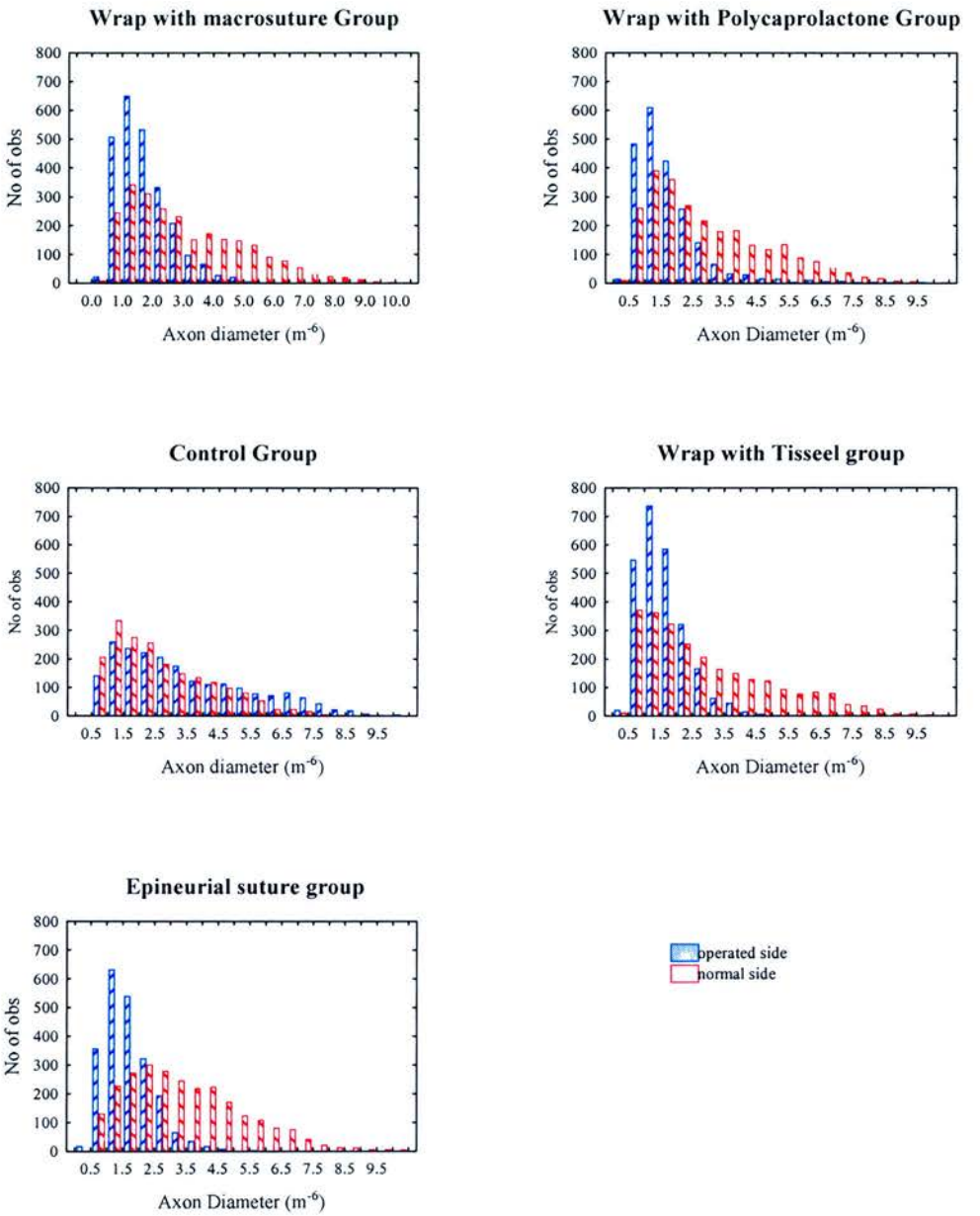

Figure 68

Histograms of axon diameter measurements (μm) from the repaired and normal nerves in all groups. There is a loss of the bimodal distribution of the axon diameters with a shift to the left in the distribution of axon diameters in the repaired nerves in comparison to the normal nerves.

Bivariate histogram of axon diameters

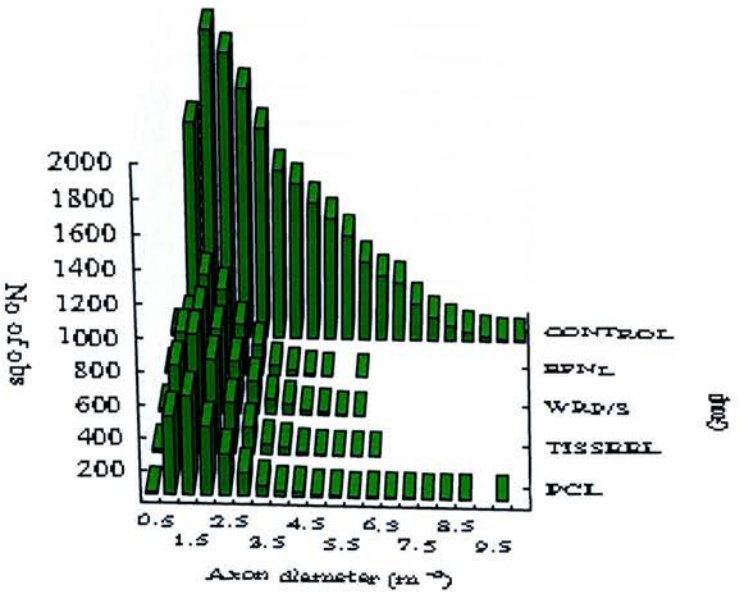

Figure 69

Bivariate histogram of axon diameter (μm) measurements in all groups. All the data for the un-operated (left) limbs and the control group are displayed cumulatively in the 'Control' column.

Myelin thickness

The *F* statistic calculated by one-way ANOVA of the myelin thickness results was significant at the 5% level therefore the null hypothesis that the ratios from each group came from populations with the same mean and variance was rejected. The mean and variance of the ratios are plotted on the box and whisker plot in figure 70.

There was a significant difference at the 5% level between the means and variance of the ratios in the control group and the ratios in each of the repair groups. In contrast to this, there was no significant difference at the 5% level when comparing the means and

variance of the ratios of the repair groups with one another—as can be seen from the results of Scheffé's tests (table 8).

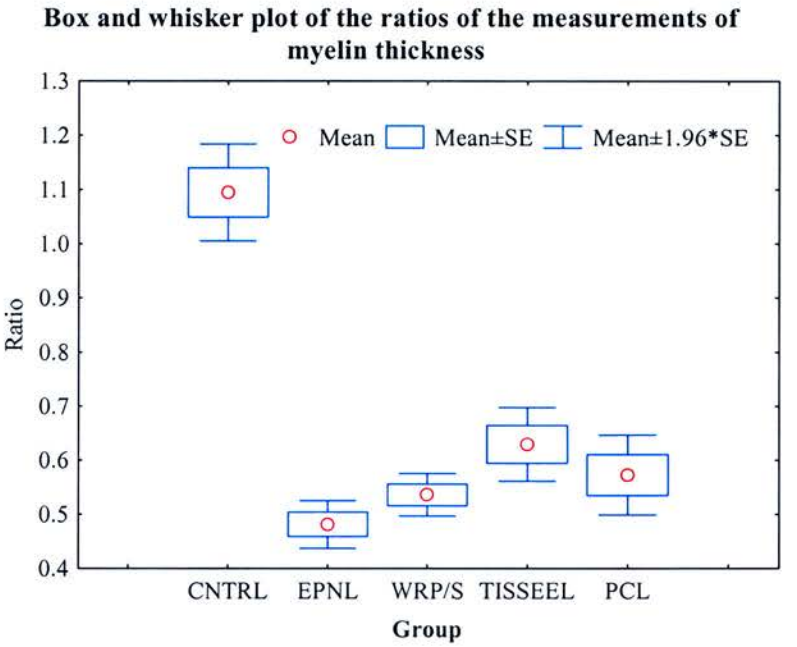

Figure 70

Box and whisker plot of the ratios of the measurements of myelin thickness in each group

	CNTRL (1.09) {0.045}	EPNL (0.48) {0.023}	WRP/S (0.54) {0.020}	TISSEEL (0.63) {0.035}	PCL (0.57) {0.038}
CNTRL [10]		0.000	0.000	0.000	0.000
EPNL [10]	0.000		0.854	0.060	0.455
WRP/S [11]	0.000	0.854		0.411	0.959
TISSEEL [11]	0.000	0.060	0.411		0.827
PCL [11]	0.000	0.455	0.959	0.827	

Table 8

The *P*-values of Scheffé's test for the ratios of the results of myelin thickness. The means of the ratios (in round brackets), the standard errors of the mean {in braces} and the group sample size [in square brackets] are shown. The *P*-values which were considered significant (<0.05) are highlighted in red.

A similar shift to the left and loss of bimodal distribution, in repaired nerves, as was seen in fibre diameter and axon diameter measurements is seen on the histograms of the myelin thickness measurements in figure 71.

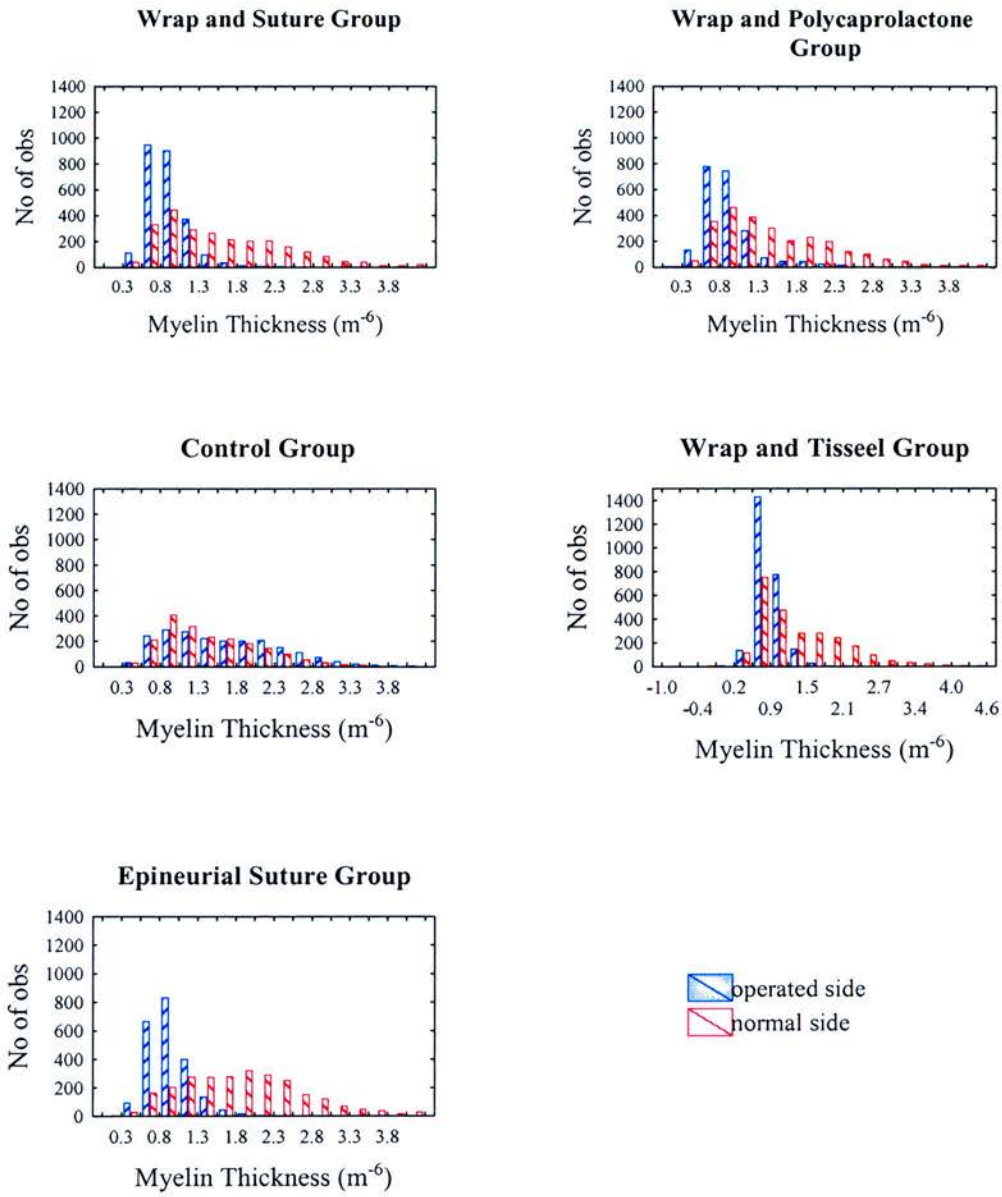

Figure 71

Histograms of myelin thickness measurements (μm) of the neurones in the right and left sides in all groups.

Bivariate histogram of myelin thickness

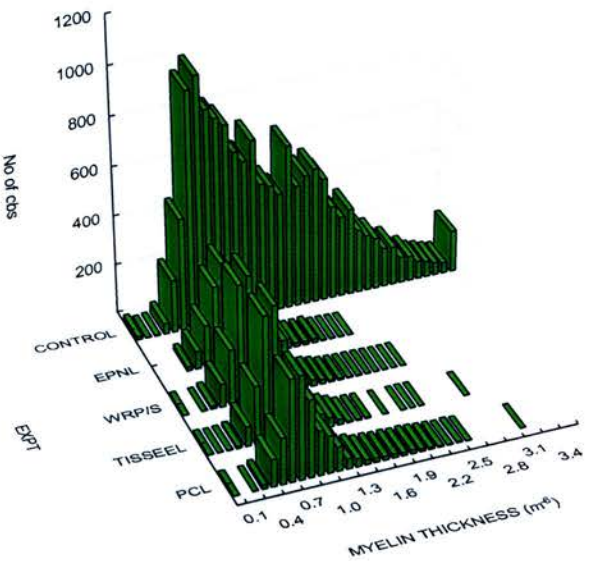

Figure 72

Bivariate histogram of myelin thickness measurements. All the data for the un-operated (left) limbs and the control group are displayed cumulatively as the 'Control' column.

The loss of bimodal distribution in the repair groups and the shift to the left in the size of the myelin thickness in the repaired nerves can be seen in the bivariate histogram of the myelin thickness measurements above in figure 72. The distribution of myelin thickness measurements peaked between 0.6 and 1.0 μm in every repair group.

G-ratio

The *F* statistic calculated for g-ratio results by one way ANOVA, unlike for fibre diameter, axon diameter and myelin sheath thickness, was not significant at the 5% level.

Therefore, the null hypothesis that the ratios of g-ratio results in the five different groups came from populations with the same mean and variance was not rejected.

The box and whisker plot of the ratios of the results of each group is shown in figure 73. It can be seen from the bivariate histogram in figure 74 that the distribution of the values for g-ratio in each group was very similar.

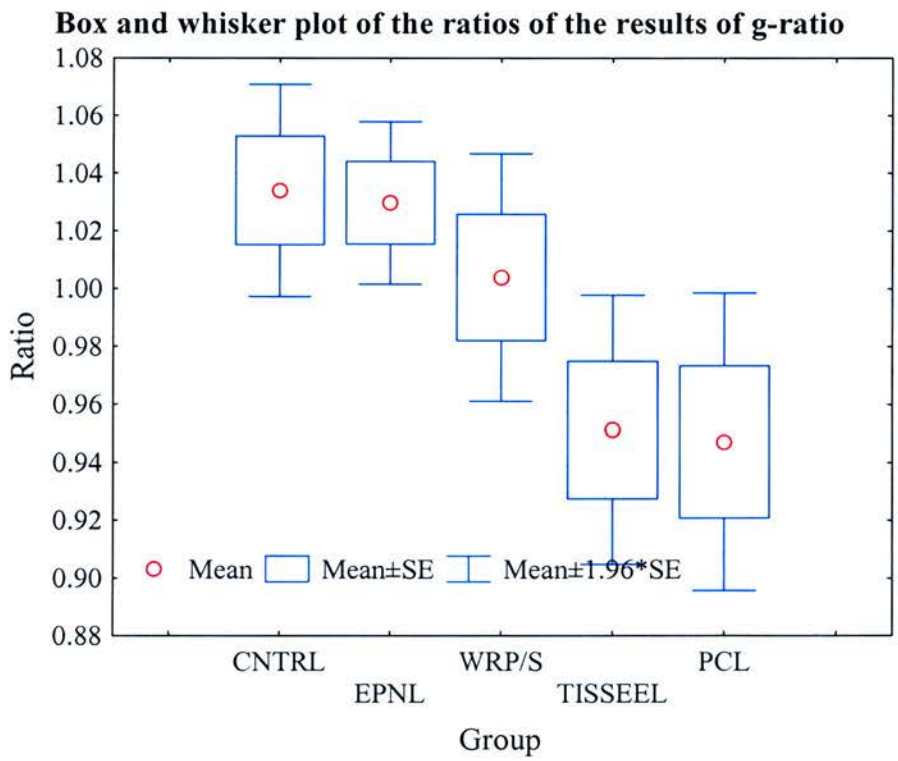

Figure 73

Box and whisker plot of the results of g-ratio. The *F* statistic of one way ANOVA was not significant at the 5% level therefore the null hypothesis that the ratios in all the groups came from the same population was not rejected

Bivariate histogram of g-ratio measurements in all groups

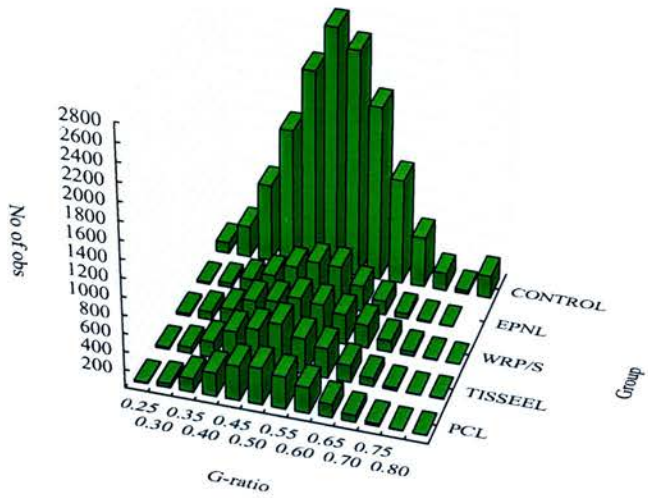

Figure 74

Bivariate histogram of the individual values for g-ratio in each group. All the data for the un-operated (left) limbs and the control group are displayed cumulatively as the 'Control' column.

Nerve sections

Nerve sections and a calibration scale were magnified by the same power through a light microscope. A camera mounted on the microscope took photographs and these were digitalized to view in an image analysis programme. The image in figure 75 shows the calibration scale used. The scale was photographed at the same magnification as the nerve specimens in figures 76-86. One small interval of the scale is equivalent to 10 μm. The specimens have been stained with osmium tetroxide which stains lipid, hence the myelin sheaths, black.

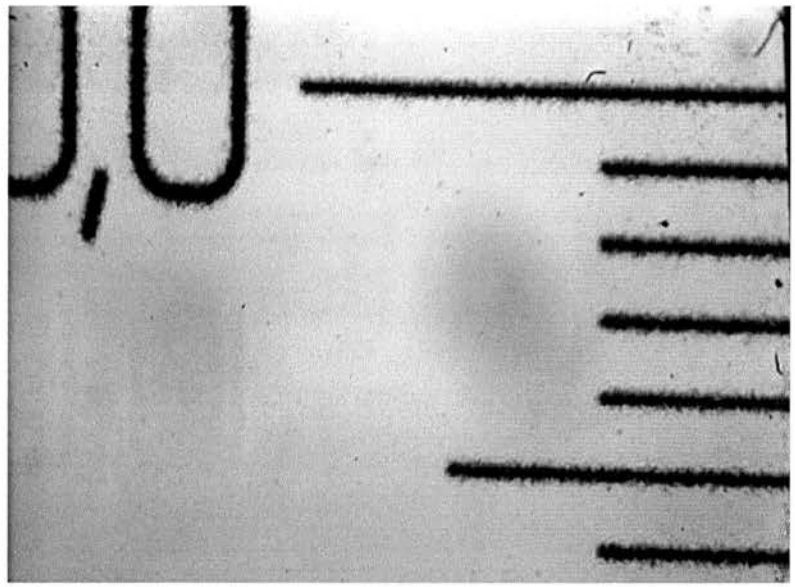

Figure 75

Each small interval of the scale is equal to 10 μm and shown at the same magnification as the photographs in figures 44–54.

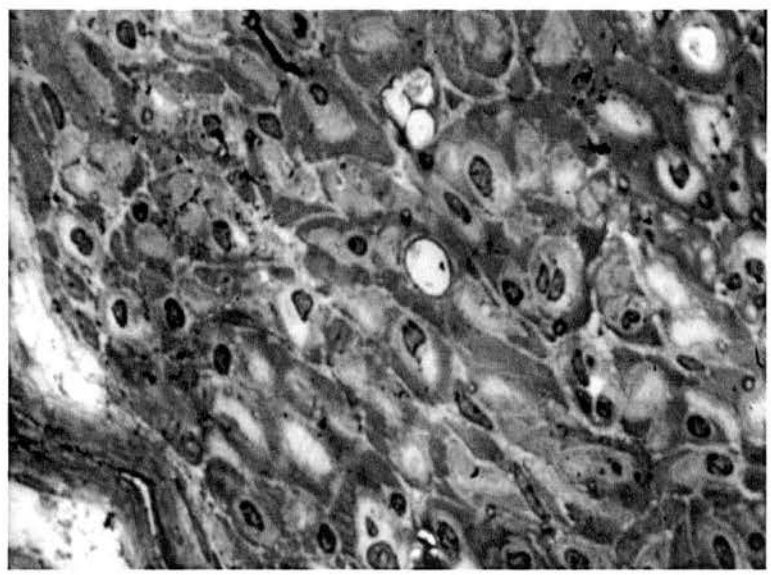

Figure 76

A semithin (1 μm) section of a sheep median nerve excised from a site distal to an epineurial suture repair site where dehiscence of the repair had occurred. No myelinated axons are visible.

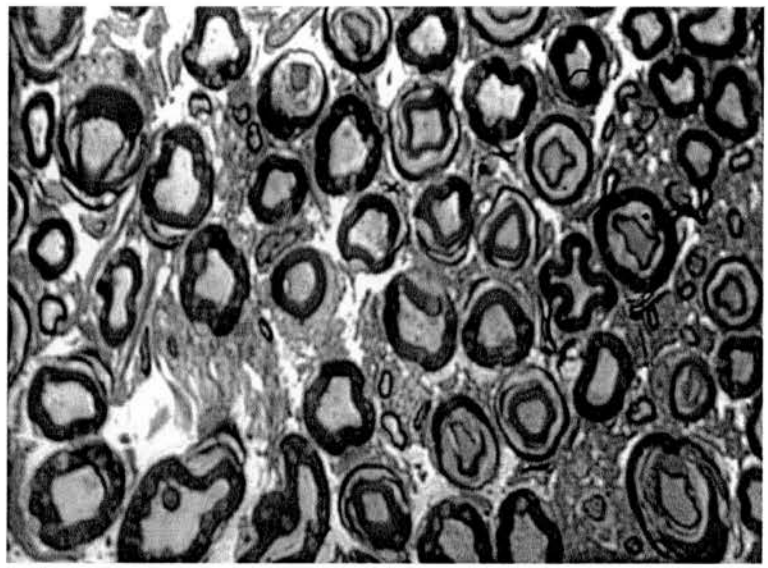

Figure 77

A semithin (1 μm) section of a normal median nerve.

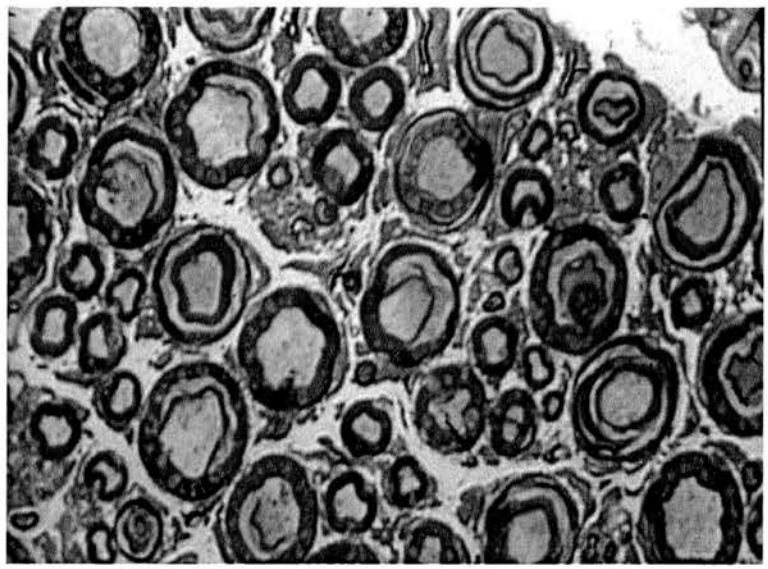

Figure 78

A semithin (1 μm) section of a normal median nerve.

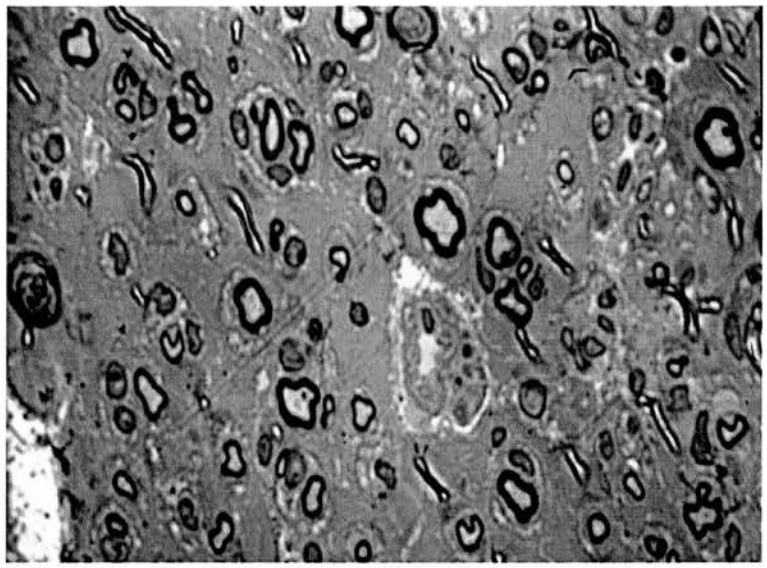

Figure 79

A semithin (1 μm) section of sheep median nerve excised from a region of nerve distal to the site of an epineurial suture repair.

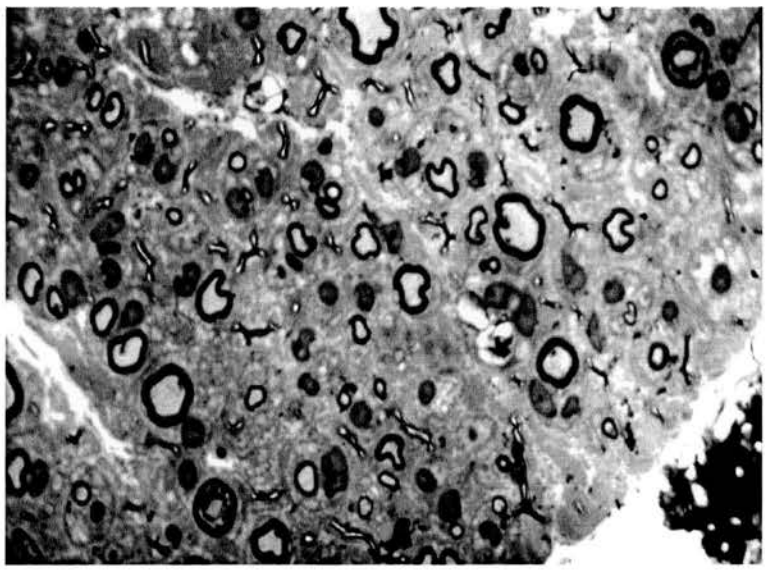

Figure 80

A semithin (1 μm) section of sheep median nerve excised from nerve distal to the site of an epineurial suture repair.

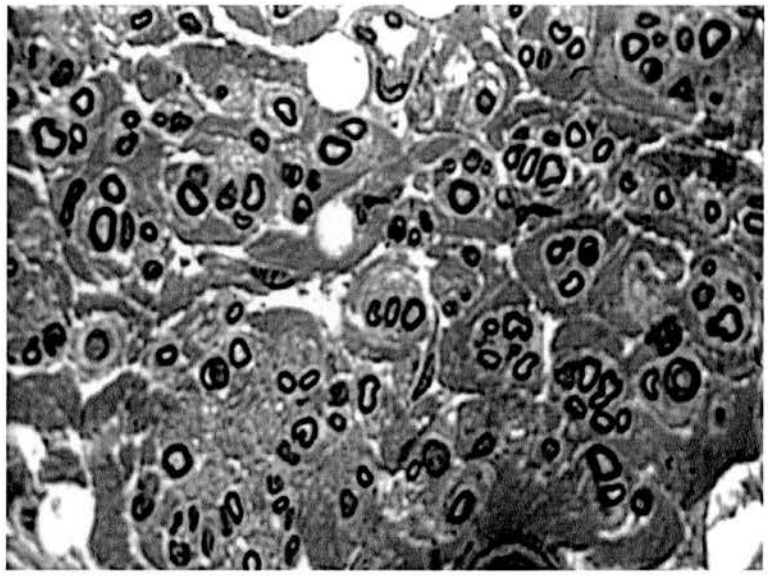

Figure 81

A semithin (1 μm) section of sheep median nerve excised from a region of nerve distal to the site of a CRG-wrap + macrosuture repair.

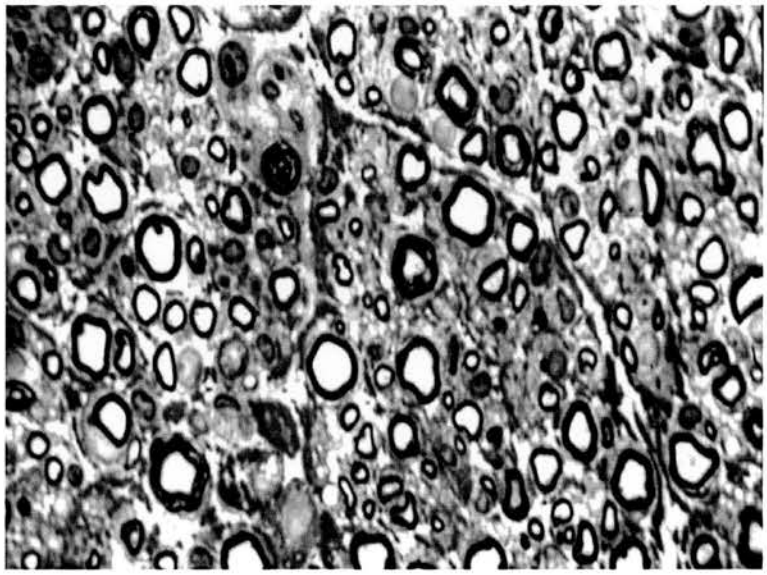

Figure 82

A semithin (1 μm) section of sheep median nerve excised from a region of nerve distal to the site of a CRG-wrap + macrosuture repair.

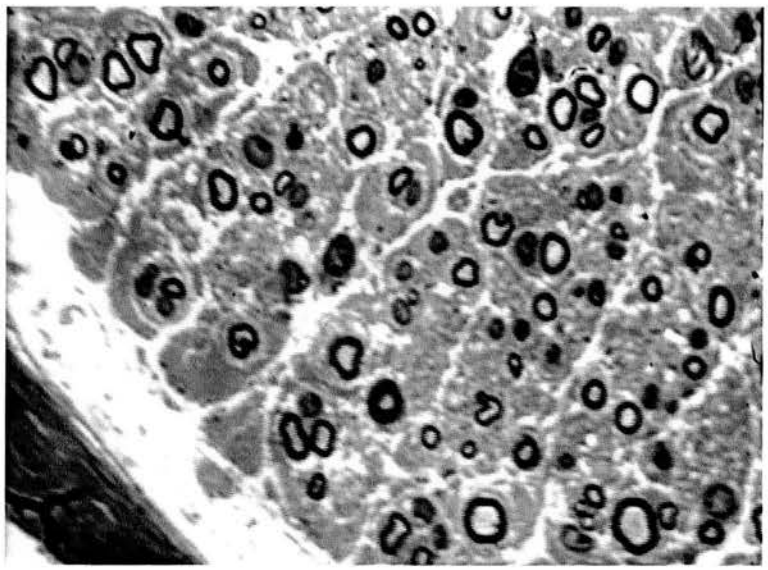

Figure 83

A semithin (1 μm) section of sheep median nerve excised from a region of nerve distal to the site of a CRG-wrap + Tisseel repair.

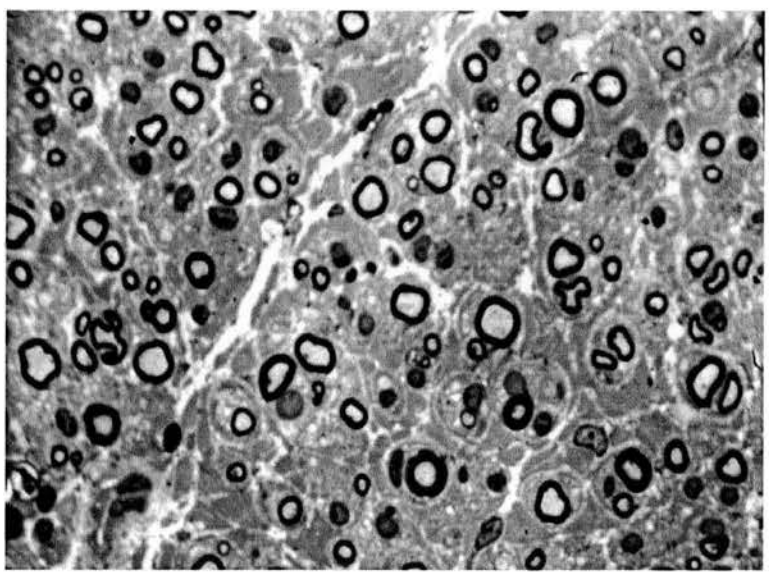

Figure 84

A semithin (1 μm) section of sheep median nerve excised from a region of nerve distal to the site of a CRG-wrap + Tisseel repair.

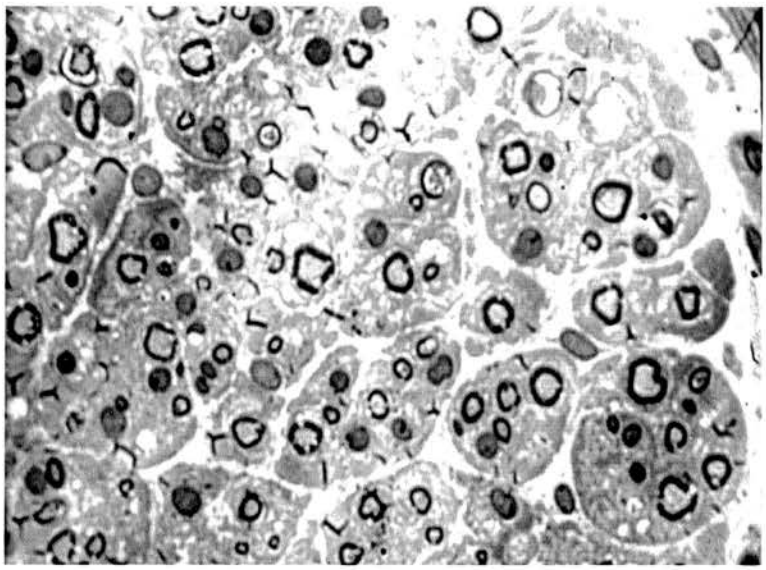

Figure 85

A semithin (1 μm) section of sheep median nerve excised from a region of nerve distal to the site of a CRG-wrap + polycaprolactone repair.

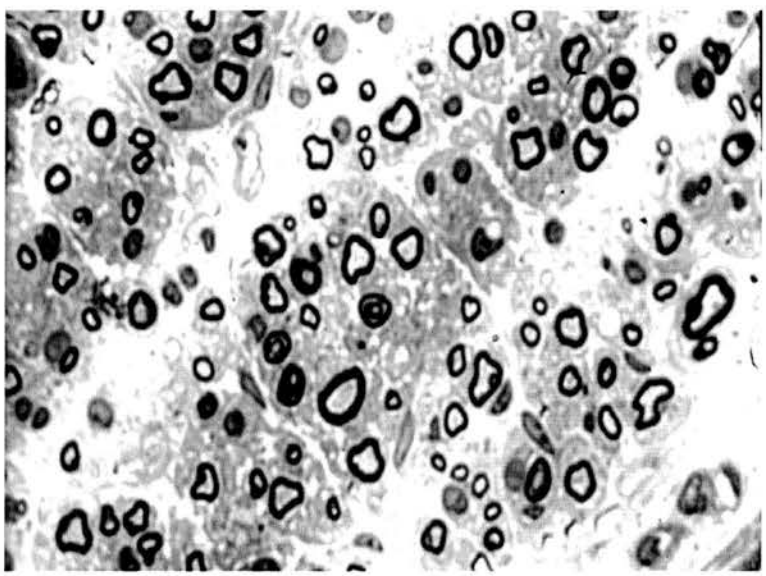

Figure 86

A semithin (1 μm) section of sheep median nerve excised from a region of nerve distal to the site of a CRG-wrap + polycaprolactone repair.

Tensile strength testing of repairs

The tensile strength of each type of repair immediately after repair had been carried out was measured. It was considered an indication of how likely dehiscence may occur *in vivo*. The force required to rupture each specimen was measured using the Instron (tensile testing machine) as previously described.

The epineurial suture repair had the highest tensile strength. Approximately 2 N were required to rupture the repair. The wrap and macrosuture repair required a force of approximately 1 N to cause the repair to rupture. The wrap with Tisseel repair required a force of less than 1 N to cause it to rupture and the repair formed by the wrap and polycaprolactone glue dehisced while being attached to the Instron machine therefore it was likely that the force required to rupture this repair was less than 1 N.

Tensile properties of repairs after 7 months

Seven months after the time of initial repair, portions of the median nerve, with the repair site at the mid point of the excised length, were taken from two sheep in each repair group. The tensile properties of the repaired nerve segments were measured. The elongation and force to rupture was recorded on the Instron machine. The results and calculated results are shown in table 9. It was important to note the position at which the specimens ruptured for two reasons; to be sure that edges of the holding blocks were not weakening the specimens and causing them to rupture at their point of attachment, and, to observe whether the repaired specimens ruptured at the site of the repair. None of the repaired nerves ruptured at the level of the repair and a half of the specimens ruptured away from their point of attachment to the holding blocks. The ultimate

NERVE	ULTIMATE STRAIN	ULTIMATE FORCE (N)	ULTI-MATE STRESS ($N M^{-2}$) (10^6)	WORK TO FAILURE (NM) (10^{-1})	NORMA-LIzED WORK TO FAILURE (N)	SITE OF break	SLIP-PAGE Y/N
T3R	0.180	79.8	9.63	3.35	8.08	LOWER EDGE	N
T11R	0.158	99.8	11.3	3.57	7.10	LOWER EDGE	N
P10R	0.216	64.1	7.66	2.43	6.55	LOWER EDGE	N
P11R		62.5	6.19			LOWER END	N
W8R	0.241	72.6	8.71	3.71	7.71	TOP END	N
W9R	0.187	97.6	12.6	3.53	7.91	LOWER END	N
S3R	0.217	55.6	4.9	2.25	4.8	LOWER END	N
S4R	0.236	58.8	8.06	2.85	6.89	TOP EDGE	?

Table 9

Results of the tensile testing of the properties of the repaired segment of nerve in each group at seven months. None of the nerves ruptured at the site of repair.

force (N), ultimate stress ($N m^{-2}$), work to failure (N m) and normalized work to failure (N) were greater on most occasions in the repairs in which a wrap had been used.

When these results are compared with the results from the same stretch test on normal and frozen nerves (shown in the table 10) it can be seen that the values for ultimate force to rupture and ultimate stress are similar in the repair groups to those in the normal and frozen nerves.

The effect of freezing on the tensile properties of nerves

The effect of freezing on the tensile strength of nerves has not previously been documented in the literature. It was important to establish this in the present study

nerve type	cross-sectional area (m^2) (10^{-6})	force at rupture (n)	ultimate stress (n m^{-2}) (10^6)	site of rupture	evidence of slippage
NORMAL 1	8.54	70.0	8.20	UPPER END	NO
NORMAL 2	5.77	80.0	13.9	MIDDLE	NO
NORMAL 3	3.23	98.0	30.4	BOTTOM EDGE	NO
NORMAL 4	6.11	54.0	8.84	UPPER END	NO
FROZEN 1	3.22	83.6	26.0	TOP EDGE	NO
FROZEN 2	4.41	59.9	13.6	BOTTOM EDGE	NO
FROZEN 3	8.09	71.7	8.86	BASE	NO
FROZEN 4	8.34	72.6	8.71	TOP END	NO

Table 10

Results of tensile testing of normal sheep median nerves and sheep median nerves that had been frozen for a mean time of four weeks at -11 °C and then thawed to room temperature.

because all the nerve repair specimens were frozen to -11 °C then thawed prior to having their tensile properties tested. To establish whether there was any change in the tensile properties of nerves with freezing then thawing, four freshly excised median nerves and

four median nerves that had been frozen at -11°C for approximately four weeks then thawed had their tensile properties measured. The results are shown in the table in table 10. No statistical analysis was made of the results because of the small group sample size. It can be seen from the results in the table however that there was no evidence of a difference in the tensile properties between the frozen and fresh nerves.

SUMMARY OF RESULTS

The results of *TSJ* and *M lat* highlighted that the outcome of regeneration compared to controls was different between the repair groups. There was no significant difference in the results of CV_{max}, *wet muscle mass*, *fibre diameter, axon diameter* and *myelin thickness* between the repair groups but the results confirmed that neurones that have regenerated after injury do not regain their original size or conduction properties. The results of F_{min} and *P lat* were not useful. The variables calculated from isometric twitch tension testing were not significantly different between any of the groups. It was decided from the results of the tensile testing that freezing then thawing of nerves had no effect on their tensile properties. The tensile strength of the repaired specimens was greater than that of normal nerves.

CHAPTER 4 — DISCUSSION

A difference among the repair groups in some of the measured variables has now been shown. Conclusions made from these differences, a critique of the experimental methods employed, and an evaluation of the techniques of securing the wrap is now presented. Also, a summary of the potential current and future uses of the CRG-wrap within the NHS and other healthcare situations will be discussed.

CRITIQUE OF THE SHEEP MODEL AND EXPERIMENTAL METHODS

The use of animals

The use of an animal model allowed the nerve involved, site of injury, mechanism of injury, time between injury and repair, experience of operator, and timing and method of assessment of outcome to be kept the same in each experimental group. This is a situation that would never possible in clinical practice. If a clinical trial was carried out using the CRG-wrap in nerve repair, the outcomes of repairs would most likely be assessed using neurophysiological tests and a clinical grading system. It may not be possible to perform a randomized controlled study comparing the use of CRG-wrap with microsurgical epineurial suture repairs because no two injuries are ever identical. Comparison of the regeneration of the neurones with respect to the time after repair would be difficult. Differences in each case such as: the age of the patient, the site of the injury, the time at which repair was carried out after the time of injury, and the presence of a vascular or soft tissue injury could not be controlled for and yet all affect nerve

regeneration (Fullarton et al 1998; Glasby, Fullarton, & Lawson 1997; Glasby et al 1998; Grieve et al 1991; Lawson & Glasby 1995).

The sheep model

The Edinburgh Peripheral Nerve Research Group (EPNRG) has used sheep now for eighteen years in experimental work. Many researchers have found the sheep to be a good model for human nerve repair with a similar potential for nerve regeneration (Fullarton et al. 2002; Fullarton et al 2001; Glasby et al 1990; Glasby & Hems 1995; Glasby et al 1992; Hems, Clutton, & Glasby 1994; Hems & Glasby 1992; Kettle 2003; Starrit 2004).

The median nerve was easily accessible at the point chosen for neurotmesis in the upper forelimb and there were no complications involving the wound. Sheep can be easily housed and handled in large numbers and in an environment no different from a working farm. They recovered well after operations, returning quickly to their normal routine. Unlike chimpanzees and rats which have a tendency to develop trophic ulcers in the skin supplied by the divided sensory nerve (Di Benedetto et al 1998; Grieve et al 1991; Kline et al 1964) there have been no trophic ulcers or skin damage in the area of skin supplied by the median nerve after its division in sheep, either in the present or previous studies (Hems 1993; Kettle 2003; Starrit 2004).

It is unfortunate that the work of the Edinburgh Peripheral Nerve Research Group is soon to finish and with it, the use of the sheep as a large animal model. Most other peripheral nerve research laboratories in the United Kingdom use rats or rabbits in experimental work on nerve regeneration. These animals (rats, rabbits, dogs) have a greater potential for nerve regeneration than humans. The results seen in such experiments may not be the

same as what could be expected in a human. For example, Nakamura et al (2004) reported that divided peroneal nerves of dogs regenerated more quickly across a gap of 15 mm through a polyglycolic acid-collagen conduit (a polyglycolic acid woven conduit that had been coated with collagen and filled with a collagen sponge) than through a nerve autograft of the same length. Peroneal nerves in dogs, however, were shown by Kline et al (1964) to regenerate over a gap length of 2–3 cm without a conduit of any type. By 14 weeks after division, Kline et al demonstrated that a gap of 2–3 cm between divided nerve ends had been bridged. In the study by Nakamura, at four months (17 weeks) the proximal nerve stump had advanced to the centre of a 15 mm nerve autograft but the distal stump had not yet reached the centre. It may be that the peroneal nerves in dogs in the experiments of Nakamura et al would have bridged the gap between the nerve ends without the presence of the collagen sponge and that, in fact, the nerve autograft probably slowed the process of nerve regeneration rather than the collagen conduit accelerating it. Humans do not have this same potential for nerve regeneration therefore growth through a collagen conduit may not exceed that through a nerve autograft in a human.

The operator

The author, who carried out most of the repairs in the experiments in the present study, had previously carried out epineurial repairs in clinical practice using loupes of × 3.5 magnification. (Loupe magnification and 9/0 polyamide, rather than the use of the operating microscope and 10/0 polyamide, are common in many centres for epineurial repair despite the opinion of Millesi (1981) that the latter technique leads to a better outcome). Instruction was given to the author in the proper use of the microscope and

microsurgical instruments prior to the commencement of the repairs in the sheep. Clinical training to carry out microsurgical epineurial repairs to an appropriately high standard requires experience (Kimura 2000). In clinical practice, most operators carrying out nerve repair unsupervised would have had around six years of basic and specialist surgical experience (i.e. a specialist registrar in plastic or orthopaedic surgery).

In contrast to this, learning to use the wrap was simple. Instruction in the techniques of application and securing of the wrap took approximately thirty minutes and in fact could be carried out without previous demonstration if the basic surgical principles were applied.

The technical points that were highlighted were:

1. To avoid placement of the macrosutures deeper than the epineurium of the nerve. This was especially difficult when putting in the uppermost sutures: the inferior sutures were placed between the nerve and the wrap with direct vision of both the epineurium and the wrap but, when placing the uppermost sutures, the wrap had been folded over the nerve stumps and their epineurium could no longer be seen. Judging how deep to place the macrosutures was difficult. In attempting to avoid placement deep to the epineurium with subsequent damage to the perineurium and neurones, the author suspects that on some occasions the uppermost sutures were not placed in the nerve at all, but only through the layers of the wrap – this still held the wrap in position and may have been a benefit.
2. When using glue, to avoid placement of the glue near the site where the cut surfaces of the nerve stumps are in contact as this could cause increased fibrosis at the repair site with a poorer outcome.

Tension between the stumps at the site of repair or too tight an apposition of the cut ends of the nerve was not possible with the wrap repair. The technique could be easily learned and carried out by someone with very limited surgical experience.

It was appropriate that a surgeon with limited experience in microsurgery carried out the repairs (the author completed most of the epineurial repairs and some of the CRG-wrap repairs, with the other repairs being carried out by the project supervisor): the ease with which CRG-wrap repairs could be carried out compared with microsurgical epineurial repairs was more obvious because the operator had limited experience in both techniques.

The control group

The control group had two important functions:

1. Any inappropriate results due to technical problems with testing on the control sheep could be discarded and results from a new animal substituted. The same was not true for the operated groups when a sheep would have to undergo an operation and then be housed for seven months until the tests could be repeated.
2. The ratios of results of the right limb to the left limb, when both limbs were normal and had not been operated on, was likely to be close to 1.0 for each measured variable. By establishing this experimentally it was demonstrated that the techniques used in measurement were accurate and gave reliable results. The mean ratios and 95% confidence intervals for the results of each measured variable are shown in figure 87.

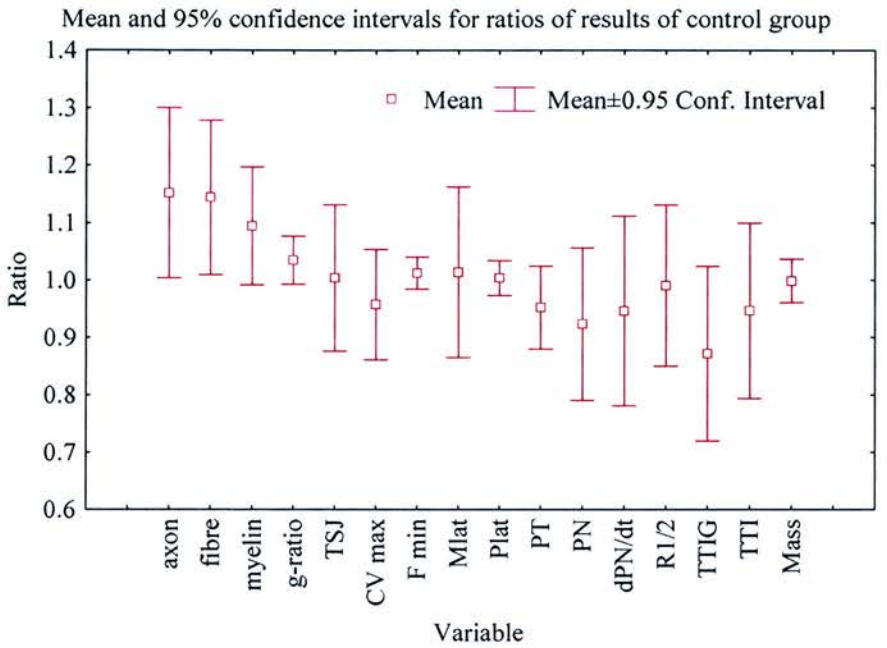

Figure 87

The mean and 95% confidence intervals for the ratios of each variable in the control group. The mean of the ratios of each variable was approximately 1.0.

The experimental methods of evaluating nerve regeneration

Measured variables that did not prove to be useful

F wave recording

Success in F wave recording was infrequent, especially in the normal limbs of the repair group sheep. No previous recorded evidence was found of how successfully F waves can be elicited in sheep. However, F waves were elicited in the control group of sheep in the present study in around 90% of limbs suggesting that they are not infrequently produced in sheep under certain conditions.

It is known that nitrous oxide, halothane and other volatile anaesthetics inhibit the production of F waves (Freidman et al 1996; Rampril & King 1996). Kennedy and Galindo (1975) showed that halothane anaesthesia prolongs the half-decay times of end plate potentials (EPPs) in Albino rat diaphragm muscle cells from 1 ms (with no halothane) to 3 ms (with halothane anaesthesia). Halothane anaesthesia also decreased the amplitude of the EPPs. They demonstrated that after administration of halothane at a concentration of 3.5% for 25–50 minutes, muscle contractions ceased; slightly lower concentrations of halothane, however, had no effect on contraction of the diaphragms after fifty minutes of delivery.

Halothane would have reached a higher concentration in the peripheral tissues at the time of measurements being made in the un-operated limbs as this limb was always examined second. It is possible that the changes caused to the EPPs by halothane anaesthesia were responsible for the low number of F waves recorded in the sheep in the present study.

Clinical Use

F_{min} is a useful measure to assess the speed of conduction in the proximal section of a nerve. If used in a clinical trial, the patient would not be anaesthetized and it is more likely that F waves would be successfully recorded. They are however still produced with a frequency of only 79% and not when stimulating near the axilla (Kimura 2000).

Central and peripheral motor conduction time

It was not possible to elicit a compound muscle action potential by electrical or magnetic stimulation of the motor cortex of the sheep. An internet search of *Pubmed* and *Medline* (1966-2005) using various combinations of the search terms 'cortical stimulation',

'magnetic cortical stimulation', 'sheep, 'cortex' and 'movements' was carried out but failed to elicit any relevant information on the production of motor responses from cortical stimulation in sheep.

Had it been possible to measure central motor latency, *peripheral motor conduction time* (*P lat*) could have been calculated using the results of F_{min} and *motor latency (M lat)*.

Clinical use

Central pathway conduction time can be measured in humans by recording cortical sensory evoked potentials in the post-central gyrus with scalp electrodes. A nerve is stimulated and evoked potentials are recorded by the scalp electrodes positioned over the post-central gyrus. In clinical practice, magnetic coil stimulation of the motor cortex can elicit motor responses with less pain and discomfort than electrical stimulation of the cortex and with no known side-effects (though both techniques should be avoided in patients with epilepsy, cardiac pacemakers or metal-implants in their head (Kimura 2000)). Electrical stimulation is too painful for the conscious subject.

Peripheral latency

The measurement of F_{min} was inconsistent and calculation of the *total motor pathway conduction time* and *peripheral latency* was therefore not possible.

Clinical use

Although not possible in the anaesthetized sheep, the measurement of peripheral latency would be easier in non-anaesthetized human subjects and would be useful in the assessment of the speed of conduction in the whole peripheral nerve from the spinal cord to the motor nerve terminals in repaired nerves.

Twitch tension measurement

The experimental arrangement in the present study used to measure isometric twitch tension had been improved upon from that used by previous researchers in the EPNRG. Starrit (2004) and Kettle (2003) used a Steinman pin through the keratinous hoof of the sheep with traction applied to equal the force of flexion produced by contraction of the flexor muscles upon stimulation of the median nerve. The olecranon was not fixed in this arrangement, and contraction of FCR produced movement of the olecranon away from the body of the sheep—and movement of the whole sheep—thus giving a falsely low measurement of isometric contraction at the distal end of FCR. Starrit (2004) did not find any significant differences between the measurements made of twitch tension between her control group and five different injury and repair groups: neurapraxia, axonotmesis, neurotmesis and repair with a nerve autograft, neurotmesis and repair with CRG-wrap, neurotmesis and epineurial suture.

The starting tension was kept the same in all the muscles in the present study. The technique of keeping the starting tension uniform was also used by Hems (1993) when he measured isometric twitch tension in the extensor digitorum longus muscle of the rabbit. He found that, although based on the presumption that all muscles had the same elasticity, measurements taken in this manner were most likely to give a maximal value for twitch tension. Unfortunately, Hems, like Starrit and the present author, found no significant difference between control and repair groups in any of the variables calculated from the recorded curves of isometric twitches.

Stevenson et al (1994) demonstrated a significant decrease in the isometric twitch force and tetanic force generated in the extensor digitorum longus muscle of rats after repair of

their peroneal nerves by an epineurial repair (n = 10) and tubular nerve guides (n = 11) compared with normal controls (n = 15). The percentage decrease from normal control values in the isometric twitch force in the repair groups was 35% in the epineurial repair group and 45% in the tubular nerve guide group. The percentage decrease from normal controls in the measured tetanic force tension was 16% in the epineurial group and 25% in the tubular repair group. There was no significant difference between the groups in the results of *time to peak tension* and *half relaxation time*. The specific methods of immobilizing the limb and ensuring the same initial tension or increase from resting length of the muscle were not described. Grieve et al (1991) also found isometric twitch measurements useful in the assessment of the effect of age on the outcome of the sciatic nerve regeneration in rats. It may be that twitch tension measurement is a more useful measure in the small animal model where immobilization of limbs is more easily carried out.

In five sheep in the Tisseel group, the maximum force of isometric twitch contraction in the repaired side was greater than in the normal side. McComas et al (1971) report that the amplitude of twitch tension of the human extensor digitorum brevis muscle was not reduced until 90% of the motor units were lost. Lewis et al (1972) and Kean et al (1974) suggest that there be more complete activation of contractile proteins in denervated muscle in response to a single action potential. These factors, working in unison, may explain why it was possible to record a larger twitch tension in the reinnervated muscle than in the normal muscle.

In summary, the methods employed in this study to measure isometric twitch tension are probably the most technically accurate of all the studies reviewed. Even with this

improved technique however, no significant difference was detected among the groups for any of the variables measured from the isometric twitch tension curves. The author concludes therefore that isometric twitch tension testing is not a useful test to compare muscle regeneration after different methods of nerve repair in a large animal model.

Variables which demonstrated differences between groups

Transcutaneous stimulated jitter (TSJ)

Use of the concentric needle

With the concentric needle, fibres within 1 mm of the leading off surface of the electrode and motor unit potential spikes were recorded (which typically consist of action potentials from around twenty muscle fibres (Thiele & Boehle 1975).) In the present study, the author found that many adjustments of the needle's position were required prior to being able to detect a single muscle fibre action potential. On occasions, two overlapping single fibre action potentials were recorded. If it was possible to discern a single straight uniform rising or falling edge in one of the potentials that was not affected by the other (see the diagram in figure 2), jitter was measured from this site. Measurements taken from overlapping action potentials can lead to an underestimation of jitter or to a difference in jitter among groups being missed (Kimura 2000). Because of the difficulty in obtaining adequate numbers of recordings, measurements from these overlapping action potentials were occasionally accepted in order to record twenty measurements of TSJ from each muscle. The electronic 'window' for latency measurements in such a case was placed near the baseline on the straight part of one

slope where the slope of the action potential was likely to be formed by only one muscle fibre's action potential (figure 88).

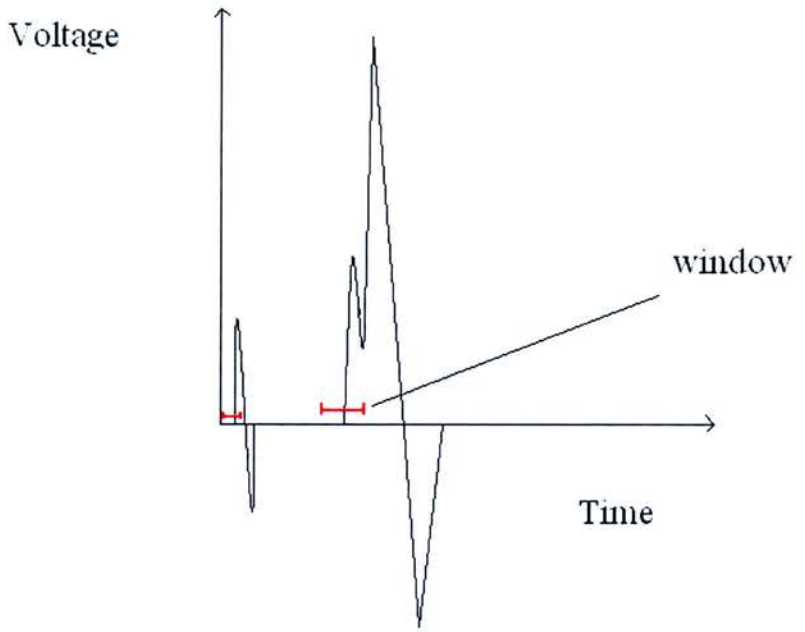

Figure 88

Diagram of positioning of SFEMJ window set-up when single motor potentials could not be recorded as separate action potentials

In summary, concentric needles are cheaper and although their design favours the measurement of motor unit potentials they can measure single fibre action potentials. They are more commonly used in clinical practice than the SFEMG needle and were used effectively in the present study.

Clinical use of jitter

In clinical practice, the most commonly measured form of jitter is *voluntary jitter* which differs from *stimulated jitter* in that the difference in latency in voluntary jitter is measured between two single fibre action potentials when a muscle is gently being contracted voluntarily. This is in contrast to measuring the difference in latency between the spike of the stimulating action potential and the muscle fibre action potential produced. Stimulated jitter is occasionally preferred if the patient cannot voluntarily contract his muscles in a controlled manner, e.g. he is under anaesthesia or sedation, is a very young child, or has loss of motor control. Care is taken on such occasions to avoid stimulation of the motor point of the muscle because damage may be caused to the motor end plates by their direct stimulation of the end plates and, activation of many motor units at once is painful (Trontelj & Stålberg 1992).

Although the measurement of *transcutaneous stimulated jitter* requires the insertion of stimulating needle electrodes into muscle, Trontelj and Stålberg (1992) consider it a useful clinical technique, even in children, and state that, 'with the stimulating cathode in a good position, stimulation is hardly perceived or may not be felt at all. Many patients will actually fall asleep during the procedure.'

In the present study, it was difficult to identify the wasted FCR muscle in the repaired limbs even though identification of FCR in a normal sheep limb is relatively easy. Recognition of particular muscle bellies is not difficult in clinical practice, even when wasted: the clinician taking the measurements is usually very experienced in the techniques used and the muscle can be identified when an associated voluntary action is

made (personal communication with Dr Moran, Clinical neurophysiologist, Western General Hospital, Edinburgh).

Maximum conduction velocity (CV_{max})

Disk electrodes effectively detected the mass action potential in the FCR muscle and were preferred to needle electrodes as they gave a better recording of the compound motor action potentials (CMAPs) produced by the whole FCR muscle. The use of tape to stick the disk electrode to the skin was found to be better than suturing as it maintained a closer contact between the disk electrode and the skin surface. The best adhesive tape was zinc oxide: it stuck well even if the skin surface was wet and molded easily to the shape of the limb surface.

In the scatterplot in figure 89 it can be seen that measurements from the control (un-operated) limbs were within a range of 60–80 m s^{-1} and are therefore consistent.

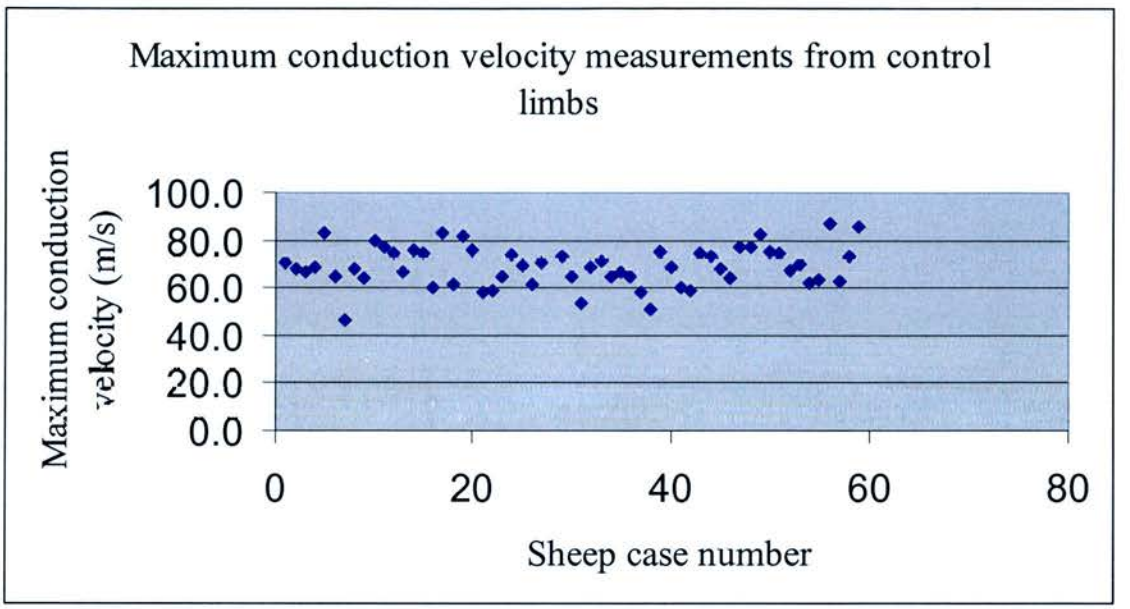

Figure 89

The measurements of CV_{max} in all un-operated limbs (these values include measurements from both limbs in the control group and un-operated limbs in the repair groups) were within a range of 60–80 m s^{-1}.

Measurement of the length between the two points of stimulation on the nerve was most easily and accurately made by laying a length of silk or linen suture along the nerve—which adhered to it by surface tension—and cutting the suture to the length between the two points of stimulation. Measurements were considered accurate to 0.5 mm.

The measurement of maximum conduction velocity is a commonly used clinical technique in the assessment of peripheral nerve function and could be easily used in a clinical trial.

The only clinical example of measurements of nerve conduction velocities for the comparison of two methods of nerve repair was in the study by Lundborg et al (2004). They measured sensory and motor conduction velocity and latency times in the ulnar and median nerves after repair of these nerves by a silicon tube (n = 17) and epineurial suture

(n = 13). Measurements from the normal contralateral limbs were not compared with the repaired side. No difference was found between the neurophysiological outcomes of the two types of repair. A difference may have been detected between the two repair groups had the ratio of the measurements taken from the repaired nerve to the measurements from the normal contralateral limb been calculated for each variable and used to compare the outcome between the groups.

Motor latency (M lat)

The median nerve divides into a large superior branch and a smaller inferior branch before it dips downwards to enter the forelimb (figure 90).

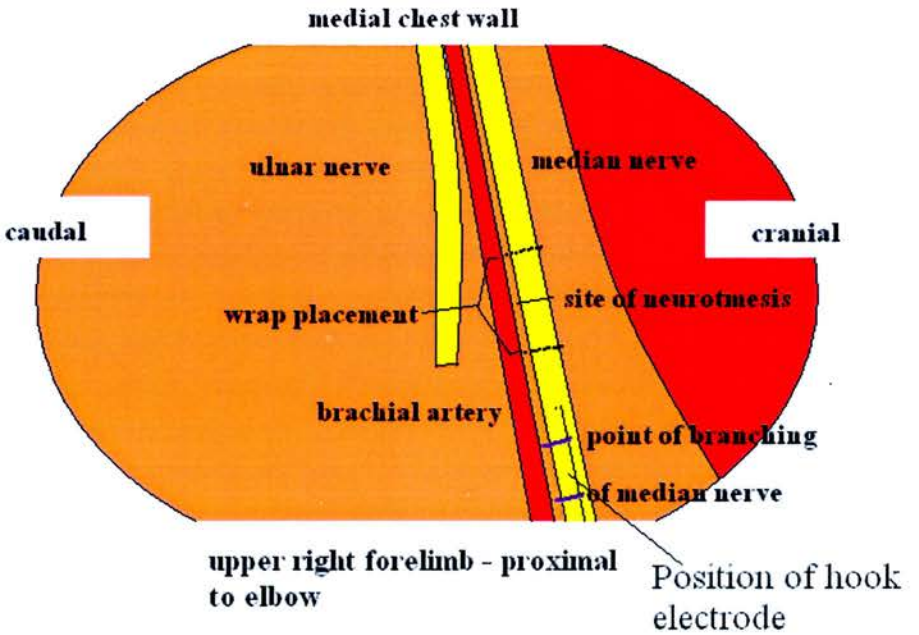

Figure 90

The position of the placement of the hook electrode for the measurement of motor latency is shown between the two mauve lines on the large superior branch of the median nerve

The length of the large, superficial branch of the median nerve was just long enough to allow the hook electrode to be positioned between its site of branching and the distal limit of dissection, and therefore the position of stimulation was uniform in each sheep.

Morphometric analysis

As with all histological fixing and staining procedures, there was a degree of shrinkage of the axons and myelin sheaths: this however would have been uniform throughout all groups. Hems (1993) used the same staining procedure as in the present experiments and suggested that the shrinkage which occurs with the method used in the present study is not greater than 10%.

Systematic randomized sampling was found to be an efficient method. The method had not previously been used in the EPNRG but was shown by Mayhew & Sharma (1984) to be an effective sampling method for the measurement of mean axon and fibre diameter from a multifascicular mixed peripheral nerve (Mayhew 1990; Mayhew & Sharma 1984a).

The mean axon and fibre diameter and myelin sheath thickness in the present study were significantly smaller than the mean values reported by Starrit, Kettle and Hems (Hems 1993; Kettle 2003; Starrit 2004). The results from different authors are shown in table 11 for comparison. A total of 200 axons and fibres were measured randomly in each of these three authors' experiments and in the present study.

Measurement	Kettle (2003) and Starrit (2004)	Hems (1993)	Present study (2005)
Light microscope magnification	× 400	× 1000	× 1000
Axon diameter (μm)	8.99		3.14
Fibre diameter (μm)	16.72	12.0 (approximate value – value was read from a histogram)	6.41
Myelin thickness (μm)	3.87		1.52
g-ratio	0.53		0.49

Table 11

Morphometry results on the median nerve from previous studies in sheep.

The authors Kettle and Starrit used a × 40 objective lens when imaging sections from which they measured axon and fibre diameters. The × 100 objective lens was used to image sections in the present study. It is the author's opinion that the many small myelinated fibres present in both the normal and repaired nerves that were measured in the present study, would not have been imaged clearly enough at the magnification obtained using the × 40 objective lens (see photographs of nerve sections in the Results chapter).

This may explain the difference between the mean values for axon and fibre diameter found by Starrit and Kettle compared with the current author.

Hems (1993) examined neurones in the ventral horn. It is likely that, at this more proximal level, the neurones were larger in diameter. (Conduction velocity is greater in the proximal section of neurones (Sunderland 1978).)

As a selection process for choosing areas of nerve on which to carry-out morphometry, Kettle and Starrit photographed six to eight random fields from each nerve: Hems chose one field from each fascicle within a multifascicular nerve and a strip of fields in a longitudinal section when examining a unifascicular nerve (Hems & Glasby 1993; Kettle 2003; Starrit 2004). Small neurones are not uniformly distributed throughout nerves (see photographs of normal nerve specimens) and in the methods used by Starrit, Kettle and Hems, observer bias could lead to the imaging of sections in which the neurones were large.

Morphometric analysis is one of the most accurate methods of assessing the success of nerve repair (Aitken & Thomas 1962). It is not possible to carry out in clinical practice however. The present study is probably the most accurate comparison of nerve repair using the CRG-wrap with epineurial repair that could be carried out.

Wet muscle mass

Wet muscle mass decreases initially on denervation and then increases after successful repair and can be used to assess muscle regeneration after different methods of nerve repair (Carter et al 1998). Many authors have used wet muscle mass to assess muscle regeneration after nerve repair in animal studies (Grieve et al 1991; Hems 1993; Kettle 2003; Starrit 2004).

Wet muscle mass is not a variable which can be measured in clinical practice. It is a better measure of reinnervation of the muscle that histology of the muscle because

muscle cyto-architecture has been shown not to vary according to the type of nerve repair in the same way in which muscle mass does (Carter et al 1998). Muscle biopsies are unlikely to be ever used in the follow-up of patients to assess the outcome of nerve repair in a clinical study.

The statistical methods

The use of ratios

The benefit of examining the ratio of the measured values of variables from the operated to the non-operated sides can be demonstrated when the results of wet muscle mass are examined. The measured values of wet muscle mass in the normal limbs and the operated limbs in the present study are displayed separately in a box and whisker plot in figure 91. There is an apparently small difference in the mean and 95% confidence intervals of the values of the operated limbs between the control group and the repair groups. When the values of the non-operated limb were examined however, there was a large increase in the mean values between the control and repair groups. The reason for this is not clear. All sheep were over one year of age and therefore fully grown when the first operation was carried out and the average of sheep was two years at the time of the second operation. The ages of sheep did vary, but old and younger sheep were used randomly throughout all of the groups and therefore this should have not affected the results. The difference in the mass of FCR in the un-operated limbs between the control and the repair groups may have been because the control groups were tested in spring and the repair groups were tested in summer (the mean mass of the sheep may have increased while they were feeding on grass).

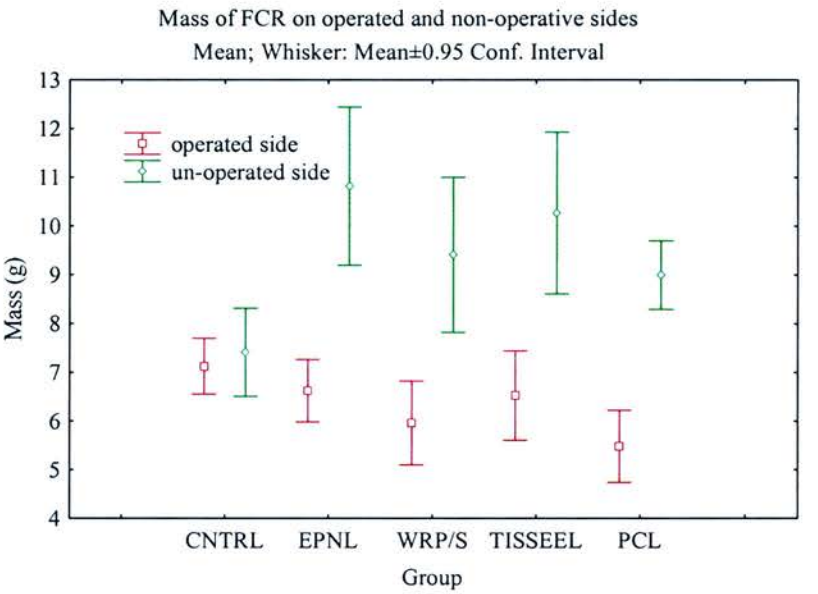

Figure 91

Mean and 95% confidence intervals for the results of wet muscle mass on the operated and un-operated sides in each group. The difference between the mass of the operated limbs and the non-operated limbs in the repair groups is much greater than the difference in the control group.

When one way ANOVA was carried out on the measurements of wet muscle mass from the operated side alone, the calculated *F* statistic was still significant at the 5% level, but the statistical power of one way ANOVA was only 0.75. This was much lower than the power of 0.99 for one way ANOVA obtained when the ratios were considered.

When Scheffé's test was carried out only on the results of wet muscle mass from the operated side (table 12), the CRG-wrap + polycaprolactone group was the only group found to be significantly different from the control group at the 5 % level.

	CNTRL (7.12) {0.257}	EPNL (6.62) {0.284}	WRP/S (5.96) {0.386}	TISSEEL (6.53) {0.410}	PCL (5.48) {0.333}
CNTRL [11]		0.902	0.225	0.816	0.030
EPNL [10]	0.902		0.768	1.000	0.263
WRP/S [11]	0.225	0.768		0.844	0.908
TISSEEL [11]	0.816	1.000	0.844		0.327
PCL [11]	0.030	0.263	0.908	0.327	

Table 12

Results of Scheffé's test for the wet muscle mass (g) of the operated side. The means of the ratios (in round brackets), the standard error of the means of the ratios {in braces}, and the sample size [in square brackets] is shown for each group. The *P*-values which were considered significant (<0.05) are highlighted in red.

Using ratios of the results of the measured values of the operated to non-operated sides therefore allows the detection of differences between groups with a greater accuracy. Perhaps, if the same method had been used by Starrit (2004), it would have been possible to detect differences between more of her groups and with a greater statistical power.

Use of ratios in the clinical setting

To exclude within-groups variation in a clinical study, measurement of *maximum conduction velocity, TSJ* and other clinical variables could be made bilaterally and the ratio of the repaired to normal side used to compare the outcomes in different groups. Taking neurophysiological measurements and carrying out clinical testing bilaterally would increase the time taken to assess each patient and cause them additional discomfort (nerve conduction studies are uncomfortable).

COMMENTS ON THE RESULTS

Clinical observation - contractures

Four contractures occurred in the Finn sheep. These sheep are bred because they tend to produce several lambs per pregnancy but are otherwise not very hardy.

Three sheep that developed a contracture had had nerve repair using wrap and polycaprolactone glue. The sites of repair in the polycaprolactone group were surrounded by more fibrosis than the sites of repair in the other repair groups. Polycaprolactone probably induced a more marked inflammatory reaction at the site of repair, therefore more pain. The Finns, being a less hardy breed, may have had more of a tendency to hold the painful limb in flexion thus allowing the ligaments around the knee to shorten.

When using the wrap in clinical practice, observation of patients would be important to document incidence of infection after operation, discomfort at the site of repair, and any evidence of joint stiffness or contractures.

Lundborg et al (2004) in their 5 year follow-up of repair with silicone tubes of the median and ulnar nerves in humans, found that eight out of seventeen patients required removal of the tubes at a later stage owing to local discomfort. There was no evidence however of an inflammatory reaction around the silicone tubes. In the present study there was little fibrosis around the sites of repair in the CRG-wrap + Tisseel group and the CRG-wrap + macrosuture group and no remnants of the CRG-wrap were could not be seen macroscopically in these two groups. It was not possible to assess the magnitude of any inflammatory reaction or pain caused by the presence of the CRG-wrap in the present

study. In a clinical study, this could be done by questioning the patients on follow-up about discomfort they experienced at the repair site.

An evaluation of the tests useful in the laboratory

Wet muscle mass

There were no significant differences found in the wet muscle mass among the repair groups confirming that the FCR muscles had regenerated by an equal amount in the CRG-wrap repair groups and the epineurial suture group. The significant decrease in the wet muscle mass of FCR in the repair groups compared with the control confirms that muscles do not regenerate fully after regeneration following neurotmesis and repair.

Morphometry

Axon diameter, fibre diameter and myelin sheath thickness

The final axon and fibre diameter of regenerated nerves depends on the peripheral connections made (Aitken et al 1947) and on an adequate repair. There was no significant difference in axon diameter, fibre diameter and myelin thickness among the four repair groups. This confirms that each CRG-wrap group had allowed neuronal regeneration and peripheral connection formation to the same degree as which occurred after the microsurgical epineurial repairs.

Axon diameter, fibre diameter and myelin thickness were significantly less in the repair groups compared with the control group. This was not surprising as neurones never regenerate, in adult mammals, to their original size or number after nerve injury (Aitken & Thomas 1962).

G-ratio

The g-ratio was not significantly different among any of the five groups. Thus, after seven months, the axon and fibre diameter and myelin sheath size had reached maturity and were not going to change further with time. It can be inferred that the mean CV_{max} and *M lat* had also reached values that were not going to change with time and therefore, while there was no significant differences among the conduction velocities of the regenerated nerve in the repair groups, the increase found in motor latency in the CRG-wrap + polycaprolactone group was unlikely to change with time.

Starrit (2004) had different findings for g-ratio when examining the neurones in the median nerve of sheep at the same level eight months after injury in five different injury and repair groups (all injuries and repairs were made on the median nerve in sheep at the same position as in the present study). There was a significant difference in the mean g-ratios between the neurapraxia group (0.48; n = 6) and the axonotmesis group (0.60; n = 6) and between the neurotmesis + CRG-wrap repair group (0.53; n = 6) and the axonotmesis group. Therefore, at eight months, the maturity of the neurones in the neurapraxia group, the neurotmesis group and the repair with CRG-wrap group was significantly less than the maturity of the neurones in the axonotmesis group. One would expect the maturity of neurones to be greater after neurapraxia compared with axonotmesis. Also, it could be concluded from the results in the study by Starrit that the maturity of neurones in the axonotmesis group was greater than in normal undamaged neurones (0.54, n = 6); this should not be the case. The current author believes that these results are probably not accurate and reflect the lower magnification at which measurements were taken and the smaller group size in the experiments of Starrit. They

do not discount the present study's finding that the neurones in all the groups had reached maturity in regeneration after seven months.

An evaluation of the tests useful in clinical practice

Transcutaneous stimulated jitter

The ratios of the measured values of *TSJ* in the operated to the non-operated limb were significantly higher in the CRG-wrap + macrosuture ($p = 0.003$) and CRG-wrap + polycaprolactone groups ($p = 0.017$) when compared with the control group. Because the g-ratios in the repair groups were no different to normal neurones, thus the neurones should have reached a state of myelination that was not going to change, it was be expected that the motor end-plates in each of the repair groups would be similarly mature. This was not the case. The regeneration of the motor end-plates must therefore continue after the maturation of the motorneurones. If serial measurements of *TSJ* and *g-ratio* had been made at several intervals after the time of initial repair up until the time of full maturation, it may have been possible to demonstrate that regeneration was slower in the CRG-wrap + polycaprolactone and the CRG-wrap + macrosuture groups than in the other two repair groups. The number of animals however which would have be required to demonstrate this would not have been ethically justifiable unless a small animal model were used (with the significant drawback of having limited relevance to repair in humans).

The conclusions that can be drawn from the statistical analyses of measured values of *TSJ* were:

1. That the epineurial suture group and the CRG-wrap + Tisseel group had developed motor end plates that were as stable as those in normal nerves.
2. That the CRG-wrap + macrosuture group and the CRG-wrap + polycaprolactone groups had regenerated motor end plates that were not as stable and therefore probably not as mature as those in normal nerves.

These findings suggest that neurones in the CRG-wrap + polycaprolactone and CRG-wrap + macrosuture group were slower to develop motor-endplates than the other two repair groups and that stabilization of the muscle cell membrane occurs after full regeneration of the supplying axon.

Maximum conduction velocity (CV_{max})

Measurement of CV_{max} in the present study was able to demonstrate with good statistical power that the fastest conducting neurones in all the repair groups had regenerated to the same degree. Conduction velocity has been shown by many authors to be one of the most reliable outcome measures in the assessment of neurone regeneration after different types of repair. It can be easily carried out in clinical practice and has clearly shown in the present study that the neurones regenerate equally after entubulation with CRG-wrap or microsurgical epineurial repair.

Motor latency

Motor latency was significantly higher in the CRG-wrap + polycaprolactone group compared with the control group. The other repair groups showed no significant

difference compared with the normal group. There was no significant difference in motor latency among any of the repair groups. The mean motor latency in the CRG-wrap + Tisseel, CRG-wrap + macrosuture, and epineurial suture groups was not significantly different from the mean motor latency in normal nerves.

The significantly longer motor latency in the polycaprolactone group must have been due to one of the following: delay in the production of an action potential in the largest motorneurones, delay in the release of neurotransmitter at the motorneurone terminals or delay in the production of a motor action potential in the muscle fibres of FCR.

Chloroform is a non-polar lipid solvent which disrupts the lipoprotein system present in myelin sheaths (Rumsby & Finean 1966) and increases the normal absolute refractory period for generation of EPPs either by depressing the nerve terminal, the nerve axon, or both (Kennedy & Galindo 1975). Chloroform evaporates rapidly at room temperature. It is possible that the presence of chloroform in the polycaprolactone glue caused irreversible damage to the myelin sheath membrane or nerve terminals when it was applied. The damage must have occurred at the time of application of the glue (it is likely that the chloroform would have evaporated rapidly) and not have recovered even with regeneration of the neurones. The motor latency was measured by stimulation of the nerve distal to the site at which the glue was applied. The chloroform could have dissolved in the tissues surrounding the site of repair and affected the nerve distal to the site at which the glue was applied.

Use of M lat in clinical practice

Measurement of motor latency was accurate and can be easily done in clinical practice at the same time as conduction velocity. In fact, in clinical practice, often the value of motor latency forms the basis for clinical diagnosis (Delisa et al 1994).

Techniques of securing the wrap

Tisseel glue

Tisseel glue was easy to use once in the 'Duploject' syringe but the requirement for a special procedure for warming and mixing the components of Tisseel glue using the 'Fibrinotherm' makes the use of Tisseel more expensive and complicated. Fibrin glue is produced by other manufacturers in more user-friendly forms, for example, Quixil (Ethicon, Johnson and Johnson Plaza, New Brunswick, NJ 08933). Quixil does not require any mixing but can be drawn up (once thawed) directly from two vials into a mixing syringe similar to the Duploject and can be applied, as with Tisseel, directly to the required site.

The use of Tisseel glue is attractive as it is already licensed for use in humans and used in some centres. When placing cable grafts in brachial plexus surgery, some surgeons use Tisseel glue alone to connect the grafts to the stumps of the residual nerves: other surgeons secure the grafts first with epineurial sutures and then place Tisseel glue around the site of repair.

Tisseel glue costs around £70 per vial. However, if more than one site of nerve division required repair, for example, in brachial plexus surgery where perhaps three nerve

autografts may require placement, one batch of Tisseel glue could secure several repair sites.

Polyglactin macrosutures

Securing the wrap with polyglactin macrosutures took longer and was a more difficult technique than securing the wrap with glue. Polyglactin sutures, however, are readily available in most surgical environments and are much cheaper than fibrin glue (around £4 per suture compared to £70 per vial of Tisseel glue). The motor end-plates in the muscle fibres in this group had not yet fully stabilized but otherwise, there was no difference in the outcome in this group compared with the epineurial suture group. The availability and ease of using polyglactin macrosutures made this technique of securing the wrap *in situ* a readily available and attractive option which may be more appropriate in the third world, surgical camps in the army, and other situations where access to fibrin glue may be limited.

Polycaprolactone glue

Polycaprolactone was the easiest technique of securing the wrap. The results of *motor latency* and *TSJ* were however significantly poorer in this group and the author would not recommend the use of polycaprolactone glue in humans. It may be possible to use other glues which are licensed for use in humans and not based on fibrin.

CONCLUSIONS

The use of the wrap in the NHS

The 'spaghetti wrist' (an injury where several structure on the volar aspect of the wrist have been divided) is not uncommon in current clinical practice and requires several hours of operative time to repair. It usually consists of several flexor tendon repairs, one or two vascular repairs and repair of the median and ulnar nerves. The use of a wrap to repair the nerves could significantly shorten the time required to complete to operation. Surgeons are often slow to adopt new techniques. It would be necessary to publish and disseminate information about the CRG-wrap widely if after a clinical trial it was found that the wrap was well tolerated in humans. The simplicity of use of the CRG-wrap, the decreased operative time that would be required and the potential for saving on costs makes the CRG-wrap an important addition to peripheral nerve repair surgery in the United Kingdom.

The use of the CRG-wrap in the third world and battlefield

The technique of using the wrap could be learned from a simple informative pamphlet or instructional DVD. A surgeon with no microsurgical experience could carry out repairs with the wrap. Time would be saved, and in surgical army hospitals, this is of great importance (personal communication with Surgeon Commander R. Rickards. R.N.). In such a situation, an immediate primary repair may be possible where it would otherwise be delayed while arranging microsurgical equipment or because of time constraints in theatre.

If fibrin glue was not available in such situations, the alternative technique of using the CRG-wrap + macrosutures would still be useful and should give an equivalent outcome to epineurial suturing after more time for regeneration.

Comparison of the CRG-wrap with alternative conduits

The type of injury examined in the present study was a simple, clean cut nerve division. Lundborg et al (2004) published results of a five year clinical follow-up of a randomized control trial comparing the repair of ulnar and median nerves in the wrist and forearm by silicone tubes or epineurial sutures using 9/0 polyamide. Seventeen patients underwent repair with the silicone tube and thirteen had epineurial repair. All injuries were clean cut divisions of the ulnar or median nerve as carried out in the present study although, unlike the present study, a gap of 3–5 mm was left between the ends of the nerves within the silicone tubes. The methods do not state whether a microscope was used for the epineurial repairs.

The patients were assessed using the 'Model for Documentation of Outcome after Nerve Repair' and the modified MRC scale for sensory function. The 'Model for documentation of outcome after nerve repair' has good reliability and validity and is based on a selection of tests of sensory and motor function (Lundborg et al 2004). The tests included are: sensory innervation (with Semmes-Weinstein filaments), static 2-point discrimination, tactile gnosis (with shape-texture identification test), dexterity (with Sollerman test), motor power, grip / strength, cold intolerance and hyperaesthesia (Weber et al 2000). Moving two-point discrimination was also measured as part of the MRC sensory grading system. The only outcome in which the two repair groups differed significantly was in that of cold intolerance. The tubular repair group had a better outcome. Unfortunately, eight out of the seventeen patients who underwent tubular repair required a further operation to remove the silicon tube because of local discomfort. While the outcome of repairs made with the silicon tubes was good, the requirement for a second operative procedure in 47% of patients makes this technique unsuitable for routine clinical use and leads Lundborg to conclude, 'Ideally, a tube used for nerve repair should be biodegradable and should not cause any local discomfort or any inflammatory reaction during its degradation.' (Lundborg et al 2004).

Weber et al compared the use of a biodegradable conduit made from polyglycolic acid with standard methods of nerve repair according to the size of the defect in the nerve. All nerve injuries were in the hand. When defects of less than 4 mm existed, patients were randomized to repair by epineurial suturing or by using a polyglycolic acid conduit. They reported 'excellent' recovery in 91% of the conduit group and 49% of the epineurial suture group. Three conduits required removal for protrusion beneath necrotic skin flaps.

When defects greater than 4 mm existed, patients were randomized to repair by nerve autograft, direct epineurial suture or PGA conduits. All defects over 8 mm were randomized to repair by nerve autograft or PGA conduit. Moving two-point discrimination was significantly better when gaps greater than 8 mm had been repaired with the PGA conduit. There was no difference between the outcomes in the groups with a gap in the nerve between 4 and 8 mm (Weber et al 2000).

The CRG-wrap is similar to the polyglycolic acid in that it is relatively inert and completely biodegradable. Similar results in humans could be expected therefore with the wrap and it has the benefit of being easier to apply (instead of having to pull the nerve ends into the conduit using 8/0 nylon sutures, the wrap can simply be secured in place with fibrin glue.)

Impermeable versus porous conduits

The potential benefit of the silicone tube which is not provided by the wrap is its impermeability and therefore its ability to accumulate tissue fluid within it that is rich in nerve growth factors. Whether this is or is not a benefit is not at all confirmed as exogenous nerve growth factor administration at the site of nerve repair has shown to increase axonal proliferation but thus increase random growth and disorganization but not necessarily improve the outcome of repair (Kelly 2002).

The problem of the gap

Having established that the wrap used in the present study, when secured with fibrin glue, provides as good nerve regeneration as that obtained with microsurgical epineurial

suturing, the next question to be considered is whether the wrap could be used to bridge gaps in nerves.

The problem of bridging gaps within a nerve is certainly one of the main current difficulties in peripheral nerve repair. A nerve autograft may be required to bridge a very small gap in a nerve, e.g. four centimetres, or for multiple long defects, for example in brachial plexus surgery where there can be nerve gaps of several centimetres in a few nerves. Despite the harvesting of the lateral and medial cutaneous nerves of the forearm and sural nerves, there may still not be enough harvested graft to repair all defects.

Enhancement of gap repairs

The potential benefit of Schwann cells to enhance neuronal regeneration because of their mitogenic action on the growth of neurones has been hampered by the requirement to culture autogeneic cells. This requires harvesting nerve tissue from a patient and culturing cells prior to repair. The subsequent reduction in the potential for regeneration due to the delayed repaired may not be compensated by the Schwann cell graft. Most studies using Schwann cells have therefore been done in animals, and, unfortunately, small animals.

Mosahebi et al (2002) suspended allogeneic or syngeneic Schwann cells within an alginate gel inside a polyhydroxybutyrate conduit and demonstrated that despite rejection of allogeneic Schwann cell implants by three weeks after implantation, there was an enhanced ability of neurones to bridge a 10 mm defect in the rat sciatic nerve when either allogeneic or syngeneic Schwann cells were present (compared with a control group of a polyhydroxybutyrate conduit alone). The quantity of axonal regeneration was however

less in the allogeneic Schwann cell group compared with both the normal conduit and syngeneic Schwann cell group.

Schwann cell mono-layers in polyethylene guides were shown by Bryan et al (1996) to allow regeneration across a 20 mm gap in the rat sciatic nerve in 60% of animals at 6 weeks.

Fibronectin mesh has been used to support nerve regeneration over a gap of 10 mm in rats. However, neurones in this study advanced more quickly into nerve autografts than into the fibronectin mesh.

Di Benedetto et al (1998) demonstrated that vein grafts with implanted segments of acellular muscle grafts could allow the bridging of gaps of 2 cm in rat sciatic nerves in five out of seven animals by fourteen weeks. The outcome with this technique was said by the authors to be similar to that which occurred with nerve autografts. Technical problems were thought to be responsible for the failure of two out of the seven cases. This highlights another benefit of the wrap; freeze-thawed muscle autografts, nerve autograft segments, or other regeneration enhancing materials could be inserted easily between the cut ends of a nerve on the open surface of the wrap prior to folding and securing of the wrap into a conduit.

Stem cells from which Schwann cells are derived, placed on a biodegradable scaffold or in a gel to sustain the cells, may allow longer lengths of nerves to regenerate without the requirement for nerve autografts.

Final conclusions

The original hypothesis, *'That, using biodegradable glass-fibre wraps held in place with glue or non-microsurgical sutures, it is possible to repair divided peripheral nerves in a large animal and obtain an outcome comparable with that found after conventional microsurgical epineurial suture repair'* is supported by the experiments described here. Nerve repair using the CRG-wrap + Tisseel glue and the CRG-wrap + macrosutures not only allowed nerve regeneration to the same standard as that which follows microsurgical epineurial repair but was also quicker, easier and more cost effective. It is suggested that CRG-wrap could be beneficially used in the developed countries, the third world and in military situations for nerve repair.

REFERENCES

Aitken JT, Sharman M, & Young JZ (1947). Maturation of regenerating nerve fibres with various peripheral connections. *Journal of Anatomy* **81**, 1-23.

Aitken JT & Thomas PK (1962). Retrograde changes in fibre size following nerve section. *Journal of Anatomy* **96**, 121-129.

Archibald SJ, Shefner J, Krarup C, & Madison RD (1995). Monkey median nerve repaired by nerve graft or collagen nerve guide tube. *J Neurosci* **15**, 4109-4123.

Ashdon RR & Done S (1984). *The Ruminants: colour atlas of veterinary anatomy* Bailliere Tindall, London.

Bennett MR (1999). The early history of the synapse: from Plato to Sherrington. *Brain Research Bulletin* **50**, 95-118.

Birch R, Bonney G, & Wynn Parry CB (1998). *Surgical disorders of the peripheral nerve*, pp. 408. Churchill Livingstone.

Birch R & Raji ARM (1991). Repair of median and ulnar nerves. Primary suture is best. *Journal of Bone and Joint Surgery* **73**, 154-157.

Borschel GH, Kia KF, Kuzon WM, & Dennis RG (2003). Mechanical properties of accelular peripheral nerve. *J. Surg. Reg.* **114**, 133-139.

Bowden RE & Guttmann E (1944). De-nervation and re-innervation of human voluntary muscle. *Brain* **67**, 273.

Boyd IA & Davey MR. Composition of peripheral nerves. 1968. Edinburgh, Livingstone.
Ref Type: Report

Boyes JH (1976). *On the shoulders of giants: notable names in hand surgery* JB Lippencott, Philadelphia.

Braun RM (1966). Comparitive studies of neurorrhaphy and sutureless peripheral nerve repair. *Surg Gynecol Obstet* **45**, 15-17.

Brunelli GA (2004). Sensory nerve transfers. *Journal of Hand Surgery* **29**, 557-563.

Brunelli GA & Brunelli F (1990). Strategy and timing of peripheral nerve surgery. *Neurosurg Rev* **13**, 95-102.

Brunelli GA, Battison B, Vigasio A, Brunelli G, & Marocolo D (1993). Bridging nerve defects with combined skeletal muscle and vein conduits. *Microsurgery* **14**, 247-251.

Brunelli GA, Vigasio A, & Brunelli GR (1994). Different conduits in peripheral nerve surgery. *Microsurgery* **15**, 176-178.

Bryan DJ, Wang K-K, & Chakalis-Haley DP (1996). Effect of Schwann cells in the enhancement of peripheral-nerve regeneration. *Journal of Reconstructive Microsurgery* **12**, 439-446.

Bunge RP (1981). Contributions of tissue culture to our understanding of basic processes in peripheral nerve regeneration. In *Postraumatic Peripheral Nerve Regeneration; Experimemental Basis and Clinical Implications*, eds. Gorio A, Millesi H, & Mingrino S, pp. 105-113. Raven Press, New York.

Carter AJ, Kristmundsdottir F, Gilmour J, & Glasby MA (1998). Changes in muscle cytoarchitecture after peripheral nerve injury and repair. A quantitative and qualitative study. *J Hand Surg [Br]* **23**, 365-369.

Chen Y-S, Chang J-Y, CHeng C-Y, Tsai F-J, Yao C-H, & Liu B-S (2005). An in vivo evaluation of a biodegradable genepin-cross-linked gelatin peripheral nerve guide conduit material. *Biomaterials* **26**, 3911-3918.

Chen Y-S, Hsieh CL, Tsai CC, Chen TH, Cheng WC, Hu CL, & Yao CH (2000). Peripheral nerve regeneration using silicone rubber chambers filled with collagen, laminin and fibronectin. *Biomaterials* **21**, 1541-1547.

Cragg BG & Thomas PK (1964). The conduction velocity of regenerated peripheral nerve fibres. *J Physiol* **171**, 164-175.

Dahlin LB, Anagnostaki L, & Lundborg G (2001). Tissue response to silicone tubes used to repair human median and ulnar nerves. *Scand. J. of Plastic and Reconstructive Surgery and Hand Surgery* **35,** 29-34.

Delisa JA, Lee HJ, Baran EM, Lai K-S, Spielholz N, & MacKenzie K (1994). *Manual of nerve conduction and clinical neurophysiology*, 3rd ed. Raven Press, New York.

Dellon AL (2004). History of peripheral nerve surgery. In *Youmans Neurological Surgery*, ed. Winn HR, pp. 3798-3808. Elsevier Inc., Philedelphia.

Dellon Al, & Mackinnon SE (1988). An alternative to the classical nerve graft for the management of the short nerve gap. *Plastic and reconstructive surgery* **82**, 849-856.

Di Benedetto GD, Zura G, Mazzucchelli R, Santinelli A, Scarpelli M, & Bertani A (1998). Nerve regeneration through a combined autologous conduit (vein plus acellular muscle grafts). *Biomaterials* **19**, 173-181.

Driscoll PJ, Glasby MA, & Lawson GM (2002). An in vivo study of peripheral nerves in continuity: biomechanical and physiological responses to elongation. *J Orthop Res* **20**, 370-375.

Freidman Y, King BS, & Rampril IJ (1996). Nitrous oxide depresses spinal F waves. *Anesthesiology* **85**, 135-141.

Frykman GK, McMillan PL, & Yegge S (1988). A review of the experimental methods measuring peripheral nerve regeneration in animals. *Orthop Clin N Amer* **19**, 209.

Fullarton AC, Glasby MA, & Lawson GM (1998). Immediate and delayed nerve repair using freeze-thawed muscle allografts. Associated long-bone fracture. *J Hand Surg [Br]* **23**, 360-364.

Fullarton AC, Lenihan DV, Myles LM, & Glasby MA (2002). Assessment of the method and timing of repair of a brachial plexus traction injury in an animal model for obstetric brachial plexus palsy. *J Hand Surg [Br]* **27**, 13-19.

Fullarton AC, Lenihan DV, Myles LM, & Glasby MA (2000). Obstetric brachial plexus palsy: a large animal model for traction injury and its repair. Part 1: age of the recipient. *J Hand Surg [Br]* **25**, 52-57.

Fullarton AC, Myles LM, Lenihan DV, Hems TE, & Glasby MA (2001). Obstetric brachial plexus palsy: a comparison of the degree of recovery after repair of a C6 ventral root avulsion in newborn and adult sheep. *Br J Plast Surg* **54**, 697-704.

Gasser HS & Grundfest H (1939). Axon diameters in relation to the spike dimensions and the conduction velocity in mammalian fibres. *Journal of Physiology* **127**, 393.

Gattuso JM, Glasby MA, Gschmeissner SE, & Norris RW (1989). A comparison of immediate and delayed repair of peripheral nerves using freeze-thawed autologous skeletal muscle grafts--in the rat. *Br J Plast Surg* **42**, 306-313.

Gilchrist T, Glasby MA, Healy DM, Kelly G, Lenihan DV, McDowall KL, Miller IA, & Myles LM (1998). In vitro nerve repair--in vivo. The reconstruction of peripheral nerves by entubulation with biodegradeable glass tubes--a preliminary report. *Br J Plast Surg* **51**, 231-237.

Glasby MA, Carrick MJ, & Hems TE (1992a). Freeze-thawed skeletal muscle autografts used for brachial plexus repair in the non-human primate. *J Hand Surg [Br]* **17**, 526-535.

Glasby MA, Clutton RE, Drew SJ, O'Sullivan MG, & Whittle IR (1995). Repair of the facial nerve in the cerebellopontine angle using freeze-thawed skeletal muscle autografts. An experimental surgical study in the sheep. *Acta Neurochir (Wien)* **136**, 151-159.

Glasby MA, Evans S, & Huang CLH (1989). Nerve regeneration through treated muscle graft during experimental treatment with antileprotic drugs. *Neuro-Orthopedics* **8**, 1-7.

Glasby MA, Fullerton AC, & Lawson GM (1998). Immediate and delayed nerve repair using freeze-thawed muscle autografts in complex nerve injuries. Associated arterial injury. *J Hand Surg [Br]* **23**, 354-359.

Glasby MA, Gilmour JA, Gschmeissner SE, Hems TE, & Myles LM (1990). The repair of large peripheral nerves using skeletal muscle autografts: a comparison with cable grafts in the sheep femoral nerve. *Br J Plast Surg* **43**, 169-178.

Glasby MA, Gschmeissner S, Hitchcock RJ, & Huang CL (1986a). Regeneration of the sciatic nerve in rats. The effect of muscle basement membrane. *J Bone Joint Surg Br* **68**, 829-833.

Glasby MA, Gschmeissner SE, Huang CL, & De Souza BA (1986b). Degenerated muscle grafts used for peripheral nerve repair in primates. *J Hand Surg [Br]* **11**, 347-351.

Glasby MA, Gschmeissner SG, Hitchcock RJ, & Huang CL (1986c). The dependence of nerve regeneration through muscle grafts in the rat on the availability and orientation of basement membrane. *J Neurocytol* **15**, 497-510.

Glasby MA & Hems TE (1995). Repairing spinal roots after brachial plexus injuries. *Paraplegia* **33**, 359-361.

Glasby MA, Hems TE, & Pell AC (1992b). The use of coaxially aligned freeze-thawed skeletal muscle autografts in the repair of the cauda equina--in the sheep. *Acta Neurochir (Wien)* **117**, 210-214.

Glasby MA, Mountain RE, & Murray JA (1993). Repair of the facial nerve using freeze-thawed muscle autografts. A surgical model in the sheep. *Arch Otolaryngol Head Neck Surg* **119**, 461-465.

Grabb WC & Arbour A (1968). Median and ulnar nerve suture. An experimental study comparing primary and secondary repair in monkeys. *J Bone Joint Surg Br* **50A**, 964-972.

Grieve FJ, Kristmundsdottir F, & Glasby MA (1991). The effect of age on the recorvery of reinnervated muscles. After nerve repair with autografts. *Neuro-Orthopedics* **12**, 1-17.

Guttmann E & Saunders FK (1943). Recovery of nerve fibres and diameters in the regeneration of peripheral nerves. *Journal of Physiology* **101**, 489-518.

Haber S, Finklestein SD, Benowitz LI, Sladek JRJr, & Collier TJ (1988). Matrigel enhances survival and integration of grafted dopamine neurons into the striatum. *Progress in Brain Research* **78**, 427-433.

Hems TE, Clutton RE, & Glasby MA (1994). Repair of avulsed cervical nerve roots. An experimental study in sheep. *J Bone Joint Surg Br* **76**, 818-823.

Hems TE & Glasby MA (1992b). Repair of cervical nerve roots proximal to the root ganglia. An experimental study in sheep. *J Bone Joint Surg Br* **74**, 918-922.

Hems TE & Glasby MA (1993). The limit of graft length in the experimental use of muscle grafts for nerve repair. *J Hand Surg [Br]* **18**, 165-170.

Hems TE & Glasby MA (1992a). Comparison of different methods of repair of long peripheral nerve defects: an experimental study. *Br J Plast Surg* **45**, 497-502.

Hems TEJ. An experimental study to define the surgical application of freeze-thawed muscle autografts in peripheral nerve repair. 1993. University of Oxford. Ref Type: Thesis/Dissertation

Holmes W & Young JZ (1942). Nerve regeneration after immediate and delayed suture. *Journal of Anatomy* **77**, 63-96.

HMSO *Home Office Animals (Scientific procedures) Act 1986* (1986). Ref Type: Bill/resolution.

Huang CL-H, Glasby MA, Gschmeissner S, & De Souza BA (1997). Regeneration of rat sciatic nerve through polyhydroxybutyrate grafts. *Neuro-Orthopedics* **117**.

Itoh S, Suzuki M, Yamaguchi I, Kobayashi H, Shinomiya K, Tanaka J (2003a). Development of a nerve scaffold using a tendon chitosan tube. *Artif. Organs* **27**, 1079-1088.

Itoh S, Yamaguchi I, Suzuki M, Ichinose S, Takakuda K, Kobayashi H, Shinomiya K, & Tanaka J (2003b). Hydroxyapatite-coated tendon chitosan tubes with adsorbed laminin peptides facilitate nerve regeneration in vivo. *Brain Res* **993**, 111-123.

Kean CJC, Lewis DM, & McGarrick JD (1974). Dynamic properties of denervated fast and slow twitch muscle of the cat. *J Physiol (Lond)* **237**, 103-113.

Kelleher MO, Al-Abri RK, Eleuterio ML, Myles LM, Lenihan DV, & Glasby MA (2001). The use of conventional and invaginated autologous vein grafts for nerve repair by means of entubulation. *Br J Plast Surg* **54**, 53-57.

Kelly G. The effects of neurotrophic factors in facial nerve repair. 2002. University of Edinburgh.
Ref Type: Thesis/Dissertation

Kennedy RD & Galindo AD (1975). Comparative site of action of various anaesthetic agents at the mammalian myoneural junction. *Br J Anaesthesia* **47**, 533-540.

Kettle S. The use of end-to-side repair of peripheral nerves for neurotization after loss of nerve tissue in a large animal model. 2003. University of Edinburgh. Ref Type: Thesis/Dissertation

Kiernan JA (2003). Carbohydrate histochemistry. In *Histological and Histochemical Methods. Theory and practice.* pp. 213-242.

Kim DH, Connolly SE, Zhao S, Beuerman RW, Voorhies RM, & Kline DG (1993). Comparison of macropore, semipermeable and nonpermeable collagen conduits in nerve repair. *J Reconstr Microsurg* **9**, 415-420.

Kimura J (2000). *Electrodiagnosis in diseases of nerve and muscle; principles and practice.*, 2nd ed. Philadelphia.

Kline DG (1981). Proximal segement of the nerve: mechanisms of nerve sprouting. In *Posttraumatic Peripheral Nerve Regeneration: Experimental Basis and Clinical Implications*, eds. Gorio A, Millesi H, & Mingrino S, pp. 102. Raven Press, New York.

Kline DG, Hayes GJ, & Morse AS (1964). A comparitive study of response of species to peripheral-nerve injury: I.Severence. *J Neurosurg* **21**, 968-979.

Kline DG, Hudson AR, Hackett ER, & Bratton BR (1981). Clinical and experimental reflections on the lesion with interruption without serious gap. In *Posttraumatic Peripheral Nerve Regeneration; Experimental Basis and Clinical Implications*, eds. Gorio A, Millesi H, & Mingrino S, pp. 287-296. Raven Press, New York.

Krarup C, Archibald SJ, & Madison RD (2002). Factors that influence peripheral nerve regeneration: an electrophysiological study of the monkey median nerve. *Ann Neurol* **51**, 69-81.

Lasek RJ, McQuarrie IG, & Wujek JR (1981). The central nervous system regeneration problem: neuron and environment. In *Posttraumatic Peripheral Nerve Regeneration: Experimental Basis and Clinical Applications*, eds. Gorio A, Millesi H, & Mingrino S, pp. 59-70. Raven Press, New York.

Lawson GM & Glasby MA (1995). A comparison of immediate and delayed nerve repair using autologous freeze-thawed muscle grafts in a large animal model. The simple injury. *J Hand Surg [Br]* **20**, 663-700.

Lawson GM & Glasby MA (1998). Peripheral nerve reconstruction using freeze-thawed muscle grafts: a comparison with group fascicular nerve grafts in a large animal model. *J R Coll Surg Edinb* **43**, 295-302.

Lenihan DV. New methods for the repair and assessment of peripheral nerve injury. 2000. University of Edinburgh.
Ref Type: Thesis/Dissertation

Lenihan DV, Carter AJ, Gilchrist T, Healy DM, Miller IA, Myles LM, & Glasby MA (1998a). Biodegradable controlled release glass in the repair of peripheral nerve injuries. *J Hand Surg [Br]* **23**, 588-593.

Lenihan DV, Carter AJ, & Glasby MA (1998b). An electrophysiological and morphological comparison of the microwave muscle graft and the freeze-thawed muscle graft. *Br J Plast Surg* **51**, 300-306.

Lewis DM (1972). The effect of denervation on the mechanical and electrical properties of fast and slow mammalian twitch muscle. *J Physiol (Lond)* **222**, 51-75.

Lundborg G (1988). *Nerve injury and repair*, 1st ed.

Lundborg G (1981). Mechanical effects on circulation and nerve function. In *Posttraumatic Peripheral Nerve Regeneration. Experimental Basis and Clinical Implications*, eds. Gorio A, Millesi H, & Mingrino S, pp. 157-158. Raven Press, New York.

Lundborg G, Rosen B, Dahlin L, Holmberg J, & Rosen I (2004). Tubular repair of the median or ulnar nerve in the human forearm: a 5-year follow-up. *J Hand Surg [Br]* **29**, 100-107.

Mackinnon SE & Dellon AL (1988). Clinical nerve reconstruction with a bioabsorbable polyglycolic acid tube. *Plastic and Reconstructive Surgery* **85**, 419-424.

Maeda T, Mackinnon SE, Best TJ, Evans PJ, Hunter DA, & Midha RT (1993). Regeneration across 'stepping-stone' nerve grafts. *Brain Res* **618**, 196-202.

Matsumoto K, Ohnishi K, Kiyotani T, Sekine T, Ueda H, Nakamura T, Endo K & Shimizu Y (2000a). Peripheral nerve regeneration across an 80-mm gap bridged by a polyglycolic acid (PGA)-collagen tube filled with laminin-coated fibres: a histological and electrophysiological evaluation of regenerated nerves. *Brain Res* **868**, 315-328.

Matsumoto K, Ohnishi K, Sekine T, Ueda H, Yamamoto Y, Kiyotani T, Nakamura T, Endo K, & Shimizu Y (2000). Use of a newly developed artificial nerve conduit to assist peripheral nerve regeneration across a long gap in dogs. *ASAIO J* **46**, 415-420.

May DSM (1970). *The anatomy of the sheep*, 3rd ed., pp. 21-24. Watson Ferguson & Co., South Brisbane, Australia.

Mayhew TM (1988). An efficient sampling scheme for estimating fibre number from nerve cross sections: the fractionator. *Journal of Anatomy* **157**, 127-134.

Mayhew TM (1990). Efficient and unbiased sampling of nerve fibre number and size. *Methods in Neuroscience* **3**, 172-187.

Mayhew TM & Sharma K (1984a). Sampling schemes for estimating nerve fibre size. I. Methods for nerve trunks of mixed fascicularity. *Journal of Anatomy* **139**, 45-58.

Mayhew TM & Sharma K (1984b). Sampling schemes for estimating nerve fibre size. II. Methods for unifascicular nerve trunks. *Journal of Anatomy* **139**, 59-66.

McKay HA, Wiberg M, & Terenghi G (2003). Exogenous leukaemia inhibitory factor enhances nerve regeneration after late secondary repair using a bioartificial nerve conduit. *Br J Plast Surg* **56**, 444-450.

Millesi H (1981). Neurorrhaphy. In *Posttraumatic Peripheral Nerve Regeneration; Experimental Basis and Technique*, eds. Gorio A, Millesi H, & Mingrino S, pp. 215-228. Raven Press, New York.

Millesi H, Meissl G, & Berger A (1972). The interfascicular nerve-grafting of the median and ulnar nerves. *J Bone Joint Surg Br* **54A**, 727-750.

Miloro M, Halkias LE, Mallery S, Travers S, & Rashid RG (2002). Low-level laser effect on neural regeneration in Gore-Tex tubes. *Oral Surg Oral Med Oral Pathol Oral Radiol Endod* **93**, 27-34.

Miyamoto Y & Tsuge K (1981). Effects of tension on intraneural microcirculation in end-to-end neurorrhaphy. In *Posttraumatic Peripheral Nerve Regeneration; Experimental Basis and Clinical Implications*, eds. Gorio A, Millesi H, & Mingrino S, pp. 81-91. Raven Press, New York.

Mosahebi A, Fuller P, Wiberg M, & Terenghi G (2002). Effect of allogeneic Schwann cell transplantation on peripheral nerve regeneration. *Exp Neurol* **173**, 213-223.

Mountain RE, Glasby MA, Sharp JF, & Murray JA (1993). A morphological comparison of interposed freeze-thawed skeletal muscle autografts and interposed nerve autografts in the repair of the rat facial nerve. *Clin Otolaryngol* **18**, 171-177.

Myles LM, Gilmour JA, & Glasby MA (1992). Effects of different methods of peripheral nerve repair on the number and distribution of muscle afferent neurons in rat dorsal root ganglion. *J Neurosurg* **77**, 457-462.

Nakamura T, Inada Y, Fukuda S, Yoshitani M, Nakada A, Itoi S, Kanemaru S, Endo K, & Shimizu Y (2004). Experimental study on the regeneration of peripheral nerve gaps through a polyglycolic acid-collagen (PGA-collagen) tube. *Brain Research* **1027**, 18-29.

Norris RW, Glasby MA, Gattuso JM, & Bowden RE (1988). Peripheral nerve repair in humans using muscle autografts. A new technique. *J Bone Joint Surg Br* **70**, 530-533.

Pereira JH, Palande DD, Subramanian A, Narayanakumar TS, Curtis J, & Turk JL (1991). Denatured autologous muscle graft in leprosy. *Lancet* **338**, 1239-1240.

Petrie A & Sabin C (2000). *Medical statistics at at glance* Blackwell Science Ltd.

Rampril IJ, & King BS (1996). Volatile anaesthetics depress spinal motor neurons. *Anesthesiology* **85**, 129-134.

Robinson PH. *Artificial conduits in reconstructive microsurgery* (1989). Ref Type: Thesis/Dissertation

Rodriguez FJ, Verdú E, Ceballos D, & Navarro X (2000). Nerve guides seeded with autologous schwann cells improve nerve regeneration. *Experimental Neurology* **161**, 571-584.

Rosberg HE, Carlsson KS, Höjgård S, Lindgren B, Lundborg G, & Dahlin LB (2005). Injury to the human median and ulnar nerves in the forearm - amalysis of costs for treatment and rehabilitation of 9 patients in Southern Sweden. *Journal of Hand Surgery* **30**, 35-39.

Rumsby MG & Finean JB (1966). The action of organic solvents on the myelin sheath of peripheral nerve tissue - I: Methanol, ethanol, chloroform and chloroform-methanol(2:1 v/v). *Journal of Neurochemistry* **13**, 1501-1507.

Sanders FK & Whitteridge D (1946). Conduction velocity and myelin thickness in regenerating nerve fibres. *Journal of Physiology* **105**, 152-174.

Schmidt FO & Bear RS (1939). The ultrastructure of the nerve axon sheath. *Biol Rev* **14**, 27.

Seddon HJ. *Peripheral nerve injuries*. 282. 1954. London, HMSO. Special reports. Ref Type: Report

Shen ZL, Berger A, Hierner R, Allmeling C, Ungewickell E, & Walter GF (2001). A schwann cell-seeded intrinsic framework and its satisfactory biocompatibility for a bioartificial nerve graft. *Micorsurgery* **21**, 6-11.

Smahel J & Jentsch B (1986). Stimulation of peripheral nerve regeneration by an isolated nerve segment. *Annals Plastic Surgery* **16**, 494-501.

Sorbie C & Porter TL (1969). Reinnervation of paralysed muscles by direct motor nerve implantation. An experimental study in the dog. *J Bone Joint Surg Br* **51**, 156.

Stålberg E, Mihelin M, & Trontelj JV (1992). Electrical microstimulation with single fibre electromyography: a useful method to study the physiology of the motor unit. *J Clinical Neurophysiology* **9**, 105-119.

Stålberg.E. & Trontelj JV (1994). *Single fibre electromyography. Studies in healthy and diseased muscle.*, 2nd ed. Raven Press Ltd., 1185 Avenue of the Americas, New York, New York 10036.

Stanec S & Stanec Z (1998a). Reconstruction of upper-extremity peripheral-nerve injuries with ePTFE conduits. *J Reconstr Microsurg* **14**, 227-232.

Stanec S & Stanec Z (1998b). Ulnar nerve reconstruction with an expanded polytetrafluoroethylene conduit. *Br J Plast Surg* **51**, 637-639.

Starrit NE. An electrophysiological and morphometric study of the effect of different methods of surgical repair in motor and mixed nerves - A comparison of the repair of the facial nerve and median nerve in a large animal model. 2004. University of Edinburgh.
Ref Type: Thesis/Dissertation

Stevenson TR, Kadhiresan VA, & Faulkner JA (1994). Tubular nerve guide and epineurial repair: comparison of techniques for neurorrhaphy. *Journal of Reconstructive Microsurgery* **10**, 171-174.

Strauch B, Ferder M, Lovelle-Allen S, Moore K, Kim DJ, & Llena J (1996). Determining the maximal length of a vein conduit used as an interposition graft for nerve regeneration. *Journal of Reconstructive Microsurgery* **12**, 521-527.

Sunderland S (1978). *Nerve and nerve injuries*, 2nd ed., pp. 240-241. Churchill Livingstone, New York.

Sunderland S & Bradley KC (1961). Stress strain phenomenon in denervated peripheral nerve trunks. *Brain* **84**, 125.

Terris DJ, Toft K, Moir M, Lum J, & Wang M (2001). Brain-derived neurotrophic factor-enriched collagen tubule as a substitute for autologous nerve grafts. *Arch Otolaryngol Head Neck Surg* **127**, 294-298.

Thesleff S, Vyskocil F, & Ward MR (1974). The action potential end plate and extrajunctional regions of rat skeletal muscle. *Acta physiol scand* **91**, 196.

Thiele B & Boehle A. Number of single muscle fibre action potentials contributing to the motor unit potential. 5th International congress of electromyography. 21-25. 1975. 1975.
Ref Type: Conference Proceeding

Thiele B & Stålberg E (1974). The bimodal jitter:a single fibre elctromyographic finding. *J Neurol Neurosurg Psychiatry* **37**, 403-411.

Trontelj JV & Stålberg E (1992). Jitter measurements by axonal micro-stimulation. Guidelines and technical notes. *Electroencephalography and Clinical neurphysiology-electromyography and motor control* **85**, 30-37.

Vowles GH & Francis RJ (2002). Amyloid. In *Theory and Practice of Histological Techniques*, eds. Bancroft JD & Gamble M, pp. 303-324. Churchill Livingstone.

Wang H & Lineaweaver WC (2003). Nerve conduits for nerve reconstruction. *Operative Techniques in Plastic and Reconstructive Surgery* **9**, 59-66.

Wang KK, Cetrulo CL, & Seckel BR (1999). Tubulation repair of peripheral nerves in the rat using an inside-out intestine sleeve. *J Reconstr Microsurg* **15**, 547-554.

Wang KK, Costas PD, Jones DS, Miller RA, & Seckel BR (1993). Sleeve insertion and collagen coating improve nerve regeneration through vein conduits. *J Reconstr Microsurg* **9**, 39-48.

Weber RA, Breidenbach WC, Brown RE, Jabaley ME, & Mass DP (2000). A randomized prospective study of polyglycolic acid conduits for digital nerve reconstruction in humans. *Plastic and Reconstructive Surgery* **106**, 1036-1045.

Weiss P, & Edds MV (1946). *Nerve and Nerve Injuries*, 145th edn.

Whitworth IH, Brown RA, Dore C, Green CJ, & Terenghi G (1995a). Orinetated mats of fibronectin as a conduit material for use in peripheral nerve repair. *Journal of Hand Surgery* **20B**, 429-436.

Whitworth IH, Dore CJ, Green CJ, & Terenghi G (1995b). Increased axonal regeneration over long nerve gaps using autologous nerve-muscle sandwich grafts. Microsurgery **16(12)**, 772-778.

Woodhall B & Beebee GW (1956). *Peripheral nerve repair: A follow-up study of 3,656 World War II injuries.*

Yoshimura M, Amaya S, Tyujo M, & Nomura S (1989). Experimental studies on the traction injury of peripheral nerves. *Neuro-Orthopedics* **7**, 1-7.

Young JZ, Holmes W, & Sanders FK (1940). Nerve regeneration. *Lancet* **3**, 128-130.

Young RC, Wiberg M, & Terenghi G (2002). Poly-3-hydroxybutyrate (PHB): a resorbable conduit for long-gap repair in peripheral nerves. *Br J Plast Surg* **55**, 235-240.

Yu X, & Bellamkonda RV (2003). Tissue-engineered scaffolds are effective alternatives to autografts for bridging peripheral nerve gaps. *Tissue Eng.* **9(3)**, 421-430.

Zhao Q, Lundborg G, Danielsen N, Bjursten LM, & Dahlin LB (1997). Nerve regeneration in a 'pseudo-nerve' graft created in a silicone tube. *Brain Res* **769**, 125-134.